NANYANG TECHNOLOGICAL UNIVERSITY

DESIGN AND PERFORMANCE OF STONE MASTIC ASPHALT IN SINGAPORE CONDITIONS

QIU YUNFENG

SCHOOL OF CIVIL & ENVIRONMENTAL ENGINEERING

2007

Design and Performance of Stone Mastic Asphalt in Singapore Conditions

Qiu Yunfeng

School of Civil & Environmental Engineering

A thesis submitted to Nanyang Technological University
in fulfillment of the requirement for the degree of
Doctor of Philosophy

2007

ACKNOWLEDGEMENTS

I wish to express my deepest appreciation to my supervisor, Dr. Lum Kit Meng, for his unreserved guidance and encouragement throughout the course of this research. Without his constant support and enthusiastic participation in the work, this research would not have been finished. I benefited a lot from his philosophical perspectives and visions. Outside research, I also learned a lot of valuable things from him in many other aspects.

I also wish to thank the Transportation laboratory of Nanyang Technological University for providing me the invaluable assistance and facilities to carry out this research work. Special thanks to the technicians, Choi Siew Pheng, Mai Ju An, Ng Choo Hiang, and Liew Kai Liang for their help during the course of the experiments of this work.

Thanks are also due to the Nanyang Technological University for the financial support and research grant.

Finally, I wish to express my gratitude for the love of my family, especially my wife, whose constant inspiration and support has always played an important role throughout the course of my research work.

TABLE OF CONTENTS

LIST OF TABLES

LIST OF FIGURES

LIST OF ABBREVIATIONS

AASHTO	American Association of State Highway Transportation Officials
AC	Asphalt Content
AI	Asphalt Institute
ANOVA	Analysis of Variance
APA	Asphalt Pavement Analyser
AS	Australian Standard
ASTM	American Society for Testing Materials
BPS	Break Point Sieve
BSI	British Standard Institution
CA	Coarse Aggregate
CMHB	Coarse Matrix High Binder
COV	Coefficient of Variation
DEM	Discrete Element Method
DUW	Design Unit Weight
DSR	Dynamic Shear Rheometer
E	Elastic Modulus
EAPA	European Asphalt Pavement Association
FA	Fine Aggregate
FA_c	Fine Aggregate Coarse Portion
FA_f	Fine Aggregate Fine Portion
f_t	Asphalt Film Thickness

FEM	Finite Element Modelling
G_1, G_2, G_N	Individual Specific Gravities of Aggregate
G_b	Specific Gravity of Asphalt
G_{mb}	Bulk Specific Gravity of Mixture
G_{mm}	Maximum Specific Gravity of Mixture
G_R	Shear Relaxation Modulus
G_{sb}	Bulk Specific Gravity for the Total Aggregate
G_{se}	Effective Specific Gravity of Aggregate
GTM	Gyratory Test Machine
HMA	Hot Mix Asphalt
K_R	Bulk Relaxation Modulus
LTA	Land Transport Authority
LUW	Loose Unit Weight
M_R	Resilient Modulus
MATTA	Material Testing Apparatus
NAPA	National Asphalt Pavement Association
NAT	Nottingham Asphalt Tester
NCAT	National Centre for Asphalt Technology
NCHRP	National Cooperative Highway Research Program
NMAS	Nominal Maximum Aggregate Size
NSSGA	National Stone, Sand and Gravel Association
NTU	Nanyang Technological University
P_1, P_2, P_N	Individual Percentages by Mass of Aggregate
P_b	Asphalt Content, Percent by Mass of Total Mixture
P_{ba}	Absorbed Asphalt, Percent by Mass of Aggregate
P_{be}	Effective Asphalt Content, Percent by Mass of Total Mixture
P_{mm}	Percent by Mass of Total Loose Mixture

P_s	Aggregate Content, Percent by Mass of Total Mixture
PMB	Polymer Modified Binder
RUW	Rodded Unit Weight
SA	Aggregate Surface Area Factor
SHRP	Strategic Highway Research Program
SGC	Servopac Gyratory Compactor
SMA	Stone Mastic Asphalt
SPS	Secondary Point Sieve
SST	Simple Shear Test
TPS	Tertiary Point Sieve
UVCATA	Uncompacted Void Content of Aggregate Testing Apparatus
υ	Poisson's Ratio
VCA	Voids in the Coarse Aggregate
VCA_{dry}	Voids of the Coarse Aggregate in the Dry Rodded Condition
VCA_{mix}	Voids of the Coarse Aggregate in the Mixture
V_a	Air Voids in Compacted Mixture
VFA	Voids Filled with Asphalt
VMA	Voids in the Mineral Aggregate
VTM	Voids in the Total Mixture
W	Mass of the Compacted Mixture in the Water
W_a	Mass of the Compacted Mixture in the Air
WWT	Wessex Wheel Tracker

ABSTRACT

Stone Mastic Asphalt (SMA) mixtures are gap-graded mixtures that contain a coarse aggregate skeleton and a high asphalt binder content mortar. SMA mixtures are used to improve the mixtures' resistance to rutting and also to improve the durability of pavements. This rutting resistance is mostly attributed to the coarse aggregate skeleton component that exhibits "stone-to-stone" contact due to its gap-graded gradation. However, guidance is lacking in the selection of the design aggregate structure for achieving stone-to-stone contact and on the understanding of the interaction of the aggregate structure with the mixture properties.

The objective of the research is to provide a methodology of quantifying coarse aggregate stone-to-stone contact in SMA with different aggregate packing to yield high rutting resistance; thus, developing a new mix design procedure (refer to Appendix A) and leading to an improved SMA mixture design and performance. The concepts that utilised aggregate interlock and aggregate packing were proposed to develop coarse aggregate stone-to-stone contact, meet volumetric criteria and provide adequate mechanical properties. These proposed concepts relied on coarse aggregate for the skeleton of the mixture with the appropriate amount of fine aggregate to provide a proper packed aggregate structure.

A total of thirty-seven mixtures were tested in this study for developing and analysing coarse aggregate stone-to-stone contact in SMA mixtures. Each mixture composed of different combinations of aggregate gradations that were selected with

a rational approach to determine the relative amounts of coarse and fine aggregates and asphalt binder. Laboratory performance tests were conducted to characterise the volumetric properties, resilient modulus, resistance to permanent deformation, and rut susceptibility of these mixtures.

The experimental results indicated that the SMA mixtures developed in this study exhibited good coarse aggregate stone-to-stone contact, thus had a better rutting resistance than the conventional dense-graded mixtures. Different combinations of coarse and fine aggregates by volume would develop different degrees of coarse aggregate stone-to-stone contact. When the design unit weight of coarse aggregate is between 95 and 105% of the rodded unit weight of coarse aggregate, stone-to-stone skeleton would develop. Also, the higher the rodded unit weight of coarse aggregate, the higher would be the degree of stone-to-stone contact, thus having a higher rutting resistance.

Only crushed granite aggregate was used in the experimental test of this study. This limited the experimental findings to one type of aggregate (crushed granite). In order to expand the laboratory test results to analyse the permanent deformation potential of SMA, a two dimensional dynamic finite element procedure was developed. Advanced material model of visco-elastic was incorporated into the 2-D dynamic finite element procedure. The numerical simulation results indicated that the developed finite element procedure reflected well the inter-granular interactions between aggregate and asphalt mastic of SMA. This procedure can be expanded to different aggregate shape, angularity and maximum aggregate size to investigate their coarse aggregate stone-to-stone contact.

The results in this study improved the SMA mixture design by providing a method to characterise coarse aggregate stone-to-stone contact in SMA mixtures through the

fundamental principles of particle packing. The design concepts outlined in this study would provide the foundation for a new procedure of SMA mixture design.

CHAPTER ONE

INTRODUCTION

1.1 BACKGROUND

Stone Mastic Asphalt (SMA), which has been used in Europe for approximately 40 years (Bellin, 1992), was first developed to provide high resistance to abrasion by studded tyres. After that, it was found that this mixture was not only successful in its intended purpose but also offered high resistance to rutting. Consequently, application of this technology continued to grow even after the use of studded tyre was discontinued in some European countries.

SMA is perhaps best explained as a two-component hot mix asphalt (HMA) mixture: a coarse aggregate skeleton and a high asphalt binder content mortar. The exceptional rut resistance performance of SMA is mostly attributed to the coarse aggregate skeleton component that exhibits "stone-to-stone" contact due to its gap-graded gradation. These two components combined address both the concern

on mixture stability and durability. The interlocking stone skeleton provides stability to withstand heavy traffic loads with minimal rutting. The high asphalt binder content of the mortar promotes durability. In addition, the mortar properties are also important to prevent draindown at mixing and placement temperatures and to assist the stone skeleton in preventing rutting. The high mineral filler content promotes both stability and durability by producing a stiff mortar that not only resists rutting but also aids in holding the coarse aggregate particles in place.

Compared with dense-graded asphalt mixtures, coarse aggregate in SMA are in close particle-to-particle contact. Figure 1.1 shows the difference between SMA and dense-graded asphalt mixture. The SMA structure provides high internal friction and high shear resistance, thus a high resistance to plastic deformation or rutting.

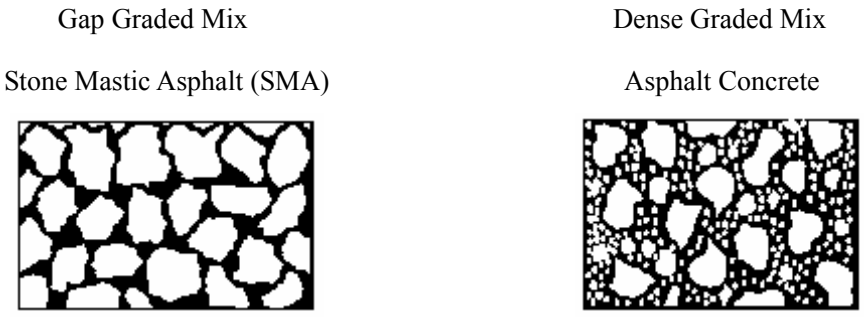

Figure 1.1 The Structure of SMA and Asphalt Concrete

The stone skeleton of SMA is composed of the coarse aggregate which is defined as the aggregate fraction retained on the 4.75 mm sieve. The sieve size is used to distinguish the relative proportions of coarse and fine aggregates (Haddock, 1998). In order to provide proper rutting resistance (i.e. load bearing capacity), it is imperative that the stone skeleton be designed to have “stone-to-stone” contact.

1.2 PROBLEM STATEMENT

Although SMA can provide an extremely rut resistant and durable HMA mixture, it must be correctly designed to maximise its performance. The design involves a careful proportioning of each of the components to ensure a proper stone skeleton and durable mortar. Literature review has indicated that the strength of SMA relies heavily on the stone-to-stone aggregate skeleton. Therefore, aggregate quality is a major factor in determining the stone-to-stone contact and the performance of SMA. However, design guide as to the degree of coarse aggregate stone-to-stone contact and an understanding on the interaction of aggregate structure with SMA mixture design, construction and performance are not readily available and are not objectively understood. Also, not much can be found in the literature on the influence of aggregate size (gradation), shape, angularity, and surface texture on the stone-to-stone contact of coarse aggregate. In general, designers rely on their experience when designing SMA based on the components involved, especially in regard to a well-blended aggregate gradation.

In 1995, the National Centre for Asphalt Technology (NCAT) developed a mixture design method for SMA. The procedure was primarily applicable to SMA having a nominal maximum aggregate size of 19 mm and was documented in an interim report published in May of 1995 (Brown et al., 1995). This interim report provided a review of the literature on SMA as well as the initial research data in the United States. In a draft final report dated September 1996, additional guidance was provided on materials, gradation, and mixture proportioning (Brown et al., 1996). Although this design method provides some guidance on the application of SMA, it only reflects local conditions and properties of available material sources in the United States. No procedure is outlined for understanding the interaction of aggregate blending and the resulting mixture volumetrics. This lack of guidance in

the selection of the blend of aggregate requires that local experience dictates the mix designer to the appropriate design.

In Singapore, the Land Transport Authority (LTA) specifies the gradation of SMA as shown in Table 1.1. But preliminary investigations as carried out in Nanyang Technological University (NTU) (Phoon, 1997; Toh, 1998; and Lau, 1999) revealed that the aggregate gradation as specified by LTA appeared not to be truly gap-graded in nature. As such, these mixtures did not approach SMA mixture gradations. They often lacked stone-to-stone contact and did not have the binder rich mortar that is a characteristic of SMA mixtures. No direct guidance is given to the selection of aggregate gradation for achieving the stone-to-stone skeleton.

Table 1.1 LTA SMA Mix Specifications

Maximum size of Aggregate	**14 mm**	
Sieve size (mm)	**% Passing**	**Mid value**
14	90-100	95
9.5	65-90	77.5
6.3	40-60	50
3.35	25-37	31
2.36	22-34	28
1.18	16-28	22
0.6	12-24	18
0.3	7-19	13
0.075	5-10	7.5

Therefore, it is necessary to understand the combination of aggregates and their packing to quantify the aggregate gradation especially coarse aggregate

stone-to-stone contact; it is imperative that the mixture be designed with a well-packed coarse aggregate skeleton. If a good mixture design procedure is to be adopted, it should be possible to improve the performance of SMA.

1.3 OBJECTIVES

The objective of the research is to provide a methodology of quantifying coarse aggregate stone-to-stone contact in SMA with different aggregate packing to yield high rutting resistance; thus, developing a new procedure and leading to an improved SMA mixture design and performance. The new design procedure would help to develop stone-to-stone aggregate skeleton, give better resistance to permanent deformation (rutting), while maintaining volumetric properties that provide resistance to environmental distress.

The main tasks according to the objective are as follows:

(1) To review the history and development of stone mastic asphalt (SMA) mixture.

(2) To search for published research results on coarse aggregate stone-to-stone contact in SMA mixtures.

(3) To review the published literature on addressing the combination of aggregates and their packing.

(4) To establish a laboratory method by which the coarse aggregate stone-to-stone contact may be credibly identified and measured.

(5) To use the developed method to identify and evaluate statistically the effects of aggregate packing and coarse aggregate stone-to-stone contact on the volumetric and mechanical properties of SMA mixtures.

(6) To derive predictive relationships relating the volumetric and mechanical properties of SMA mixtures to the aggregate stone-to-stone contact and asphalt binder such as aggregate ratio and asphalt film thickness.

(7) To conduct a two dimensional dynamic finite element analysis procedure to expand the laboratory test results to analyse the permanent deformation potential of SMA.

1.4 SCOPE

This study developed SMA mixture design concepts that utilised aggregate interlock and aggregate packing to develop aggregate stone-to-stone contact for Singapore conditions.

In this study, "Singapore conditions" mainly referred to the use of certain aggregate and asphalt materials and testing conditions relevant to the context of Singapore:

- Crushed granite aggregate of 14 mm nominal maximum size was used for SMA mixture.
- Polymer modified asphalt (Cariphalte) was used as the binder.
- Physical property tests such as repeated load uniaxial test and wheel tracking test were carried out at 50 °C , which is suitable for Singapore climate condition.

Research work was performed to evaluate the effect of various aggregate combinations on the stone-to-stone contact of SMA. The testing was done using the Uncompacted Void Content of Aggregate Testing Apparatus (UVCATA). Mixtures were also prepared and tested in the laboratory to evaluate the effect of various aggregate packing on the volumetric and mechanical properties of SMA.

The laboratory performance of the mixtures was characterised through fundamental engineering property tests. The engineering property tests conducted in this study included:

- Draindown;

- Volumetrics;
- Indirect tensile resilient modulus at 25 °C ;
- Repeated load uniaxial test at 50 °C ; and
- Wheel tracking test at 50 °C .

In order to expand the results from fundamental mixture characterisation and to predict SMA performance, a two dimensional finite element analysis procedure to analyse the permanent deformation potential of SMA was developed. In the numerical analysis, a visco-elastic model was developed to describe the stress-strain relationship of SMA mixtures. Different volume fractions of coarse aggregate and different coarse aggregate size, shape, and angularity were selected to validate the material models and the finite element procedures. After model validation, the numerical simulation results were compared to the experimental measurements.

1.5 SIGNIFICANCE

The research conducted in this study was designed to overcome the limitations of the current procedures used to design and analyse SMA. In Singapore, SMA is an alternative surfacing layer to the dense-graded bituminous mixture. The research was aimed at establishing the coarse aggregate stone-to-stone contact and evaluating the fundamental engineering properties of SMA for potential applications in Singapore. It is a scientific effort to quantify aggregate stone-to-stone contact pertaining to the SMA mixture design procedures. The resulting performance test will measure aggregate stone-to-stone contact correlated to SMA rutting and will play a key role in the quality control (QC) and quality acceptance (QA) of HMA mixtures.

The developed micromechanical models using finite element modelling technique in this study can simulate fundamental material properties of SMA based on the properties of the individual constituents. Micromechanical modelling has tremendous potential benefits in the field of asphalt technology, for reducing or eliminating costly tests to characterise asphalt-aggregate mixtures for the design and control of these materials.

1.6 ORGANISATION

This thesis is composed of seven chapters. Chapter One introduces the problem with a brief discussion of the background information related to the SMA mixture design, and a description of the objectives to be accomplished. Chapter Two provides a summary of the literature search and review on the development of SMA mixtures, the introduction of the particle packing for use in the design of aggregate gradation, and the evaluation of rutting resistance tests. The development of numerical simulation of asphalt mixture was also discussed. The third chapter presents the methodology used in laboratory testing, describing step-by-step the testing protocol used to design and quantify aggregate stone-to-stone contact in SMA mixtures. Chapter Four presents the comprehensive laboratory investigation. The equipment and test methods used to conduct laboratory tests were briefly summarised. Chapter Five presents and discusses the results obtained from the testing programme and statistical analysis. The significant factors are identified and predictive equations are developed and evaluated. Chapter Six describes the theoretical development of material characterisation to predict SMA mixture permanent deformation. A two dimensional dynamic finite element analysis, in which visco-elastic material model was applied for the asphalt mixtures, was developed. The conclusions of this research and recommendations for its

application and further development are presented in Chapter Seven.

CHAPTER TWO

LITERATURE REVIEW

Relevant literatures were reviewed and were included as a part of this document. Literature review covered the development of SMA mixtures, aggregate gradation analysis and the particle packing for use in aggregate stone-to-stone contact, the evaluation of rutting resistance test, and the development of numerical simulation of asphalt mixture.

2.1 STONE MASTIC ASPHALT

Stone Mastic Asphalt (SMA) was developed in Germany in the mid 1960's (Bellin, 1992) to combat the excessive wear and damage caused by the use of studded tyres. The mixture became known in Europe as Splittmastixasphalt or Stone Mastic Asphalt and as Stone Matrix Asphalt in the United States. Today, this mixture is probably best known by the acronym "SMA". This mixture was not only successful in its intended purpose but was found to be highly resistant to rutting. Consequently, application of this technology has become widespread throughout the world.

The concept of SMA is not complex. A tough, durable, crushed stone aggregate structure is bound by mastic comprising a high asphalt binder and mineral filler content. While an adequate amount of mortar is also essential to ensure durability, it is imperative that an excess of mortar be avoided in order to maintain "stone-to-stone" contact among the coarse aggregate particles. The exceptional rut resistance of SMA is mostly derived from this coarse aggregate skeleton component of the mixture. Thus, proper proportioning of the components to provide aggregate stone-to-stone contact is the challenge of SMA mixture design.

2.1.1 Development

Since SMA inception in Germany, trials were conducted in Sweden and then in Denmark. Germany's early work was the basis for the first European specifications (Germany Specification, 1984). However, these specifications were essentially recipes, which dictated mixture ingredients and proportions that seemed to work well. As use of the mixture became more widespread in Europe, a proliferation of specifications and methodologies evolved that aimed to suit the materials used within a given region or nation. While these various European specifications provided prospective users with useful information, such specifications and empirical methods were not directly applicable to all situations. Hence, similar satisfactory results could not be expected with certainty when different materials were used or when criteria and/or methods were compromised.

In the late 1980's, news about SMA began to circulate through technical information exchanges between asphalt technologists in the United States and Europe (Bellin, 1992). A group of pavement specialists from the United States conducted a fourteen-day tour of six European countries in 1990. One of the objectives of the tour was to investigate pavements and asphalt technology. While in Europe, these pavement specialists examined SMA pavements firsthand and learned more of the technology through technical presentations such as the one provided by Liljedahl (1990). The European Asphalt Study Tour resulted in the publication of a

report (AASHTO, 1991), which documented the findings of the team. The report provided the state of the practice regarding the use of SMA in various European and Scandinavian nations.

The basic features which are typical of SMA in Europe such as gap-grading, high crushed stone content, high filler content and high binder contents are characteristics of SMA in the United States and have served as the framework for mixture design. However, some early U.S. specifications required minimum Marshall Stability and voids in the mineral aggregate (VMA) values. In contrast, these parameters were not part of European SMA Specifications. In fact, the German specification (1984) made no mention of VMA at all.

2.1.2 Materials

Quality materials are essential for any quality hot mix asphalt (HMA) product. However, this is particularly true for SMA. In fact, aggregate properties are most important for stone-to-stone contact of SMA. The other component, the mortar, is actually a blend of asphalt binder, filler, and most often some types of stabiliser to minimise drainage of the binder during production and construction. Therefore, proper selection and use of quality mortar ingredients to ensure satisfactory mortar quality is also essential for good quality SMA mixture.

- **Asphalt Binder**

The literature review clearly indicated that when the use of SMA mixtures began in Europe and Scandinavia, “neat”, or unmodified, penetration graded asphalt binders were used (Kast, 1985; Sardal, 1988; and Rinckes, 1989). The standard European designation for asphalt binders is the letter “B” followed by the penetration grade of the binder. Thus, a B65 simply indicates an asphalt binder with the penetration grade of 65. The binders most often used appear to be a B65, B80, B100, and B200. Indeed the German SMA specification contains mixtures with B65, B80, and B200

penetration graded asphalt binders (Germany Specification, 1984). Although the earliest SMA mixtures used these straight run asphalt binders, modified asphalt binders with and without fibre have also been used in Europe (Tappeneir, 1990).

When the use of SMA began in the United States, both straight run and modified asphalt binders were employed. The first SMA pavement in the United States used an 80-100 penetration graded asphalt binder. Other projects had used AC-20 and AC-30. With the advent of Superpave performance graded binders, grades such as PG 64-22 and others are now used (Cooley and Brown, 2003).

The optimum asphalt content for SMA mixtures is above 6.0 percent and in some specifications is required to be above 6.5 percent (Brown et al., 1996). The voids are filled with mastic, which contains fines, asphalt cement and special stabilisers or fibres. For SMA mixtures which contain organic or mineral fibres, the range of optimum asphalt content is normally slightly higher than that required when polymers are used as stabiliser (Brown, 1993b). The high asphalt contents and mastic provide a mixture that has excellent durability.

- **Aggregate**

The importance of aggregate quality is acknowledged in a number of specifications. In the United States, a model guideline on materials (NAPA, 1994) addressed the issue of aggregate quality. Numerous gradations used for SMA appeared throughout the literature. In Europe, the maximum aggregate size for SMA mixes can vary from 6.35 mm (1/4 inch) to as large as 25 mm (1 inch), but most SMA mixes tend to use relatively smaller coarse aggregate particles. The size of the largest particles typically used is 4.75 mm (3/16 inch), 8 mm (5/16 inch) or 11 mm (7/16 inch) (Nobel Industry, 1991). These maximum sizes appeared reasonable since the mixture was developed and has primarily been used as a wearing course.

In 1997, the National Centre for Asphalt Technology completed a survey of all

SMA projects completed in the United States through 1996 (Brown et al., 1997b). The survey was completed for the Federal Highway Administration. Of the 136 pavement sections constructed during this period, 70 mixtures had a 19 mm Nominal Maximum Aggregate Size (NMAS), 2 had a 16 mm NMAS. Although 57 were 12.5 mm NMAS mixtures and 7 had a NMAS of 9.5 mm, they could also have been classified as 19 mm NMAS mixtures. No nominal maximum size mixtures smaller than 9.5 mm or larger than 19 mm were evaluated since none had been constructed as of 1996. In addition, since that time, there were no documented cases of SMA mixtures having nominal maximum sizes smaller than 9.5 mm or larger than 19 mm until 2003 that Cooley and Brown (2003) studied "fine" SMA (4.75 mm NMAS) and used it as a viable option for thin overlay.

- **Mineral Filler**

A central issue in the design of SMA mortar is the role of the mineral filler. The term "filler" is a generic one used to describe dust-size particles. In general, 8-12 percent of the total amount of aggregate in the mix passes the 0.075 mm sieve (Davidson and Kennepohl, 1992). This large amount of filler plays an important role in the properties of SMA mixture particularly in terms of air voids, voids in the mineral aggregate and optimum asphalt content (Nobel Industry, 1991 and Davidson and Kennepohl, 1992). Since the amount of material passing the 0.075 mm sieve is relatively large, the SMA is handled and performs very differently from other HMA mixtures (Davidson and Kennepohl, 1992). A primary difference between SMA and open graded mixtures is the low air voids (approximately 3-4 percent) in the SMA mixture, whereas open graded friction courses may have more than 20 percent air voids.

- **Stabiliser**

SMA mixtures have higher asphalt binder contents than regular dense-graded mixtures, which render them vulnerable to draindown of the binder during storage

or while the material is being hauled to the paving site. In order to prevent draindown in SMA mixtures, stabilisers are used. There are two kinds of stabilisers: fibre stabiliser and polymer stabiliser.

Fibres, as a stabiliser agent, are usually added to reduce the draindown of the binder material during mixing, hauling and placing operations (Scherocman, 1992). Loose organic fibres, such as cellulose, are typically added at the rate of 0.3 percent by weight of mixture. Mineral fibres are often added at a rate of 0.4 percent by weight of mixture (Brown, 1993b).

Polymer stabilisers have also been used on a limited basis in SMA mixtures. In some cases, the polymers are pre-blended with the asphalt binder and added to the mix during the mixing process. One purpose of the polymer stabiliser is to minimise the asphalt binder draindown during the hauling, mixing, and placing operations (Scherocman, 1992). The other purpose is to increase the stiffness of the asphalt at high, in-service temperature and/or to improve the low temperature properties of the binder material (Scherocman, 1992). Polymers are typically added to the mix at a rate of 3.0 to 8.0 percent by weight of asphalt binder (Brown, 1993b).

2.1.3 Stone-to-Stone Contact

There is a consensus in the SMA literature that the use of SMA continued to rise due to its ability to withstand heavy traffic without rutting. This ability is derived from a stone-to-stone coarse aggregate skeleton. Obviously, aggregate quality especially the percent of coarse aggregate has an important effect on this stone-to-stone contact. However, a quantitative method to establish this condition is lacking. Traditionally, the SMA gradation specification has been used to help ensure an adequate coarse aggregate skeleton. For example, in Sweden where SMA had been used successfully for many years, the specifications (Sardal, 1988) generally followed what has become known as the “30-20-10 rule.” This rule suggests that an SMA should have approximately 30 percent passing the 4.75 mm sieve, 20 percent

passing the 2.36 mm sieve, and 10 percent passing the 0.075 mm sieve. The first major use of SMA in the United States was designed following this rule (Scherocman, 1991).

The use of quantitative test procedures to determine when coarse aggregate stone-to-stone contact is achieved in SMA was discussed by Haddock et al. (1993). In their paper on an Indiana SMA project, the authors noted the importance of a coarse aggregate skeleton and presented a method for determining whether SMA mixtures have an adequate skeleton. Their method involved compacting the coarse aggregate only fraction of the mixture and determining its density. Two percent asphalt cement by mass of total mixture is used to aid in the compaction process. After SMA mixture specimens have been compacted and their densities determined, the density of the coarse aggregate skeleton in the total SMA mixture is calculated. This skeleton density is then compared to the density of the coarse aggregate only fraction previously determined. If the SMA coarse aggregate skeleton density is greater than or equal to the coarse aggregate only fraction density, the SMA mixture is determined to have a stone-to-stone coarse aggregate skeleton.

Brown and Mallick (1995) discussed a similar method for determining when coarse aggregate stone-to-stone contact exists in a SMA mixture. Their method is based on the relationship between voids in the coarse aggregate (VCA) and the percent fine aggregate (material passing the 4.75 mm sieve) in the mixture. By comparing a series of mixtures, Brown and Mallick were able to clearly show that as the percent fine aggregate in a mixture decreases, the VCA decreases. This approximately linear relationship persists until the percent fine aggregate reaches about 30 percent. At this point, the VCA becomes more or less constant. The point at which the VCA ceases to decrease with a further decrease in percent fine aggregate was interpreted to be the point at which coarse aggregate stone-to-stone contact exists.

Based on their findings, Brown and Mallick suggested using the dry-rodded unit weight apparatus (ASTM C29, 1998) to determine when coarse aggregate

stone-to-stone contact exists in a SMA mixture. To use this approach, the coarse aggregate only fraction of the SMA mixture is placed in the unit weight bucket and its density determined. The density is used to calculate the VCA for the coarse aggregate only fraction. In this state, coarse aggregate stone-to-stone contact obviously exists since only the coarse aggregate is present. The entire SMA mixture is then compacted using conventional methods and the density of the mixture is determined. From this information, the VCA of the SMA aggregate skeleton can be calculated. If the SMA aggregate skeleton has a VCA less than or equal to the coarse aggregate only fraction VCA, the SMA mixture is judged to have developed stone-to-stone contact.

2.1.4 Mixture Design

The SMA mixture design procedure is developed to ensure that SMA mixtures have an adequate coarse aggregate skeleton and satisfactory mixture volumetric. The five basic steps in the mixture design procedure are:

(1) Select constituent materials;
(2) Determine optimum aggregate gradation;
(3) Determine optimum asphalt binder content;
(4) Evaluate asphalt binder draindown potential; and
(5) Evaluate moisture susceptibility.

Although the first SMA was placed in 1991 in the United States and many subsequent projects built thereafter, no standard mixture design procedure was available in the early 1990's. Consequently, material specifications and design procedures used for the early U.S. trials were a reflection of those of the Europeans. The 1991 Wisconsin project and those that followed were documented in the trade press and later in more detailed reports published by research agencies or state departments of transportation (Pryor, 1991; Drake, 1991; Eaton, 1991a; Eaton, 1991b; Warren, 1991; Kuennen, 1991; and Parson, 1991). Most of these trials were deemed successful although sufficient time had not transpired to make complete

performance assessments. However, despite these early successes, there remained lack of objectivity as to the appropriate material specifications and design procedures. Even when the desirable material properties were determined and the correct materials obtained, the problem of how to correctly design SMA in relating to environment outside their locations and its associated performance remained to be answered. No standard design and mixture evaluation tests were specified by the Europeans. This is apparent because no standard design methods were used in Europe as exemplified by Bellin's (1992) explanation that no specific design method existed in Germany. Many practitioners in the United States were more comfortable with some types of test that designers could rely on to indicate expected performance. Unfortunately, little work had been done to correlate physical tests such as creep properties or rutting resistance with SMA performance.

- **Recent European Mixture Design Methodologies**

In 1998, Bellin (1998a) presented a state-of-the-art summary of SMA used in Germany. In his work, he described the origin and development of Stone Mastic Asphalt. He also provided details regarding material selection and design. The design described involves the preparation of trial specimens using Marshall Compaction. Recommendations regarding aggregate gradation were given; however, details concerning the selection of the aggregate structure were not provided. The optimum asphalt binder content was specified as the one yielding air voids between 3 and 4 percent. Marshall Stability and Flow were not recommended and the performance indicators such as wheel tracking tests were not required.

Also in 1998, Bellin (1997) prepared a report entitled *Designing Stone Matrix Asphalt Mixtures* that was submitted to the Technical Committee of the European Asphalt Pavement Association (EAPA). The purpose of this report was to provide a summary of SMA used in Europe and to present the European Product Standard for SMA. The EAPA subsequently published Bellin's report in a document entitled *Heavy Duty Surfaces: The Arguments for SMA* (Bellin, 1998b). In this report, Bellin

again summarised the German applications and design practices. However, he also included specifications and design procedure for the following European nations, namely, the Czech Republic, Denmark, France, Hungary, Italy, Netherlands, Norway, Portugal, Sweden and the United Kingdom. The report specifically provided information regarding material gradations/nominal maximum aggregate sizes, mix design procedures, mixture criteria, and performance testing. Notable points from the report for each country are shown in Table 2.1. The information given in Table 2.1 illustrates the proliferation of SMA specifications used in Europe. The use of Marshall Compaction seems to be a common practice although 50, 75 and even 100 blows per face were reported. There obviously were debates regarding the most appropriate performance test as virtually every nation recommends something different. Interestingly, Table 2.1 shows that some Europeans continued to employ the Marshall Stability test despite recommendations made by the German and U.S. researchers to the contrary.

Bellin (1998b) also presented the European Product Standard for SMA in the EAPA report. These specifications are shown in part in Table 2.2. Notably, gradations having a range in nominal maximum aggregate size from 4 mm to 22 mm were given. However, Bellin indicated that the 4 mm, 20 mm and 22 mm mixtures were not being used at that time. The report stated that the final compaction procedure had yet to be determined although the Marshall hammer (50 blows) was recommended in the interim. Likewise, voids content had yet to be recommended, but 2.0 to 6.0 percent was recommended as a first proposal. Performance testing was not yet incorporated into the proposed standard approach either. However, empirical performance testing in the form of some type of wheel tracking and a fundamental performance evaluation, most likely triaxial compression testing was expected to be included.

In the EAPA report, Bellin (1998b) explicitly stated that SMA is appropriate for all surface and resurfacing applications. He also mentioned the use of SMA as a base or binder layer was also being considered by the Swedish. Therefore, specifications

for these larger stone size SMA mixtures were included in the proposed European standard as shown in Table 2.2. However, Bellin expressed some doubts as to the potential benefit to be gained versus the additional cost of these mixtures.

- **The U.S. Mixture Design Procedure**

Mix design for early U.S. projects relied heavily upon European recipe specifications. However, most of these projects were successful which sparked greater interest in this mix type and amplified the need for a formal, rational approach to its design.

In 1995, the National Centre for Asphalt Technology (NCAT) developed a tentative mixture design method for SMA. The work was completed for the Transportation Research Board through the National Cooperative Highway Research Program (NCHRP) Project 9-8 (Brown et al., 1995). This version of the procedure was applicable to SMA having a nominal maximum aggregate size of 19 mm and was documented in an interim report published in May of 1995. The interim report also provided a review of the literature on SMA and as well as the initial research data. Table 2.3 listed the suggested requirements of SMA mixture design. In a draft final report dated in September 1996, additional guidance was provided regarding materials, gradation, laboratory compaction and mixture proportioning (Brown et al., 1996).

Table 2.1 Notable Points of SMA Specifications of Various European Nations (Bellin, 1998b)

European Nation	SMA Mixture NMAS, mm	Laboratory Compaction	Min or Typical Binder Content, %	Air Voids (%)	VMA (%)	Performance Tests**
The Czech Republic	8, 11	Marshall	6.5-7.0 or 7.2	3.0-4.5	Not Specified	MS, NAT
Denmark	8, 11, 16	Marshall	Not Specified	1.5-4.0	Min 16.0	Not Specified
France	6, 10	Not Specified	Min 5.6	Not Specified	Not Specified	CIR, FR, CM, F
Germany	5, 8, 11	Marshall	Min 7.2, 7.0, 6.5	2.0 or 3.0-4.0	Not Specified	Not Specified
Hungary	8, 12	Marshall	5.7-7.0	2.5, 3.5-4.0	Not Specified	LCPC, DC
Italy	10, 15	Marshall	5.5-7.0	1.0-4.0	Not Specified	MS, ITS, IT
The Netherlands	6, 8, 11	Marshall	7.4, 6.9, 6.5	4.0	Not Specified	Not Specified
Norway	11, 16	Marshall*	6.3, 6.0	1.5, 2.5	Not Specified	MS, S
Portugal	9.5, 12.5	Marshall	Min 5.0	3-5 or 6	Not Specified	Not Specified
Sweden	8, 11, 16, 22	Marshall	Min 5.9, 5.7, 5.5	2.0-5.4***	Not Specified	Not Specified
United Kingdom	10, 14	Not Specified	Not Specified	Not Specified	Not Specified	Not Specified

* 75 blow

** Performance test: MS – Marshall Stability; CM – Complex Modulus; ITS – Indirect Tensile Stiffness;
NAT – Nottingham Asphalt Tester; F – Fatigue (type not specified); IT – Indentation Test;
CIR – Compression/Immersion Ratio; LCPC – Wheel tracking; S – Stiffness (type not specified).
FR – French Rut Tester; DC – Dynamic Creep;

*** Specific range varies for each NMAS mixture

Table 2.2 European Standard for SMA (Bellin, 1998b) (Gradations shown as percentage passing)

Sieve Size, mm	SMA Mixture ("D" – Designation, NMAS shown in mm)									
	D4	**D6 (1)**	**D6 (2)**	**D8**	**D10**	**D11**	**D14**	**D16**	**D20**	**D22**
31.5									100	100
22.4								100		90 – 100
20.0							100		90 – 100	
16.0						100		90 – 100		60 – 80
14.0					100		90 – 100		60 – 80	
11.2				100		90 – 100		45 – 75		35 – 60
10.0			100		90 – 100		50 – 75		35 – 60	
8.0		100		90 – 100		45 – 75		25 – 40		25 – 40
6.3			90 – 100		30 – 50		20 – 35		20 – 35	
5.6	100	90 – 100								
4.0	90 – 100			25 – 45		25 – 40		20 – 35		20 – 35
2.0	30 – 40	30 – 40	25 – 35	20 – 30	20 – 30	20 – 30	15 – 30	15 – 30	15 – 30	15 – 30
0.063	8 – 12									
Binder Content Range, %	7.0 – 8.0	6.5 – 7.5	6.5 – 7.5	6.0 – 7.0	6.0 – 7.0	6.0 – 7.0	5.8 – 6.8	5.8 – 6.8	5.7 – 7.2	5.7 – 7.2
Additives	0.3 – 1.5									

Table 2.3 Properties of SMA Materials and Mixtures (Brown et al., 1996)

Property	Criteria Established	Criteria Evaluated in SMA Mix Design Study
Coarse Aggregate		
L.A. Abrasion (AASHTO T96)	30% Max	√
Flat and Eongated Particles (ASTM D4791)	3:1, 20% Max	√
	5:1, 5% Max	√
Sodium Sulfate Soundness (AASHTO T104)	15% Max	
Percent Fractured Faces		
One or more	100%	
Two or more	90% Min	
Absorption (AASHTO T85)	2% Max	
Coarse and Fine Durability Index	40 Min	
(AASHTO T210)		
Fine Aggregate	100 % Crushed	
Sodium Sulfate Soundness (AASHTO T104)	15% Max	
Liquid Limit (AASHTO T89)	25% Max	
Total Aggregate – Gradation (mm)	(%)	
19	100	
12.5	85 – 95	
9.5	75 Max	
4.75	20 – 28	√
2.36	16 – 24	
0.6	12 – 16	
0.3	12 – 15	
0.075	8 – 10	√
0.02	3 Max	√

Table 2.3 Properties of SMA Materials and Mixtures (Brown, et al., 1996) (continued)

Asphalt Cement	AASHTO M226	
Mineral Filler		
PI	4 Max	
Percent Passing 0.02mm	20%	√
Stabiliser Cellulose	0.3%	
Mineral Fibre	0.4%	
Polymer	---	
Property	**Criteria Established**	**Criteria Evaluated in SMA Mix Design Study**
Stone to Stone Contact	---	√
Voids in Total Mix	3 – 4%	√
VMA	17%	√
Asphalt Content	6.0% Min	√
Compactive Effort	50 Blows	√
Draindown	0.3% Max	√

2.2 AGGREGATE GRADATION AND PARTICLE PACKING

2.2.1 Aggregate Gradation Analysis

Accurate quantification and selection of aggregate gradation is essential for a better understanding of its effect on the load carrying capacity of an asphalt mixture. This is even more applicable for SMA where stone-to-stone contact forms the cornerstone of its load carrying capacity, especially against rutting.

In the early mix design, the selection of aggregate gradation was only used to determine the asphalt content. The need for minimum amount of asphalt binder was recognised and formulas were applied to the gradation for the determination of this amount of asphalt binder to provide adequate durability.

Several researchers examined the problem of improved gradation by the 1940's. Nijboer (1948) experimentally showed that the ideal gradation for maximum packing of aggregate solids occurred when the slope of the log-log gradation chart was 0.45. This agrees with the later work by Goode and Lufsey (1962) in their establishment of the "0.45 chart."

Nijboer also pointed out the importance of aggregate particle shape in an asphalt mixture. While he found that the 0.45 slope gave the densest packing, he also recognised that the combination of round and angular aggregate may lead to a decrease in voids when compared to angular aggregate alone. He also stated that the densest state would be for the gradation that contains all round particles. This fact was verified by Huber and Shuler (1992) who concluded that rounded gravels produced mixtures with lower VMA than crushed aggregates for the same gradation.

Nijboer stressed the importance of the quantity of coarse aggregate in developing the required mechanical properties and plastic deformation in an asphalt mixture. He stated that with increasing quantities of coarse aggregate, the system would change into one in which the coarse particles would form a skeleton. This aggregate skeleton is independent of the largest aggregate size and is only a factor of the amount of coarse aggregate, where coarse aggregate is the largest size of aggregate included in the mixture. Nijboer found that the interlocking resistance provided by the coarse aggregate is the best mechanism for resisting permanent deformation in

an asphalt mixture. The interlocking resistance was found to increase with the volume concentration of coarse aggregate in the mixture.

When a mixture contains small quantities of coarse aggregate, these particles can be considered to be solids moving in a liquid formed by the asphalt and fine aggregate material. Nijboer concluded that this type of mixture would have a decreased resistance to deformation. He concluded that coarse aggregate would affect the properties mainly through the volume present in the mix, but not through the maximum particle size or the gradation. Nijboer stated that the study of the middle size aggregates was not necessary for mixtures with adequate quantities of coarse aggregate and improved filler-binder ratio.

A later study of gradation of asphalt mixtures and the resulting voids included an examination of aggregate packing. This study by Hudson and Davis (1962) pointed to the fact that the gradation specification bands were arbitrarily determined as a result of local experiences. These gradation bands were not necessarily related to the quality of the resulting mixture. Hudson and Davis stated that if the criteria based on aggregate bands are to be fully met aggregate voids must be maintained within the definite limits. This study recognised that the most important characteristic of a gradation is the resulting aggregate voids in the compacted mixture.

Recent studies on the combination of aggregates for asphalt mixture design recognise the importance of the volume of coarse aggregate for improved mixture performance. Concepts put forth by Seward et al. (1996) advocated using increased volume of coarse aggregate for improved performance. This work proposed using a standard load, applied by the Superpave Gyratory Compactor (SGC) to compact the coarse aggregate, determine the volume of voids remaining, and filling those voids

with the dry compacted volume of fine aggregate. Based on the field experience, the resulting mixtures from these proposed design methods may be considered difficult to construct and may have high permeability because of a lack of fine aggregate in the mixture.

Studies from the concrete industry on the combined gradation of aggregate in a concrete mixture have yielded similar results to those currently being presented in the asphalt industry. For concrete, it has been found that the largest possible volume fraction of coarse aggregate is advantageous with regard to strength and stiffness, creep, drying shrinkage, and permeability (Johansen and Andersen, 1991). For concrete mixtures, the cement paste may be considered the weakest part of the concrete, as it is necessary to hold the skeleton of aggregate particles together. If the aggregate is sound and of high quality it is advantageous to ensure that the aggregate skeleton is as closely packed as possible and to bind it with just the right amount of high-quality cement paste to fill the voids between the aggregate particles.

A paper by Kight and Crockford (1998) presented a method for aggregate gradation selection. The paper proposed a method for determining the coarse aggregate volume in a compacted state and filling the remaining voids with fine aggregate in a compacted state. These mixtures have been placed on the roads trafficked by extremely heavy vehicles and have out-performed the Texas Coarse Matrix High Binder (CMHB) materials and a SHRP Superpave mix. The mechanical properties of these mixtures were superior over the CMHB and Superpave mixtures when evaluated in the Rapid Triaxial Test Device.

In summary, the ideas presented on the relation of aggregate gradation to the desired properties of an asphalt mixture gave mixed recommendations on the appropriate

gradation for asphalt. With the advent of increased traffic loading and vehicle weight, it became necessary to re-examine the aggregate structure properties that would give good performance. With this re-examination, the importance of coarse aggregate in the performance of mixtures under the increased load was demonstrated. An increase in the volume of coarse aggregate has not been totally embraced because of the difficulty in the construction of these mixtures, and the perceived problems with their durability.

2.2.2 Particle Packing

- **Packing of Spheres**

The study of particle packing is necessary to understand the basis for the combination of aggregates and aggregate stone-to-stone contact in an asphalt mixture. Considerable work has been recorded on the combination of particles and the resulting voids but without a solution that provides the answer to the problem of particle packing.

The idealised packing of spheres is often used as a starting point to evaluate the packing of aggregate particles. The theoretical models for the packing of spheres are used to understand the general concepts that govern the packing of aggregate particles.

The study of uniform spheres is used as background material in rock physics, seismic analysis and ceramics (Reed, 1988 and Mavko et al., 1998). In the geometric packing of single sized spheres, several particle orientations exist for ordered packing including, cubical, orthorhombic, tetragonal, pyramidal, hexagonal, and tetrahedral. Of interest in this study is the size of the maximum sphere fitting in

the narrowest channel created by the packing of the unit sphere. These sizes can be used to calculate a particle diameter ratio $(\frac{\text{Particle Fitting in Void}}{\text{Large Particle Creating Void}})$. This particle diameter ratio has a range from 0.42 for the simple cubical packing to 0.15 for the tetrahedral or hexagonal close packing (Bourbie et al., 1987 and Reed, 1988).

Several models exist for evaluating the densities resulting from combining two sizes (binary packing) of spheres. These models are generally divided into two distinct groups, those with particle diameter ratios below 0.22 and those with particle diameter ratios above 0.22 (Johansen and Andersen, 1991). Experimental results with the packing of spheres showed that the model by Aim and Goff (1967) gave the best fit to the experimental data for particle diameter ratios below 0.22. The model by Toufar et al. (1976 and 1977) gave the best fit for particle diameter ratios above 0.22. Toufar et al. stated that the smaller particles, for diameter ratios greater than 0.22, would actually be too large to be situated within the interstices between the larger particles. Based on the split in applicability of the models naturally occurring at a particle diameter ratio of 0.22 it is felt that this ratio is applicable for describing a particle size that fills the void, rather than a particle size that is larger than the created void.

In the study of gap gradations for asphalt, Davis (1980) had suggested that the proper size of a sphere to perfectly fill the void created by the intersection of other spheres would have a diameter ratio of 0.3. In his paper, Davis did not give the background for such an assumption, but did state that there was a considerable increase in the volume concentration of aggregate when in a binary mixture of spheres the second size particles has a diameter ratio of 0.3 or smaller.

Optimisation of Aggregate Packing

The study of optimisation of packing has primarily been undertaken in the concrete industry (Shilstone, 1990; Shilstone, 1993; Roy et al., 1993; de Larrard and Sedran, 1994; and Goltermann et al., 1997). Work in the optimisation of aggregate gradation had improved the state-of-the-art and the rheological properties of cement and concrete, which had led to an improved performance in many applications.

The development of ultra high performance concrete has also utilised the ideas of particle packing (de Larrard and Sedran, 1994). When developing an ultra high performance concrete, it is necessary to include aggregate to create some void space for the ultra high performance mortar. The use of properly sized aggregate is important for the creation of this material. Experimental data showed that an aggregate with a characteristic size of 250 μm was optimised with a cement mortar created by cement with a continuous gradation and nominal maximum size of 63 μm. The particle diameter ratio for the sized materials was 0.25.

Work by Shilstone in the design of concrete mixtures had received mixed reactions (Shilstone, 1990 and Shilstone, 1993). The analysis of gradation for general use concrete that was introduced is not in line with the traditional design of concrete mixtures. The Portland Cement Association method for the design of concrete mixtures advocates blending aggregates that meet the quality and gradation specifications given by ASTM but do not analyse the resulting gradation (Kosmatka and Panarese, 1988). Shilstone used the idea of blending the aggregates by volume and added an analysis of gradation for the design of mixtures with improved performance (Shilstone, 1990 and Shilstone, 1993). Shilstone advocated the use of a percent retained graphical analysis procedure to ensure balance in the gradation.

Testing of different aggregates had revealed that the percentage of voids in the compacted state ranged from 41% to 32% depending on the maximum size and gradation of the aggregate (Goltermann et al., 1997). These values were typically 33% to 38% when continuous gradation of sands was examined (Powers, 1964). When combining two aggregates, it is possible to achieve voids as low as 23%. The addition of a third aggregate source will reduce the voids to as low as 18%. These results on the voids in aggregate were very dependent on the particle shape of the aggregates (Tons and Goetz, 1967).

Recent research on the theoretical close packing of spheres showed that the random close packing of spheres was an elusive topic. The definition of close packing was arguably difficult to describe mathematically (Torquato et al., 2000). The research, which applied previously to unused packing philosophies, may change the way engineers design composite materials from solid chemicals for industrial use to Portland cement concrete and hot mix asphalt.

2.3 RUTTING RESISTANCE TESTS

In HMA design methodologies, rutting resistance tests included strength tests like the Marshall or Hveem Stability, or fundamental property tests such as Resilient or Creep Modulus. Unfortunately, little work had been done to correlate these familiar tests to SMA performance. Stuart (1992) noted that few strength or stiffness tests had been done in Europe and the applicability of diametral and tensile strength tests to SMA mixtures was not yet determined. Richter (1991) documented the use of some European tests. However, none of these were familiar outside Europe. Thus, in addition to the need for a rational mix design approach, a need also exists to adequately characterise and predict the performance of SMA mixture.

Despite the relative newness of the mixture design method and a continued lack of performance-related mixture tests, SMA mixtures appeared to be performing well as rut resistant mixtures. The SHRP researchers examined a wide variety of test methods to find the best performance test for measuring permanent deformation response. They examined and discussed four types of laboratory tests used to characterise the permanent deformation response of pavement materials.

(1) Uniaxial stress tests: unconfined cylindrical specimens in creep, repeated, or dynamic loading;
(2) Triaxial stress tests: confined cylindrical specimens in creep, repeated, or dynamic loading;
(3) Diametral tests: cylindrical specimens in creep or repeated loading; and
(4) Potential (new) tests: e.g., simple shear and hollow cylinder tests.

Of these, based on field simulation and simplicity, they ranked the simple shear test (SST) (AASHTO TP7) first, the triaxial stress test second, and the creep test third. They measured that the shear properties were the most important in rutting and that the SST provided the best means to directly measure the effects of a specific stress state and the dilation characteristics of a mix. However, the advantages of the SST were not worth the increased cost over the triaxial stress test apparatus.

Gabrielson (1992) evaluated variations of creep tests and permanent deformation tests to characterise the rutting behaviour of asphalt concrete. Repeated load deformation test was found to be the best method and was validated with field cores. A significant relationship was found between rutting performance and permanent strain. Thirteen percent permanent strain was the delineating point between “rutted” and “good” pavements.

The SHRP researchers (Monismith et al., 1994) pointed out that previous research

had suggested that the repeated load test was more sensitive to mix variables than the creep test. They found that the repeated load triaxial test provided a better measure of rutting characteristics than the creep test.

The study by Brown and Manglorkar (1993) indicated that the Marshall Stability for SMA mixtures was significantly lower than that for dense-graded mixtures. It showed that Marshall Stability may not be applicable for SMA. The quality of SMA mixtures is better controlled by the volumetric properties than by Marshall Stability.

In Taiwan, Hsu and Leu (1998) used repeated load triaxial tests to relate the permanent deformation behaviour of SMA mixtures to the energy dissipated during the test. Based on their experimental results, they concluded that a 19 mm SMA mixture provided better resistance to rutting than a 25 mm SMA or a conventional dense-graded mix.

Nunn et al. (1998) using the Nottingham Asphalt Tester (NAT) compared the repeated load axial test (both confined and unconfined) against wheel-tracking tests of the same materials and found that the repeated load test ranked the materials in a similar fashion to the wheel tracking test. They found the unconfined test inadequate for evaluating the resistance to permanent deformation. They recommended that the repeated load test be further evaluated to develop standard testing conditions.

Brown and Scholz (1998) also modified the NAT to convert the repeated load axial test into a repeated load triaxial test by using a vacuum to apply the confining stress. This approach limited the confining stress to 1 atmosphere (roughly 100 kPa) but made the test variable as a routine test. They then used the apparatus to examine two porous mixtures with the same gradation but different binders at different

temperatures and confining stresses. They found that confining the specimen emphasised the role of aggregates in resisting permanent deformation.

The National Centre for Asphalt Technology developed a procedure for a confined repeated load deformation test (Gabrielson, 1992; Foo, 1994; Mallick et al., 1994; Buncher, 1995; and Ahlrich, 1996) to evaluate the rutting of asphalt mixture. The test uses a triaxial arrangement similar to that used in soil mechanics. A confining pressure of 20 psi (138 kPa) and deviator stress of 100 psi (690 kPa) are applied to 100 mm diameter and approximately 63.5 mm thick compacted samples.

Many asphalt technologists have continued to utilise wheel tracking devices to make performance prediction of HMA mixtures including Superpave designed mixtures. Mogawer and Stuart (1994) performed tests using the French rut tester, the Georgia Loaded Wheel Tester, and the Gyratory Testing Machine and found no significant differences among the mixtures tested. Walsh (1993) also conducted wheel tracking tests and proposed a test temperature of 45 °C . Fujita (1994) indicated that a Japanese SMA was far superior to their regular dense-graded HMA in a dynamic wheel tracking test. Kandhal and Mallick (1999) concluded that the Asphalt Pavement Analyser (APA) wheel tracking device was sensitive to aggregate gradation and binder performance grade. In addition, they stated that the APA appears to have the potential to predict the relative rutting potential of HMA mixtures. Based on their research data, they also concluded that terminal rut depths after 8000 loading cycles should be less than 4.5 to 5.0 mm in order to ensure rutting resistance in the field.

In NTU, Lum and Hassabo (2003) used wheel tracking test to study binder influence type on deformation resistance of SMA. Based on their experimental results, they concluded that SMA batched polymer-modified binder and

process-modified binder had higher rutting resistance than those SMA batched with Pen 60/70 conventional bitumen.

2.4 NUMERICAL SIMULATION OF ASPHALT MIXTURE

The microstructure simulation approach can be used to predict the effect of properties of aggregate on asphalt mixtures. Although the numerical modelling of SMA is sparsely found in the literatures, the use of micromechanics in conventional asphalt mixtures and mastic and cemented particulate materials has drawn increasing attention over the past decade. Thus, a number of approaches have been investigated. They can be applied to SMA modelling with some modifications.

The literatures on finite element method (FEM) that were used to model the performance of asphalt concrete have been studied by many researchers. Tashman et al. (2000) presented a version of the element capable of modelling the permanent deformation of asphalt pavements. They developed an anisotropic viscoplastic continuum damage model. The model is based on Perzyna's formulation with Drucker-Prager yield function modified to account for the material inherent anisotropy. Schwartz et al. (2002) evaluated a constitutive model and developed it as a comprehensive material model for asphalt concrete. This model considered the visco-elastic, damage, and viscoplastic components of asphalt concrete behaviour over the full range conditions of interest for the mechanistic prediction of flexible pavement distresses. Lu et al. (2002) extended the model to consider elastic, visco-elastic, and viscoplastic components. They described a visco-elastoplastic method and implemented it in a finite element program to simulate the development of pavement rutting.

Previous studies focusing on the continuum response of asphalt materials cannot be used to describe the micromechanical behaviour between aggregate and binder. The primary deficiency of them is the inability to model particle contact and stress transmission through the aggregate skeleton. Research studies have been conducted to investigate the micromechanical behaviour of particulate, porous and heterogeneous materials. For example, studies on cemented particulate materials by Dvorkin et al. (1994) and Zhu et al. (1996a; 1996b) provided information on the load transfer between particles which are cemented together. Such mechanics provide details on the normal and tangential interparticle load transfer, and would be fundamental in developing a micromechanical theory for load distribution and failure of such materials. Some contact-based analysis of asphalt performance has recently been reported by Zhu (1998). Zhu and Nodes (2000) used the contact-based mechanism to analyse the behaviour of asphalt pavement with the effect of aggregate angularity. In the study, the contact mechanism is defined such that the execution of load/force transmission is mainly characterised by the contact-based force-displacement interaction of particles adjacent to each other. The general stress-strain relations are derived by the contact method with the assumption of round aggregates, and asphalt pavement is considered as an aggregate assembly coated by asphalt mortar.

2.5 SUMMARY

The literature review indicated that SMA mixtures consist of a large coarse aggregate content (approximately 70 percent), fine aggregate, high filler content, and asphalt cement with or without a modifier and usually a cellulose or mineral fibre. The strength of this mix is gained from stone-to-stone contact. It is designed to have 3-4 percent air voids, and has relatively high asphalt content due to the high

amount of voids in the mineral aggregate. It contains a high filler content (approximately 10 percent passing the 0.075 mm sieve), and typically contains a polymer in the asphalt cement or fibre (cellulose or mineral) in the mixture to minimise drainage of the asphalt cement.

However, most SMA design procedures still base their mix design on empirical procedures. As in most mixture designs, there is little or no mixture performance analysis involved during the design procedure, especially the analysis of coarse aggregate stone-to-stone contact. Several researchers have realised the importance of increasing coarse aggregate, yet no well-accepted design procedure that established the appropriate volume of coarse aggregate exists. They conducted limited laboratory performance tests on mixtures they studied and the results varied. This is because aggregates were combined on a weight basis in their studies of SMA. However, this method is rather limited as combining aggregates by weight cannot evaluate the degree of aggregate interlock because of differing specific gravities of fine and coarse aggregates, including mineral fillers. On the other hand, no procedure is outlined to provide an understanding on the interaction of aggregate blending and the resulting SMA mixture volumetrics. This selection of the blend of aggregates requires that local experience dictates the appropriate design. If local experience is not available, trial and error process must be used to develop an appropriate mixture. This trial and error process can be time consuming and costly, therefore, improvements in the understanding on the combination of aggregates by volume and the resulting mixture would provide a considerable improvement in the design of SMA mixture.

The particle packing concepts provide an adequate background for the continued study of aggregate gradations and aggregate stone-to-stone contact in SMA mixtures. The results of sphere packing studies can be used to be an appropriate

estimate for the geometric relations of the packing of granular materials. Further, a particle diameter ratio of 0.22 would appear to be an appropriate break-point value to study the gradation of asphalt concrete. This particle diameter ratio is considered to be the most appropriate value based on the current state-of-the-art for the examination of aggregate gradation in HMA mixture.

In essence, SMA has proven to be superior to dense-graded HMA in terms of rutting resistance. Its rutting performance is influenced by many factors, especially aggregate gradation and volumetric properties. However, little work had been done to correlate rutting resistance tests to SMA performance. Several researchers have pointed out that the repeated load axial tests and wheel-tracking tests can be used to evaluate rutting performance of SMA mixtures.

Although many researchers proposed many models to simulate asphalt mixtures and significant progress has been made in characterising the visco-elastic properties of asphalt binders, none had conducted studies on the numerical analyses of SMA mixture to describe the influence of aggregate size (gradation), shape, angularity, and surface texture on the performance of SMA mixtures.

CHAPTER THREE

RESEARCH METHODOLOGY

From Chapter 2, SMA mixtures have traditionally been designed using a trial and error procedure to select the aggregate gradation. No mix design methods were available on the design of aggregate structure, especially stone-to-stone contact in SMA mixtures. This chapter provides a methodology to develop a new procedure which helps to quantify coarse aggregate stone-to-stone contact in SMA and leads to an improved SMA mixture design and performance. Figure 3.1 shows a schematic of the whole research methodology.

Firstly, aggregate packing concepts as described in Chapter 2 were used to design and to quantify aggregate stone-to-stone contact in SMA mixtures. The presented mix design concepts are based on the following principles:

(1) The stability and rutting resistance of SMA mixture is best derived from coarse aggregate stone-to-stone contact and proper aggregate packing;

(2) The durability of SMA mixture is best attained with proper mixture design in relation to the volumetric, including air voids, voids in the mineral aggregate

(VMA), asphalt film thickness and mineral filler proportion.

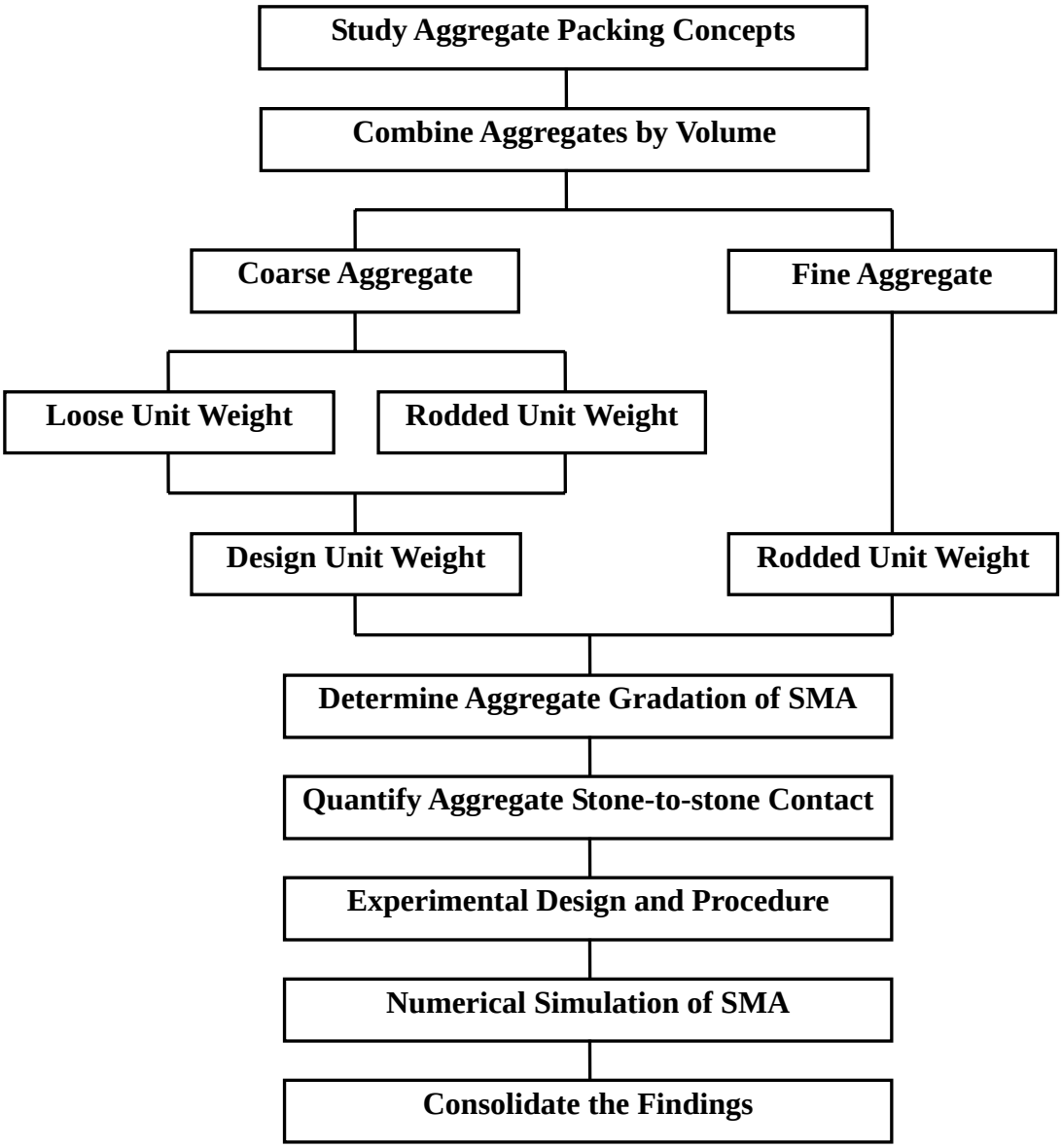

Figure 3.1 Overview of the Research Methodology

Secondly, based on the method to quantify aggregate stone-to-stone contact, experimental design and procedure were conducted. Work was performed to

evaluate the effect of various aggregate combinations on the stone-to-stone contact of SMA. Mixtures were also prepared and tested in the laboratory to evaluate the effect of various aggregate packing on the volumetric and mechanical properties of SMA.

Finally, in order to expand the results from fundamental mixture characterisation and to predict SMA performance, a two dimensional finite element analysis procedure to analyse the permanent deformation potential of SMA was developed.

3.1 COMBINATION OF AGGREGATES

The primary components in asphalt mixtures are typically defined as coarse aggregate, fine aggregate, mineral filler, and asphalt binder. These aggregate components are combined to provide an aggregate skeleton that will resist permanent deformation and cracking. It is necessary to examine the packing of aggregates and the characteristics of the components in order to understand their behaviour as a mixture and to generalise on their performance properties.

Coarse aggregate is considered the primary deformation resisting component in an asphalt mixture. The coarse aggregate particles, through their interlock, provide a path for the applied pavement stresses to be carried within the mixtures and transmitted to the lower pavement layers. The aggregate interlock also provides a stone-to-stone skeleton that resists deformation. Therefore, it is necessary to characterise and quantify this interlock to determine the load carrying capacity provided by the mixture. By understanding the load carrying capacity needed for the pavement application during design, it is possible to properly design mixtures to satisfy the requirements of the pavement. In order to quantify the amount of coarse

aggregate interlock in a mixture, an investigation of coarse aggregate packing is necessary.

Fine aggregate completes the aggregate structure by creating a supporting structure for the void spaces in the coarse aggregate. Without the inclusion of this fine aggregate, the mixture would remain open with a high percentage of voids, thus, resulting in high rutting and permeability. Fine aggregate is viewed as a filler material for the voids in the coarse aggregate. It is desired that this fine aggregate be in a compacted state, which reduces the amount of permanent deformation due to shear flow in this fraction of the aggregate blend. With the densification, and deformation of the fine aggregate minimised, it becomes possible for the coarse aggregate to carry the bulk of the applied load.

Mineral filler is used in the aggregate blend for several purposes. One purpose is to develop mastic. The properties of the mastic contribute to the properties of the mixture, especially as it relates to mixture stiffness and low temperature performance. From an aggregate combination perspective, mineral filler is used to fill the voids in the mixture that are created by the fine aggregate. It is much more important for SMA mixtures which have a high percentage of coarse aggregate.

Conventionally, aggregate is combined on a weight basis; however, this method is rather limited as combining aggregates by weight cannot evaluate the degree of aggregate interlock because of differing specific gravities of fine and coarse aggregates, including mineral fillers. Therefore, there is a need to combine aggregates by volume to determine coarse aggregate interlock or stone-to-stone contact in SMA mixtures more objectively.

Consider the case of filling a unit volume with aggregate. If the primary component

is to comprise coarse aggregates in this unit volume and to provide coarse aggregate interlock, the appropriate amount of coarse aggregates must be determined between a minimum and maximum value. To ensure aggregate interlock, the minimum volume of coarse aggregate that can be placed into the mixture is the amount to fill the unit volume with the coarse aggregate in its loosest state. This amount of coarse aggregate will provide a considerable amount of void space, which must be filled by the fine aggregate. The maximum volume of coarse aggregate that can be added to the unit volume is the amount to fill the unit volume with the coarse aggregate in a compacted state under a specified compactive effort. Asphalt mixtures with coarse aggregate volumes between the loose state and the compacted state would be considered to have a degree of aggregate interlock/stone-to-stone contact relative to this proportion of coarse aggregate and be considered to possess interlock resistance against deformation.

Upon establishing the coarse aggregate volume, which is determined as a percentage of the unit volume and selected as a unit weight of coarse aggregate desired in the mix, it becomes necessary to determine the relative percentages of the other aggregates. The amount of fine aggregate and the amount of mineral filler must be determined so that the voids established by the coarse aggregate are filled with the appropriate volume of filler aggregate and the proper mastic properties are achieved.

3.2 BREAK POINT SIEVE TO DISTINGUISH COARSE AND FINE AGGREGATES

In order to develop a method for combining aggregates to optimise the aggregate interlock and to provide the proper volumetric properties, it is necessary to

understand some of the controlling factors that affect the design and performance of these mixtures. The explanation of coarse and fine aggregates given in Section 3.1 has provided a background for the understanding on the combination of aggregates. Since coarse and fine aggregates must reflect their relevance in combining aggregates by volume to attain the coarse aggregate stone-to-stone contact, there is a need to incorporate two broad concepts:

(1) Develop a more fundamental definition to distinguish between coarse and fine aggregates; and

(2) Combine aggregates by volume to ensure coarse aggregate interlock or stone-to-stone contact.

Generally, coarse aggregate is the larger size particles typically greater than the 4.75 mm sieve size material. Fine aggregate is any aggregate that is less than the 4.75 mm sieve size material. For the purpose of this study, it is necessary to change these definitions in order to properly analyse a mixture gradation and determine the packing and aggregate interlock provided by the combination of all aggregates in the mixture. Thus, coarse aggregate can be seen as large aggregate particles creating voids when placed in a unit volume. Fine aggregate is aggregate particles that fill the voids created by the coarse aggregate. They can be distinguished by a break point sieve (BPS), which is the sieve size distinguishing coarse aggregate from fine aggregate. This break point sieve is important because it establishes what portion of the aggregate constitutes the coarse aggregate skeleton. SMA mixtures are gap-graded and the BPS is simply a point where the gap begins. Thus, ‘coarse aggregate’ in SMA mixtures can be considered as a relative term depending upon the nominal maximum aggregate size (NMAS is defined as the sieve immediately larger than the first sieve to retain at least ten percent of the material) and the selected BPS. The BPS is defined as the closest size sieve to the nominal maximum sieve size in millimetres multiplied by a particle diameter ratio.

Bourbie et al. (1987) and Reed (1988) reported that the diameter ratio is given as: $\frac{\text{Particle Fitting in Void}}{\text{Large Particle Creating Void}}$. It can be calculated from a two- and three-dimensional analysis on the packing of different shaped particles resulting from combining two sizes (binary packing) of spheres. The two-dimensional analysis of aggregate shape is the four combinations of geometry based on the following dimensional relationships:

(1) All round faced particles, shown in Figure 3.2, produces a ratio of 0.16;

(2) Two round faces, one flat face, shown in Figure 3.3, produces a ratio of 0.20;

(3) One round face, 2 flat faces, shown in Figure 3.4, produces a ratio of 0.24; and

(4) All flat faced particles, shown in Figure 3.5, produces a ratio of 0.29.

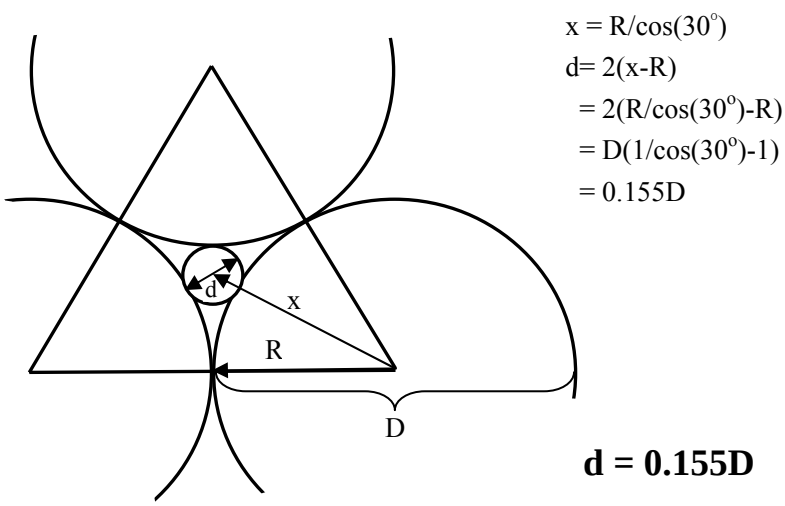

Figure 3.2 Two-Dimensional Packing of All Round Particles

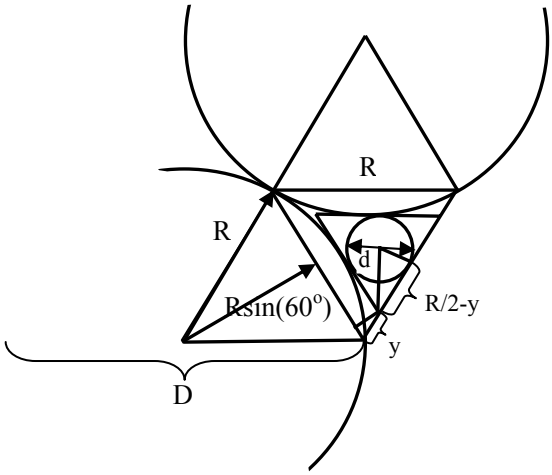

$y = (R-R\sin(60^o)/\sin(60^o)$
$= R(1/\sin(60^o)-1)$
$d = 2\tan(30^o)(R/2-y)$
$= 2R\tan(30^o)(1/2-1/\sin(60^o)+1)$
$= 0.199D$

d= 0.199D

Figure 3.3 Two-Dimensional Packing of 2- Round and 1-Flat Particles

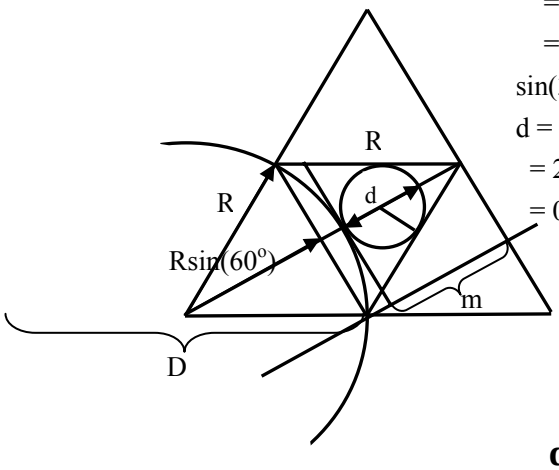

$m = R\sin(60^o)-(R-R\sin(60^o))$
$= 2R(\sin(60^o)-1/2)$
$= D(\sin(60^o)-1/2)$
$\sin(30^o) = (d/2)/(m-d/2)$
$d = 2m\sin(30^o)/(1+\sin30^o)$
$= 2D(\sin(60^o)-1/2)\sin(30^o)/(1+\sin30^o)$
$= 0.244D$

d = 0.244D

Figure 3.4 Two-Dimensional Packing of 1-Round and 2-Flat Particles

d' = Diameter of Packed Particle in condition (4)
d = Diameter of packed Particle in condition (1)

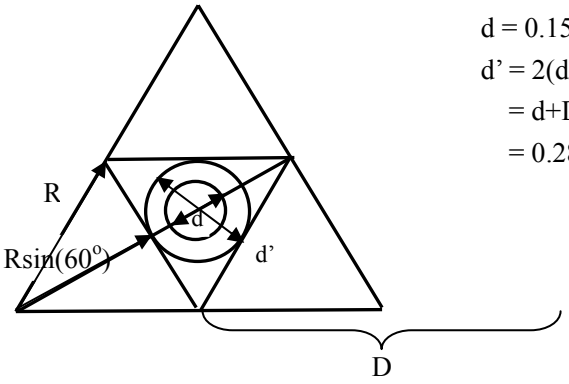

$d = 0.155D$

$d' = 2(d/2+(R-R\sin(60^o)))$
$= d+D(1-\sin(60^o))$
$= 0.289D$

$d' = 0.289D$

Figure 3.5 Two-Dimensional Packing of All Flat Particles

A 0.22 size ratio is the average of these four different combinations of two-dimensional particle, and appears to best represent the average condition. While the actual size ratio would vary depending on the particles included in the mixture, an average value is certainly typical and would seem to be applicable to particle arrangements of randomly shaped particles found in an asphalt mixture (Vavrik et al., 2002).

The diameter ratio from three-dimensional analysis has been described in Chapter 2. It has been determined that the characteristic diameter of the void in a packed system would be in the range from 0.15, from the tetrahedral packing of spheres, to 0.42, from the cubical packing of spheres (Bourbie et al., 1987; Reed, 1988; and Mavko et al., 1998). Since the packing of the aggregates is desired to be between cubical and tetrahedral, yet more similar to the tetrahedral packing, which can provide the more stable configuration, the 0.22 particle size ratio is reasonable for

use in three-dimensional particles too.

Literature has shown that the 0.22 size ratio that was presented in a two-dimensional analysis is also validated through the use of a three-dimensional analysis. Therefore, it can be seen that the 0.22 particle diameter ratio is most commonly used as the characteristic size.

The gradation for asphalt mixtures has been standardised in Singapore through the use of a standard set of sieves. These sieves are 37.5 mm, 25 mm, 19 mm, 14 mm, 9.5 mm, 6.3 mm, 3.35 mm, 2.36 mm, 1.18 mm, 0.6 mm, 0.3 mm, 0.15 mm, and 0.075 mm. Application of the particle diameter ratio to the standard set of sieves gives the break point sieve (BPS). It can be obtained from the result of the BPS formula given in Equation 3.1:

$$BPS = NMAS \times 0.22 \quad (3.1)$$

The complete list of standard sieve sizes for asphalt mixtures and the corresponding BPS size is given in Table 3.1. There is a standard sieve size matching each BPS reasonably well, therefore the standard set of sieves is adequate in analysing an asphalt gradation using the 0.22 size ratio.

As the true particle diameter ratio will change in every mixture, an analysis was performed to determine if an adjusted ratio would change the BPS when using the standard set of aggregate sieves. The results indicated that ratios in the range from 0.18 to 0.25 would give the same BPS as the 0.22 size ratio for the standard set of sieves.

For the purpose of SMA mixture design, the 0.22 relationship would adequately define the size difference between coarse aggregate and fine aggregate with

sufficient accuracy applicable to current sieve sizes. On average, it can be expected that a particle with a characteristic dimension of 0.22 will fill the void created by the larger particle. This fine aggregate particle with 0.22 or less dimension is then referred as filler aggregate, as it serves to fill the created voids.

Table 3.1 Standard Sieve Sizes and Their Associated Break Point Sieves

Particle Size (mm)	Particle Size × 0.22 (mm)	Break Point Sieve (mm)
37.5	8.25	9.5
25	5.5	6.3
19	4.18	3.35
14	3.08	3.35
9.5	2.09	2.36
6.3	1.39	1.18
3.35	0.74	0.6
2.36	0.52	0.6
1.18	0.26	0.3
0.6	0.13	0.15
0.3	0.07	0.075

3.3 COMBINATION BY VOLUME

In order to accomplish the volumetric combination of aggregates, additional information must be gathered. In this study, the aggregate volumes will be expressed as unit weights. It is easier for mix designers and quality control personnel to understand the change in the unit weight of aggregate than to understand the change in aggregate volume. Therefore, for each of the coarse aggregates the loose and rodded unit weights must be determined, and for the fine

aggregate the rodded unit weight is necessary. These measurements provide the volumetric data at the specific void structure required to evaluate interlock properties.

3.3.1 Loose Unit Weight of Coarse Aggregate

The loose unit weight of coarse aggregate is determined using procedures similar to the Uncompacted Void Content of Fine Aggregate Test Apparatus (UVCATA) (ASTM C1252, 1998). A modification to this procedure will be used for this experiment. This apparatus and its modified apparatus are as described in Chapter 4. This test deposits a representative sample of the whole coarse aggregates in a standard dimension bucket from a standard fall, resulting in the packing of the aggregates in a standard loose condition in the bucket. By knowing the volume of the bucket, the weight of aggregates deposited from a standard fall, and the coarse aggregate bulk specific gravity, the volume of voids in the coarse aggregate can be determined. This volume of voids is the volume present when the particles come into contact without any compactive effort being applied.

3.3.2 Rodded Unit Weight of Coarse Aggregate

The rodded unit weight of coarse aggregate is determined using the same apparatus as in the determination of loose unit weight of coarse aggregate test. This allows for direct comparison of the results with the loose unit weight test.

The rodded unit weight is determined by dropping the complete gradation of coarse aggregate into the bucket in three equal lifts applying 25 rods of compaction with a 16 mm diameter steel rod per lift. The rodded unit weight is combined with the

volume of the bucket and the bulk specific gravity of the aggregate to determine the volume of voids of the coarse aggregate when the particles have undergone compaction and consolidation.

3.3.3 Design Unit Weight of Coarse Aggregate

The design unit weight of the coarse aggregate sets the level of coarse aggregate interlock that will result in the aggregate blend by fixing the volume of coarse aggregate in the mixture. The design unit weight is selected by the mix designer and under the proposed method is typically chosen to be near to the loose unit weight because the loose unit weight is considered to be the lower limit of coarse aggregate interlock. The rodded unit weight is considered to be the upper limit of coarse aggregate interlock. The design unit weight can be less than the loose unit weight for a mixture. But as the design unit weight is lowered beyond the loose unit weight, theoretically, the mixture has no coarse aggregate interlock. However, it has been found that the densest gradation that can exist is when the design unit weight approximately falls 5% below the loose unit weight of coarse aggregate (Vavrik et al., 2002). The densest condition could change if the testing methods for determining the loose and rodded unit weights were modified. With the design unit weight increased close to the rodded unit weight, the amount of compactive effort required for densification would increase. For SMA mixture, to ensure stone-to-stone skeleton, the design unit weight is typically chosen to be near to the rodded unit weight and expressed as a percentage of the rodded unit weight under the proposed method. Figure 3.6 shows a schematic diagram on the design unit weight.

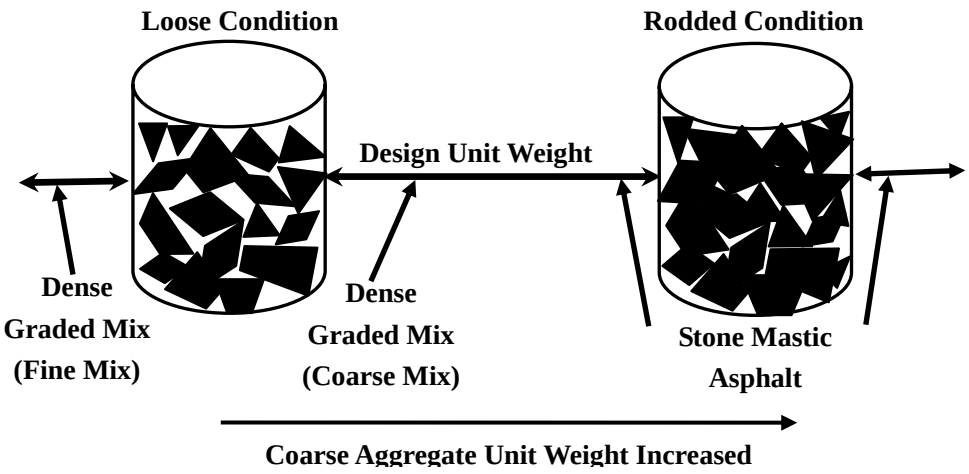

Figure 3.6 Design Unit Weight (Vavrik et al., 2002)

Upon selection of the appropriate design unit weight, it is necessary to fill the voids created by the coarse aggregate. These voids are filled with the appropriate volume of fine aggregate in its compacted state.

3.3.4 Rodded Unit Weight of Fine Aggregate

Selecting the amount of fine aggregate used to fill the voids created by the coarse aggregate is carried out with fine aggregate in a state of dry compaction. With the fine aggregate in a compacted state, the densification of the mixture due to further compaction of fine aggregate is minimised. The fine aggregate in a compacted state reduces the amount of permanent deformation due to shear flow in this fraction of the aggregate blend. This state of dry compaction is the rodded unit weight of the fine aggregate.

The rodded unit weight of fine aggregate is determined by dropping a representative sample of the whole aggregate into the standard bucket in three equal lifts with 25 rods per lift, using a 16 mm diameter steel rod. The rodded unit weight, when combined with the volume of the bucket and the bulk specific gravity of the fine aggregate, are used to determine the volume of voids of the fine aggregate when the particles have undergone compaction and consolidation.

3.4 DESIGN PROCEDURES FOR AGGREGATE STONE-TO-STONE CONTACT

Based on the analysis of aggregate packing and aggregate combination, the proposed procedure for the blending of aggregates to achieve a gradation to quantify aggregate stone-to-stone contact is as follows:

(1) Determine the loose and rodded unit weight of coarse aggregate;
(2) Determine the rodded unit weight of fine aggregate;
(3) Select the design unit weight of coarse aggregate;
(4) Fill the remaining void space created by the coarse aggregate with the rodded unit weight of fine aggregate; and
(5) Include the appropriate amount of mineral filler for proper mastic properties and mixture volumetric.

The procedure outlined above provides the direct ability to proportion aggregates to achieve varying degrees of aggregate stone-to-stone contact using measurable properties of the individual aggregates used in the mixture.

3.5 RATIOS FOR CONTROLLING AGGREGATE GRADATION

The combined gradation of an asphalt mixture can be analysed using the concepts of particle packing. The use of particle packing involves applying the appropriate particle diameter ratio (0.22) to the gradation to illustrate the void relationships that result from the filling of voids with different size particles. Studying the filling of voids with the appropriate amount and size of filler material will illustrate the resulting void structure in the combined mixture. The understanding of aggregate blending will lead to improvements to the design of SMA mixtures.

In this study, the combined blend is broken down into three distinct portions, and each portion is evaluated individually. The coarse portion of the combined blend is from the largest particle to the BPS. These particles are considered the coarse aggregates of the blend. The fine aggregate is broken down and evaluated as two portions. To determine where to split the fine aggregate, the same 0.22 diameter ratio used on the entire gradation is applied to the BPS to determine a secondary break point sieve (SPS). The SPS then becomes the break between coarse sand and fine sand. The fine sand is further evaluated by determining the tertiary break point sieve (TPS), which is determined by multiplying the SPS by the 0.22 size ratio. A schematic on how the gradation is divided into the three portions is given in Figure 3.7.

An analysis is done using ratios that evaluate packing within each of the three portions of the combined aggregate gradation. Three ratios are defined: Coarse Aggregate Ratio (CA Ratio), Fine Aggregate Coarse Ratio (FA_c Ratio), and Fine Aggregate Fine Ratio (FA_f Ratio). These ratios characterise packing of the

aggregates. By changing gradation within each portion, modifications can be made to the volumetric properties or performance characteristics of the asphalt mixture.

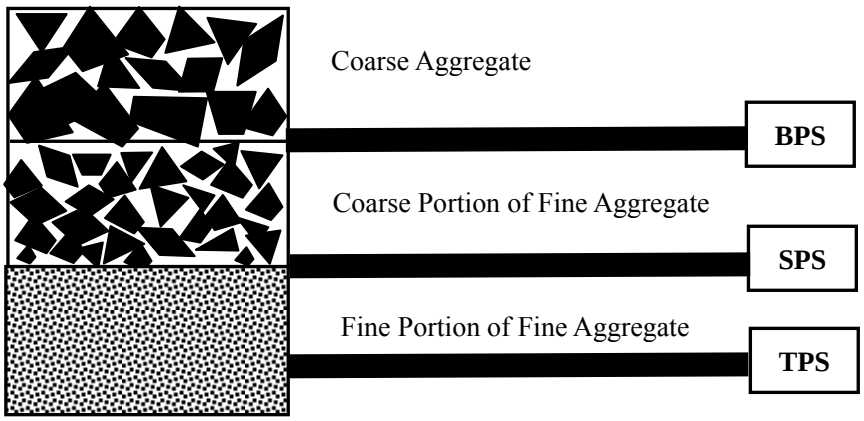

Figure 3.7 Schematic Plot of Ratios for Controlling Gradation

3.5.1 CA Ratio

The CA Ratio is used to evaluate packing of the coarse portion of the aggregate gradation and to analyse the resulting void structure and performance. Understanding the packing of coarse aggregate requires the introduction of the half sieve. The half sieve is defined as one half of the NMAS. Particles smaller than the half sieve are called “interceptors”. Interceptors are too large to fit in the voids created by the larger coarse aggregate particles and hence spread them apart. The balance of these particles can be used to adjust the mixture’s volumetric properties. By changing the quantity of interceptors, it is possible to change the VMA in the mixture to produce a balanced coarse aggregate structure. With a balanced aggregate structure, the mixture should be easy to compact in the field and should adequately perform under load.

The calculation of the CA ratio is given in Equation 3.2:

$$\text{CA Ratio} = \frac{\%\text{Passing Half Sieve} - \%\text{Passing BPS}}{100\% - \%\text{Passing Half Sieve}} \qquad (3.2)$$

3.5.2 FA_c Ratio

All of the fine aggregates (i.e., below the BPS) can be viewed as a blend by itself that contains a coarse and a fine portion and can be evaluated in a manner similar to the overall blend. The coarse portion of the fine aggregate creates voids that will be filled with the fine portion of the fine aggregate. As with the coarse aggregate, it is desired to fill these voids with the appropriate volume of the fine portion of the fine aggregate without overfilling the voids.

The calculation of the FA_c Ratio is given in Equation 3.3:

$$FA_c \text{ Ratio} = \frac{\%\text{Passing SPS}}{\%\text{Passing BPS}} \qquad (3.3)$$

3.5.3 FA_f Ratio

The fine portion of the fine aggregate fills the voids created by the coarse portion of the fine aggregate. This ratio shows how the fine portion of the fine aggregate packs together. One more sieve is needed to calculate the FA_f, the TPS. The TPS is defined as the closest sieve to 0.22 times the SPS. The FA_f Ratio is given in Equation 3.4:

$$FA_f \text{ Ratio} = \frac{\%\text{Passing TPS}}{\%\text{Passing SPS}} \qquad (3.4)$$

A complete listing of the sieve sizes and calculations for the CA Ratio, FA_c Ratio, and FA_f Ratio are given in Table 3.2. This table is given in an effort to clarify the previously presented information on ratios for the evaluation of aggregate gradation.

Table 3.2 Summary of Ratios for Controlling Aggregate Gradation

NMAS	37.5 mm	25 mm	19 mm	14 mm	9.5 mm	6.3 mm
BPS	9.5 mm	6.3 mm	3.35 mm	3.35 mm	2.36 mm	1.18 mm
Half Sieve	19 mm	14 mm	9.5 mm	6.3 mm	6.3 mm	3.35 mm
CA Ratio	$\frac{19-9.5}{100\%-19}$	$\frac{14-6.3}{100\%-14}$	$\frac{9.5-3.35}{100\%-9.5}$	$\frac{6.3-3.35}{100\%-6.3}$	$\frac{19-9.5}{100\%-19}$	$\frac{3.35-1.18}{100\%-3.35}$
SPS	2.36 mm	1.18 mm	0.6 mm	0.6 mm	0.6 mm	0.3 mm
FA_c	$\frac{2.36}{9.5}$	$\frac{1.18}{6.3}$	$\frac{0.6}{3.35}$	$\frac{0.6}{3.35}$	$\frac{0.6}{2.36}$	$\frac{0.3}{1.18}$
TPS	0.6 mm	0.3 mm	0.15 mm	0.15 mm	0.15 mm	0.075 mm
FA_f	$\frac{0.6}{2.36}$	$\frac{0.3}{1.18}$	$\frac{0.15}{0.6}$	$\frac{0.15}{0.6}$	$\frac{0.15}{0.6}$	$\frac{0.075}{0.3}$

3.6 EXPERIMENTAL DESIGN AND PROCEDURES

The overall purpose of experimental design and procedures is to gather objective details on how the physical properties of SMA mixtures is related to aggregate stone-to-stone contact; thus, developing a new procedure and leading to an improved SMA mixture design and performance. The details are discussed in Chapter 4.

3.7 NUMERICAL SIMULATION OF SMA

Numerical simulation is used to expand the results on the physical properties of SMA mixtures. It presents a micromechanical model on SMA mixtures that gives a simple analytical constitutive relation in terms of measurable mix parameters like the volume fractions of coarse aggregate and coarse aggregate size, shape, and angularity. The details are discussed in Chapter 6.

3.8 SUMMARY

The concepts given in this chapter provided an outline for a design procedure that will ensure coarse aggregate interlock through measurable properties of the individual component aggregates. The establishment of this interlock is expected to provide coarse aggregate stone-to-stone contact, thus, contributing to high deformation resistance and desired volumetrics.

Ratios for controlling aggregate gradation will help to provide insight into the packing of the aggregate structure. These ratios include: CA Ratio, FA_c Ratio, and FA_f Ratio. The control of aggregate packing should provide the ability to specify the mixture properties and eliminate the trial and error process normally used in the determination of aggregate gradation.

The concepts discussed will provide a valuable tool in the evaluation of aggregate stone-to-stone contact in SMA mixture. With knowledge of the actual aggregate components, one can determine the degree of aggregate stone-to-stone contact of the SMA mixture, thus, leading to a more fundamental understanding of SMA mixture performance.

CHAPTER FOUR

EXPERIMENTAL DESIGN AND PROCEDURES

This chapter describes the method and procedures applied in this study. Section 4.1 presents the experimental testing plan of the study. Section 4.2 describes the selection of aggregates and characterises the aggregate testing used in this study. The first part of Section 4.3 describes the development of SMA mixture design. The mixture performance test procedures are then introduced. Section 4.4 describes the equipment and test methods used to conduct the laboratory tests.

4.1 EXPERIMENTAL TESTING PLAN

The new procedure to design and evaluate aggregates provides the basis for an improved design method for SMA mixture. Blending aggregates by volume provides a methodology of quantifying coarse aggregate stone-to-stone contact in SMA with different aggregate packing. In order to validate these concepts leading to an improved SMA mixture design and performance, a testing plan that examines

aggregate gradations and the combination of aggregates was conceptualised and conducted. It can be divided into three stages. The first stage involved preliminary aggregate testing to understand the change in the aggregate packing properties with changes in aggregate gradation and provided the information necessary to develop aggregate blending in SMA mixtures. The second stage involved the design of the SMA mixtures based on the developed procedure of aggregate blending. While the third stage involved the actual testing of the SMA mixtures prepared in the second stage. Figure 4.1 shows a schematic representation of the overall test plan.

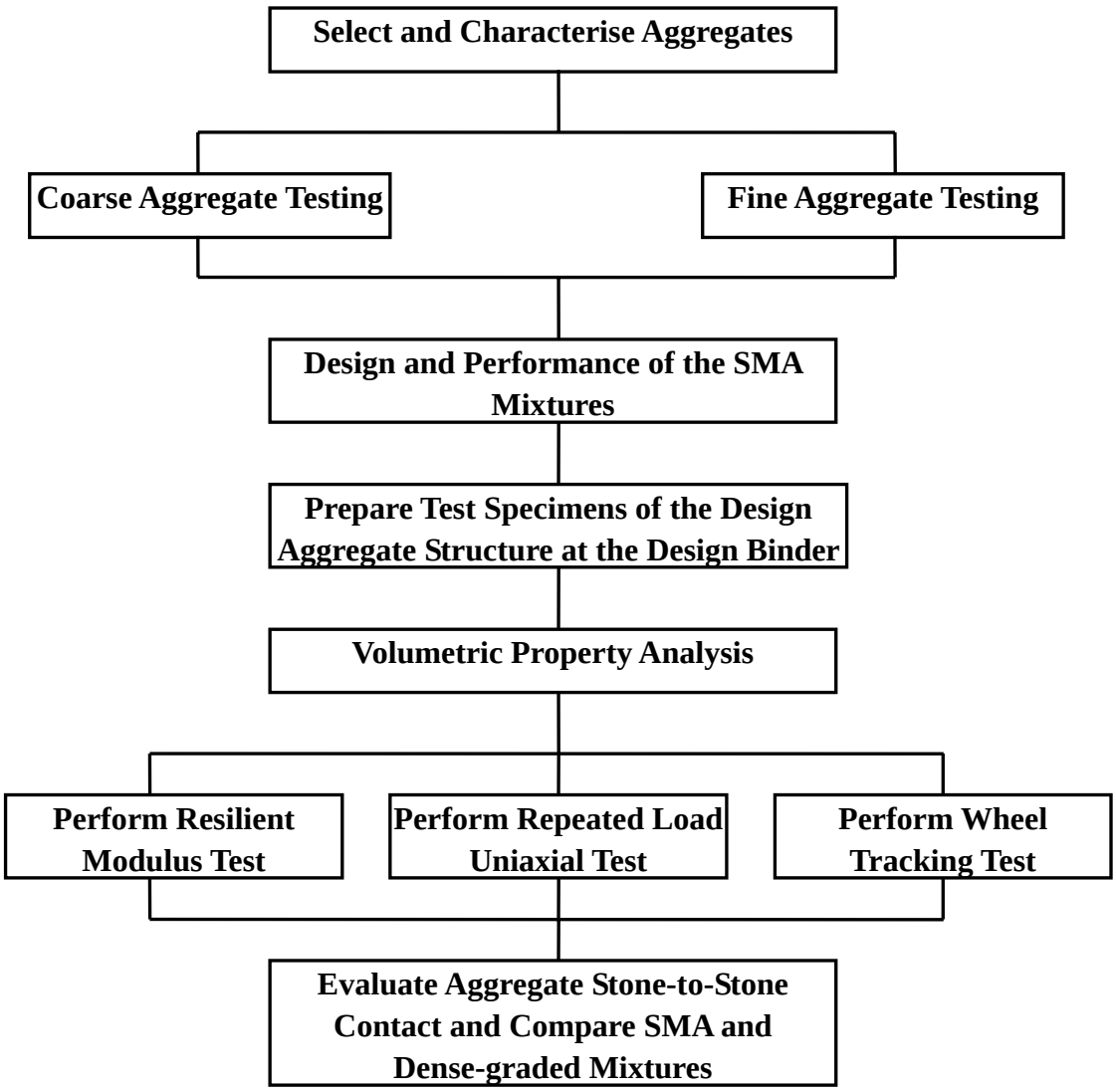

Figure 4.1 Overall Test Plan

4.2 AGGREGATE TESTING

Aggregate testing was performed using the modified Uncompacted Void Content of Fine Aggregate Test Apparatus (UVCATA) as described in Section 4.4.1. Coarse and fine aggregates were tested to illustrate the effect of combined gradation of aggregate materials. All aggregate testing was performed on aggregates with precisely controlled gradations for coarse and fine aggregates. The gradations were varied from the lower to the upper limit allowed by the appropriate specification in Singapore.

Typical aggregate used for Singapore roads is the crushed granite aggregate of 14 mm nominal maximum size, therefore, the break point sieve (BPS) as determined according to Equation 3.1 was 3.08 mm. As there is no such a sieve size, the closest 3.35 mm sieve size was chosen as the BPS to differentiate between coarse and fine aggregates (See Table 3.1). Three target aggregate gradations for coarse and fine aggregates were designed. These target gradations were chosen as the upper limit, medium limit, and lower limit of the specification in Singapore and are given in Tables 4.1 and 4.2, respectively. The mineral filler content is kept constant at 10% for all aggregate gradation designs as discussed in Chapter 2.

Table 4.1 Aggregate Test Gradations for Coarse Aggregate

Sieve (mm)	Percent Passing (%)		
	Upper	Medium	Lower
14	80	90	100
9.5	55	70	85
6.3	20	30	40
3.35	0	3.5	7

Table 4.2 Aggregate Test Gradations for Fine Aggregate

Sieve (mm)	Percent Passing (%)		
	Upper	Medium	Lower
3.35	100	100	100
2.36	66	75	83
1.18	58	58	58
0.6	33	37	41
0.3	20	24	28
0.075	0	0	0

These aggregate gradations were then evaluated in the modified UVCATA. The modified tests performed included the uncompacted voids, voids with 10 rods compaction, and voids with 25 rods compaction (similar to unit weight). The results from this testing are discussed in Chapter 5.

4.3 SMA MIXTURE DESIGN AND PERFORMANCE

With the selection and testing of the individual dry coarse and fine aggregate components completed, the aggregates were combined in precise percentages to produce SMA mixtures which should exhibit controlled levels of coarse aggregate stone-to-stone contact. These combinations were tested to relate the compaction characteristics, mixture volumetric, and mechanical properties with changes in the coarse and fine aggregate gradations, the corresponding aggregate ratios, and asphalt binder contents. Mechanical property testing of these mixtures was performed to evaluate the performance properties of the mixtures.

4.3.1 Mixture Design Procedures

Mixture design is an experimental procedure that determines the optimum aggregate gradation and asphalt binder content for a given compaction effort. Although no standard procedure for the design of SMA mixture can be found, there existed some key procedural steps from literature review. For instance, five basic steps for the mixture design method are illustrated in Figure 4.2, which shows the method involves the selection of materials, design of the aggregate structure, design of the binder content, asphalt binder draindown potential evaluation, and a moisture susceptibility evaluation. Since the main objective of this study is to provide a methodology of quantifying coarse aggregate stone-to-stone contact in SMA with different aggregate packing to develop a new procedure and leading to an improved SMA mixture design and performance, the moisture susceptibility evaluation will not be studied.

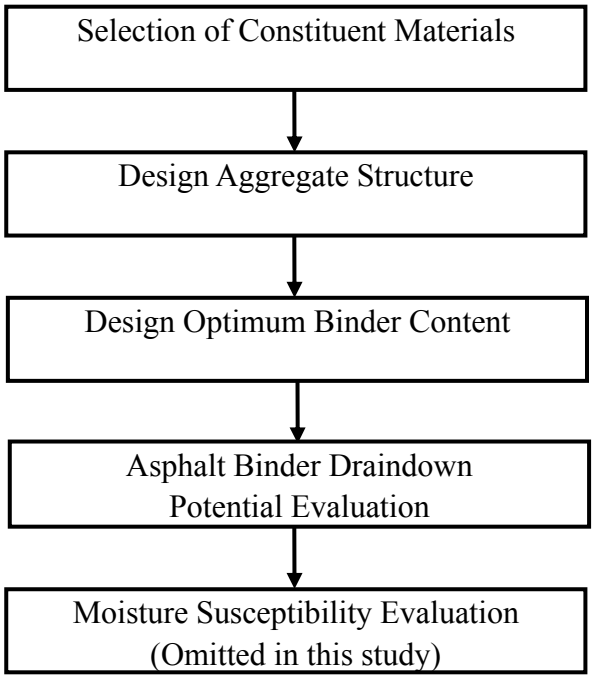

Figure 4.2 Basic Procedural Steps for SMA Mixture Design

Selection of Constituent Materials

SMA composes of coarse and fine aggregates, asphalt binder, mineral filler, and stabilising additive. The asphalt binder is selected based on the climate and traffic loading for Singapore conditions. As SMA contains about 70% of coarse aggregate and about 5-8% by weight of binder, it is susceptible to binder draindown when batched with conventional bitumen. However, one can either use conventional bitumen with cellulose fibres added or polymer modified binders (PMB) to prevent binder drainage. In this experimental design, it was the intent to study SMA batched with PMB and thus, only PMB was used in the experimental design. Both coarse and fine aggregates used in SMA must be crushed and conform to the quality requirements. Filler must consist of finely divided mineral matter such as crusher fines, lime or fly ash. In this experimental design, Indonesian granite aggregates were used. The pertinent material properties and specification requirements for each of these are given in Tables 4.3 and 4.4, respectively.

Design Aggregate Structure

The selection of a design aggregate structure is one of the major features of SMA mixture design method. The procedures for the blended aggregates outlined in the methodology as described in Chapter 3 would provide a direct ability to proportion aggregates by volume to achieve varying degrees of aggregate packing.

Table 4.3 Aggregate Properties of Indonesian Granite

Properties	Method of Testing	Indonesian Granite	Allowable Standard	Status
Bulk Specific Gravity	--	2.63	--	
L.A. Abrasion	ASTM:1985	24%	25%	OK
10% Fines Value	SS73:1974	167 kN	>130 kN (NZ)	OK
Polished Stone Value	BS 812:1990	55	> 45 (DOT, 1976)	OK
Aggregate Crushing Value	SS73:1974	11%	< 25%	OK
Aggregate Impact Value	SS73:1974	12%	< 25%	OK

Table 4.4 Polymer Modified Bitumen Properties

Test	PMB (Cariphalte)	Test Method
Penetration at 25 °C (0.1 mm)	> 50	ASTM D5-86
Softening Point (Ring & Ball Temperature)	> 80 °C	ASTM D36-86
Brookfield Viscosity, SR 9.30 (170 °C)	< 600	ASTM D789
Torsional Recovery	> 80	
SHRP Performance Grading	PG 82	
Polymer Content	6.0	
Specific Gravity at 25 °C	1.0 – 1.1	ASTM D70

The coarse aggregate was separated into individual standard sieve sizes and recombined to an upper, medium, and lower limit gradation as shown in Table 4.1. The fine aggregate was similarly assembled to an upper, medium, and lower limit gradation as shown in Table 4.2. For each combination of coarse and fine aggregate listed in Tables 4.1 and 4.2, the percentage of coarse and fine aggregates was varied to produce different levels of aggregate stone-to-stone contact and aggregate ratios that would result in changes in the volumetric properties and mechanical properties. The gradations, which were based on the principles outlined in Chapter 3, were developed by selecting the design unit weight to be at the following five levels:

- Rodded Unit Weight – 10% (90% RUW)
- Rodded Unit Weight – 5% (95% RUW)
- Rodded Unit Weight (100% RUW)
- Rodded Unit Weight + 5% (105% RUW)
- Rodded Unit Weight + 10% (110% RUW)

● Design Binder Content

As mentioned, once the design aggregate structure of the mixture has been determined, it may be necessary to increase the asphalt binder content to obtain the designed amount of air voids in the mixture. The design procedure begins with the compaction of specimens of the design aggregate structure. In this experimental design, three asphalt binder contents at 5.5%, 6.0% and 6.5% were evaluated for the mixtures according to the results studied by Toh (1998) and Lau (1999) at Nanyang Technologic University (NTU).

The optimum asphalt binder content is chosen to produce 3 to 4 percent air voids in the mixture (Bellin, 1997; Brown and Mallick, 1994). It is recommended that approximately 4 percent air voids should be the design criterion in warmer climates

and a value closer to 3 percent for colder climates.

Once the designed binder content has been established, mortar draindown potential is to be assessed according to the test procedure developed by the National Centre for Asphalt Technology and standardised by the American Society for Testing Materials given as Method D6390 (2001). Suggested SMA guidelines currently recommend a maximum draindown limit of 0.3 percent for SMA mixtures.

After SMA mixture design procedure, samples were combined using precise gradation control and different asphalt binder contents. The main task of this research is to study the effect of change in gradation of the coarse and fine aggregate portions of an aggregate blend while changing the volume of coarse and fine aggregates and the effect of change in asphalt binder content. There were four factors to be analysed in this study: coarse aggregate gradation (upper, medium, and lower), fine aggregate gradation (upper, medium, and lower), asphalt binder content (5.5%, 6.0%, and 6.5%), and design unit weight of coarse aggregate (90% RUW, 95% RUW, RUW, 105% RUW, and 110% RUW). Thus, a comprehensive experimental testing matrix using fractional factorial experimental method was developed. Table 4.5 gives the overall test matrix. Block 1 was chosen to evaluate the effect of different asphalt binder content. Blocks 2 and 3 were used to analyse the effect of different gradation of the coarse and fine aggregate portions of an aggregate blend. For Blocks 1, 2, and 3, there are five different design unit weights to evaluate aggregate stone-to-stone contact in SMA mixtures. Block 4 was chosen for the purpose of comparing SMA mixtures with dense-graded mixtures.

Table 4.5 Test Matrix for Experimental Design

Block		Coarse Aggregate Gradation	Fine Aggregate Gradation	Asphalt Binder Content	Design Unit Weight
1	1	Medium	Medium	5.5%	90% RUW 95% RUW RUW 105% RUW 110% RUW
	2	Medium	Medium	6.0%	
	3	Medium	Medium	6.5%	
2	1	Upper	Medium	5.5%	90% RUW 95% RUW RUW 105% RUW 110% RUW
	2	Medium	Medium	5.5%	
	3	Lower	Medium	5.5%	
3	1	Medium	Upper	5.5%	90% RUW 95% RUW RUW 105% RUW 110% RUW
	2	Medium	Medium	5.5%	
	3	Medium	Lower	5.5%	
4		Medium	Medium	5.5%	LUW 80% LUW
Note: Blocks 1.1, 2.2, and 3.2 are the same asphalt mixtures					

4.3.2 Preparation of Test Specimens

All mixture samples were carefully prepared to ensure precise gradation control. The individual aggregate samples were dried and then sieved into their component sizes by mechanical sieve machine. The aggregates were then sieved by hand for 1 minute to ensure proper size characterisation of the aggregate materials. These materials were combined to precisely controlled gradations. The percentage passing 0.075 mm material remained constant for all mixtures. All aggregate samples were mixed with the designed asphalt binder content.

Cylindrical specimens were fabricated for fundamental engineering property tests in this study. The specimens were compacted in the Servopac Gyratory Compactors

(SGC) to a diameter of 100 mm and a designed height of about 63.5 mm. The steps in preparing the specimens are described in the following:

(1) For each specimen to be prepared, the batch weights for different aggregate fractions were weighed into a pan;

(2) The aggregate was heated in an oven at a temperature of approximately 10 °C higher than the established mixing temperature. Mixing bowls, spatulas and the other tools used were also heated;

(3) The asphalt binder was heated to the proper mixing temperature;

(4) The compaction moulds and base plates were placed in an oven at the compaction temperature;

(5) The heated mixing bowl was placed on the scale and scale was zeroed. Heated aggregate was poured into the bowl and dry mixed for several seconds. Hot asphalt binder was added to the aggregate to achieve the desired batch weight;

(6) The mixing was done with a mixer shown in Figure 4.3 for proper mixing and coating of the aggregate;

(7) The mould and base plates were removed from the oven and a paper disk was placed at the top of the base plate. The mixture, at the proper compaction temperature, was then placed in the mould and another paper disk was placed on the top of the material;

(8) The mould containing the specimen was loaded into the compactor and was placed in the compactor. The specimens were then compacted to 100 gyrations; and

(9) After compaction was completed the specimen was removed from the mould, labelled, and stored at room temperature.

Figure 4.3 Mixing Bowl and Mixer for Mixing Asphalt Samples

4.3.3 Mixture Testing

Compared with dense-graded asphalt mixtures, SMA developed coarse aggregate stone-to-stone skeleton and provided high internal friction and high shear resistance, thus a high resistance to rutting. Therefore, this study focused on the rutting problem to measure the mechanical performance properties of the SMA mixtures. Sample preparation and testing was performed on the mixtures in the above described fractional factorial experiment (Table 4.5). The following tests were conducted to evaluate the performance of SMA mixtures:

(1) Draindown Test – ASTM D6390

(2) Bulk Specific Gravity of Compacted Mixtures – ASTM D2726

(3) Maximum Theoretical Specific Gravity of Mixtures – ASTM D2041

(4) Resilient Modulus Test

(5) Repeated Load Uniaxial Test

(6) Wheel Tracking Test

The first test was used to determine the amount of draindown in SMA mixtures. The second and third tests were used to determine the volumetric properties of the asphalt mixtures. The remaining tests were used to evaluate mechanical performance of SMA mixtures.

According to these tests and the overall test matrix for the experimental design (Table 4.5), 37 asphalt mixtures were evaluated in this experiment (It is noted that Blocks 1.1, 2.2, and 3.2 are the same asphalt mixtures.). For each of the 37 mixtures, different numbers of samples were produced in the SGC. Additionally, 7 rolling compacted slabs of asphalt mixtures chosen from the fraction of the overall test matrix were produced in the rolling compactor. This fraction scheme from the overall test matrix is given in Table 4.6. All asphalt samples were performed on mixtures according to the following schedule:

(1) Two uncompacted samples from each mixture of Block 1 in the experimental design were selected for draindown testing;

(2) Two uncompacted samples from each mixture were selected for maximum theoretical specific gravity testing (G_{mm});

(3) Six gyratory cylindrical samples prepared for each mixture were used for volumetric analysis.

Table 4.6 Test Matrix for the Rolling Compacted Slabs

	Coarse Aggregate Gradation	Fine Aggregate Gradation	Asphalt Binder Content	Design Unit Weight
Block 2.1	Upper	Medium	5.5%	RUW
Block 2.2	Medium	Medium	5.5%	90% RUW RUW 105% RUW 110% RUW
Block 2.3	Lower	Medium	5.5%	RUW
Block 4	Medium	Medium	5.5%	80% LUW

After volumetric analysis, the same six gyratory compacted samples and seven additional rolling compacted slabs were performed for the mechanical property testing accordingly to the following schedule:

(1) Six same gyratory compacted samples used in volumetric analysis were used for resilient modulus test. This test provided the measurement of resilient modulus;

(2) Six same gyratory compacted samples from resilient modulus test (Since resilient modulus is a non-destructive test, the tested samples can be used in other test) were used for the repeated load uniaxial test for the evaluation of resistance to permanent deformation;

(3) Each of the seven rolling compacted slabs for different asphalt mixtures was cut into four $200\text{mm} \times 50\text{mm}$ cylindrical cores. These samples were used to determine the rutting depth for the mixture in the wheel tracking test.

4.4 TESTING EQUIPMENT AND METHODS

The testing methods used in this experiment to determine the voids characteristics of aggregates and mechanical properties in SMA mixtures include aggregate and mixture testing on several types of accepted testing apparatus. The test equipment used in the evaluation of these mixes includes:

- Uncompacted Void Content of Aggregate Test Apparatus (UVCATA);
- Draindown Test Apparatus;
- IPC Servopac Gyratory Compactor (SGC);
- IPC Material Testing Apparatus (MATTA); and
- Wessex Wheel Tracker (WWT).

4.4.1 Uncompacted Void Content of Aggregate Test

This test method describes the determination of the loose uncompacted void content of a sample of aggregate. It can be used to determine the loose unit weight of aggregates.

ASTM C1252 is the standard test method for determining the uncompacted void content of a sample of fine aggregate. However, there is no standard test method for determining the uncompacted void content of coarse aggregate. Ahlrich (1996) proposed an uncompacted void content test for coarse aggregate which is similar to the uncompacted void content test for fine aggregate, ASTM C1252. In order to accommodate larger size (4.75 mm to 19 mm) aggregate, a 102 mm orifice funnel and a 152 mm diameter cylindrical measure were proposed. A schematic of the proposed equipment is shown in Figure 4.4 along with the equipment for the fine aggregate test. The cylindrical measure is the same as used in dry rodded unit weight (ASTM C29, 1998). The drop distance, 114 mm, was kept the same as that of fine aggregate. Ahlrich (1996) proposed two methods of measuring uncompacted voids, i.e., as received gradation and individual sizes. Five thousand grams of samples of material passing 19 mm but retained on 4.75 mm sieve were proposed.

Coarse and fine aggregate tests were performed in the proposed Uncompacted Void Content of Aggregate Test Apparatus (UVCATA). The apparatus is shown in Figure 4.5. An aggregate sample is allowed to flow through a funnel from a fixed height into a cylinder of known volume. The weight of material in the cylinder was measured and, with aggregate specific gravity, used to compute void content.

There are three methods of measuring uncompacted voids. Method A is for standard graded sample, method B for individual one-size materials while test method C is

for as received gradation. The test method used in the experiment follows method C. Method C of the proposed test procedure requires the use of the stockpile gradation. For the aggregates used in this experiment, the test was performed on the controlled gradations as outlined in Table 4.1 for the coarse aggregates and Table 4.2 for the fine aggregates. These aggregates were mechanically sieved into component sieve sizes and recombined to achieve the target gradation.

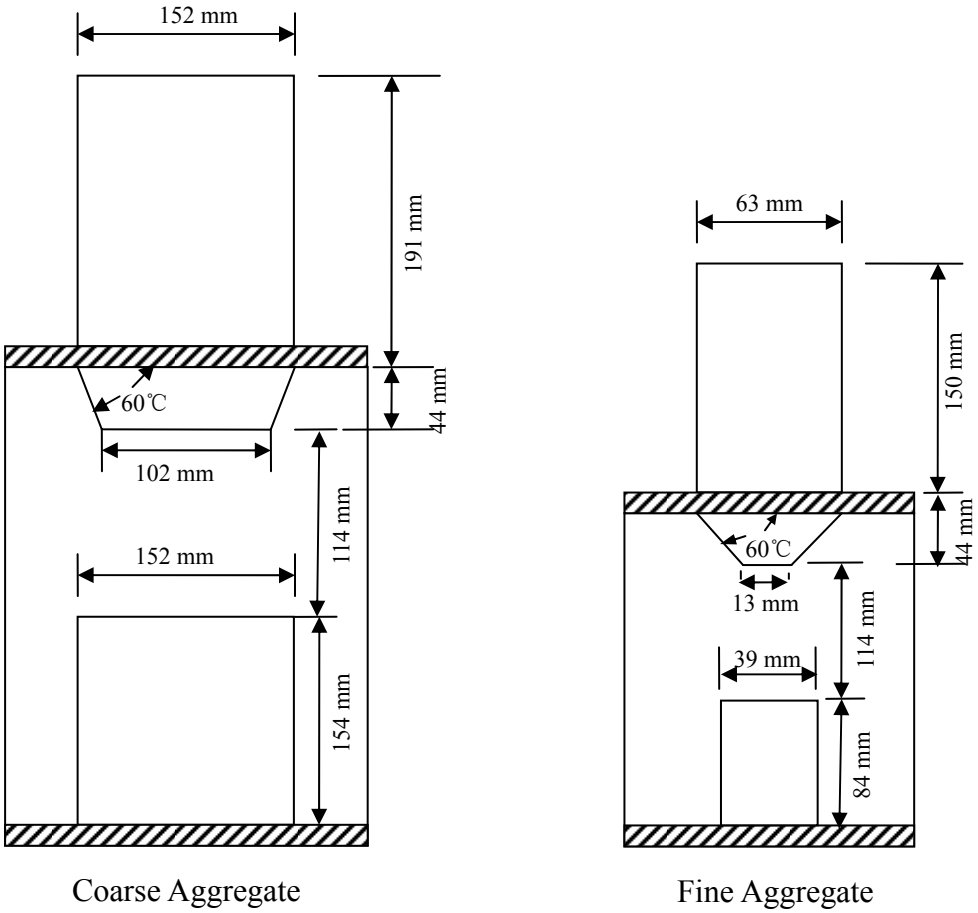

Figure 4.4 Schematic of Apparatus for Uncompacted Void Content of Aggregates

Figure 4.5 Uncompacted Void Content of Aggregate Test Apparatus

In addition to the standard testing, all of the aggregates for this study were tested under two levels of compactive effort. The standard container used in the UVCATA served as the standard container for the compaction of the aggregates and the determination of unit weight. Each aggregate was tested with 10 rods and 25 rods of compaction.

For each of the rodded tests, the aggregates were dropped into the bucket in a similar manner. The aggregates, which are of the specified stockpile gradation, were dropped into the container in three lifts with each lift being rodded the appropriate amount. The rodding proceeded as outlined in ASTM C29, Unit Weight and Voids in Aggregate.

The reported results from this testing include:

- Loose unit weight and uncompacted voids of aggregate;

- Rodded unit weight and rodded voids of aggregate (10 rods); and
- Rodded unit weight and rodded voids of aggregate (25 rods).

4.4.2 Draindown Test

When compared to conventional hot mix asphalt (HMA), SMA mixtures generally have a higher asphalt content and higher percentage of coarse aggregates. As a result, stabilising additive may be added to retain the asphalt binder during production and placement.

Draindown test is a fast, simple, and inexpensive test that measures the potential for asphalt binder to drain from the coarse aggregate structure while the mix is held at an elevated temperature. The test is performed in accordance with ASTM D6390, Test Method for Determination of Draindown Characteristics in Uncompacted Asphalt Mixtures (ASTM D6390, 2001). To run this test, a sample is prepared in the laboratory (during mix design) or obtained from field production. The sample is placed in a wire basket that is put onto a suitable container of known mass (generally a paper plate). The sample, basket, and container are then placed into a forced draft oven for an hour at or above the anticipated production temperature. At the end of the hour, the mass of asphalt binder draining from the sample that is retained in the container is determined and the amount of draindown calculated. Figure 4.6 shows the apparatus used for draindown test.

Figure 4.6 Typical Wire Mesh Basket Used for Draindown Test

4.4.3 Gyratory Compaction

The Gyratory Compactor is currently accepted as the most appropriate device to assess the compaction characteristics of asphalt mixtures. This is derived from the fact that the volumetric properties of mixtures can be better controlled using gyratory compaction as well as it simulates field rolling of asphalt mixtures more closely than the conventional falling hammer method. The gyratory compactor also provides the ability to investigate the material properties at void levels representing construction and throughout the life of the pavement.

The SGC is a fully functional feedback controlled testing machine, which is designed to meet and exceed the specification for SGC compaction. The compactor is fully automated, servo-controlled and designed to compact asphalt mixes by means of the fixed angle and vertical pressure gyratory compaction technique. The simultaneous action of static compression and the shearing action resulting from the mould being gyrated through an angle about its longitudinal axis achieve the gyratory compaction. The compactor is shown in Figure 4.7. Additionally, Figure

4.8 shows the configuration of a SGC mould, which has an inside diameter of 100 mm and a nominal height of 300 mm. A base plate fits at the bottom of the mould to confine the specimen during compaction.

Figure 4.7 Servopac Gyratory Compactor

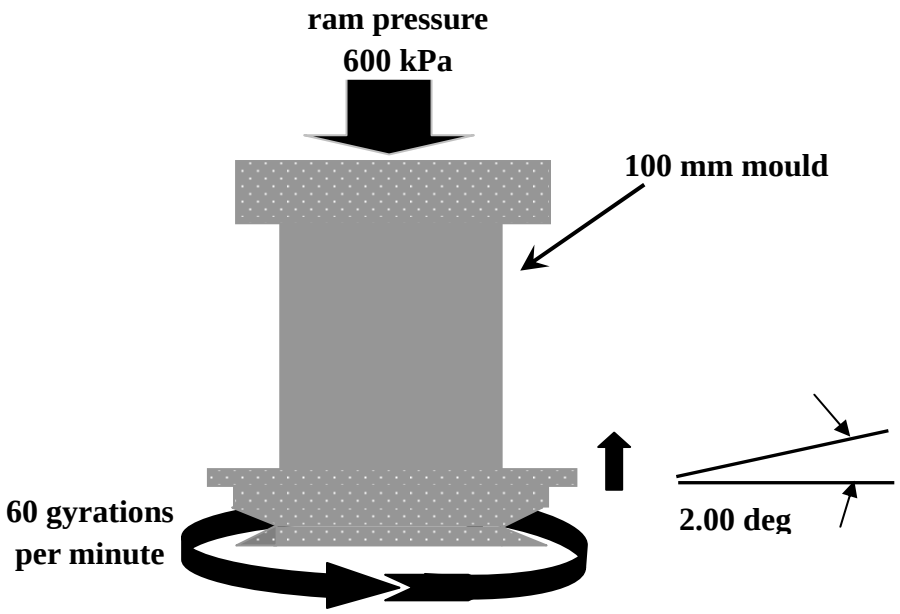

Figure 4.8 SGC Mould Configuration and Compaction Parameters

The IPC SGC is a second-generation gyratory compactor from Australia. The closed loop feedback control electronics allow for precise control of the critical parameters involved in the gyratory compaction process. The compactor is fitted with a pressure transducer in the pressure lines of the three vertical actuators that control the gyration. This pressure, when combined with the other gyratory inputs, allows calculation of the shear resistance of the asphalt material during compaction. The algorithm for determining this shear resistance is similar to that of the Gyratory Test Machine (GTM) of the U.S. Army Corps of Engineers, which is described in detail by Sigurjonsson and Ruth (1990) on the study of shear resistance of various mixtures with different gradations and asphalt contents. In the GTM, as the angle decreases it has the effect of compressing an "air-roller" at a distance L (lever arm distance) from the vertical axis of rotation to generate an air pressure P. The gyratory shear stress (S_G) in a specimen of area A and height h is calculated using Equation 4.1:

$$S_G = \frac{2PL}{Ah} \qquad (4.1)$$

The measurement of shear stress in the SGC uses a similar algorithm where P is the average pressure measured in gyratory actuators and L is the distance to the midpoint of the actuators.

The gyratory compaction data will be examined to determine if a relationship exists between coarse aggregate stone-to-stone contact, aggregate ratios, mixture volumetrics, the compaction curve (height vs. gyrations), and the shear resistance characteristics in the gyratory compactor. It is presumed that a relationship exists with these variables that will show the gyratory compactor to be an improved tool in the examination of asphalt mixtures.

4.4.4 Volumetric Properties

Volumetric properties of HMA, including asphalt content, voids in the total mix (VTM), voids in the mineral aggregate (VMA), voids in the coarse aggregate (VCA), and the voids filled with asphalt (VFA), are important parameters for durability and performance (AI, 1993). The volume or amount of asphalt binder is critical for durability of asphalt mixtures. There should be enough asphalt to provide adequate coating of the aggregates. The gradation of the aggregate determines the aggregate surface area, and together with asphalt content and absorption determine the amount of free asphalt available to coat the aggregates. What follows is a summary of some of the important volumetric properties currently used in the volumetric mix design. Figure 4.9 shows a schematic of the volumetric properties.

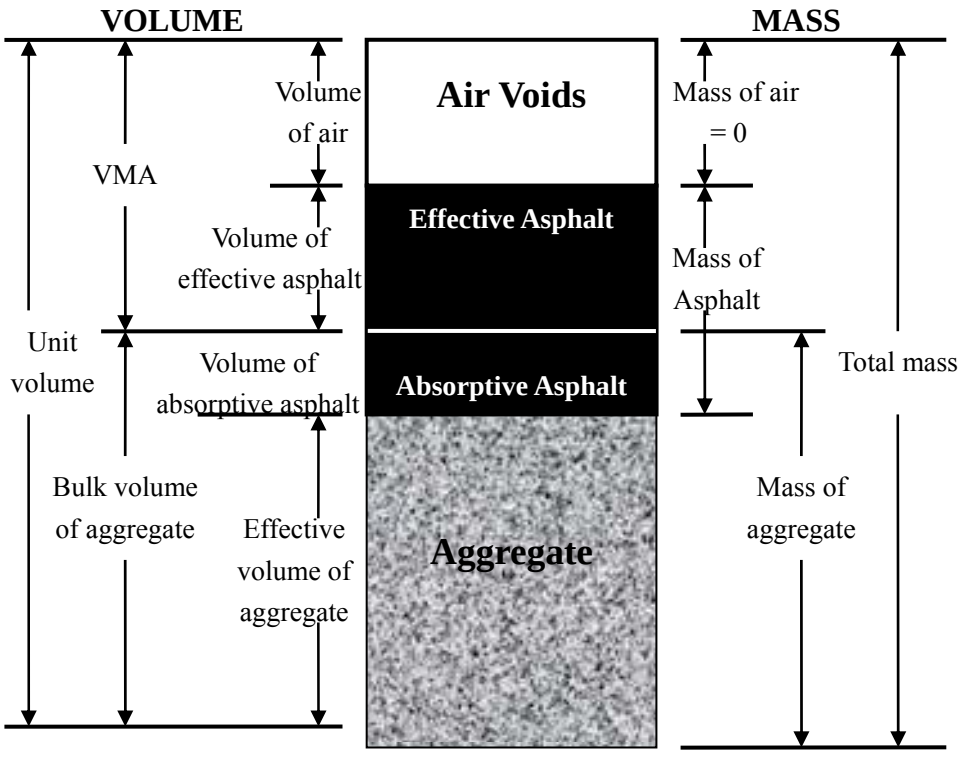

Figure 4.9 Component Diagram of Compacted SMA Sample (Walter, 2000)

- **Aggregate Bulk Specific Gravity**

The bulk specific gravity of total aggregate is calculated from Equation 4.2 when the total aggregate consists of separate aggregate fractions of coarse aggregate, fine aggregate and mineral filler.

$$G_{sb} = \frac{P_1 + P_2 + \cdots + P_N}{\frac{P_1}{G_1} + \frac{P_2}{G_2} + \cdots + \frac{P_N}{G_N}} \qquad (4.2)$$

where

G_{sb} = bulk specific gravity for the total aggregate;

P_1, P_2, P_N = individual percentages by mass of aggregate; and

G_1, G_2, G_N = individual bulk specific gravities of aggregate.

The bulk specific gravity of mineral filler is hard to determine accurately so the apparent specific gravity is generally used.

- **Aggregate Effective Specific Gravity**

The effective specific gravity of aggregate, G_{se} (Equation 4.3) includes all void spaces in the aggregate particles except those that absorb asphalt.

$$G_{se} = \frac{P_{mm} - P_b}{\frac{P_{mm}}{G_{mm}} - \frac{P_b}{G_b}} \qquad (4.3)$$

where

G_{se} = effective specific gravity of aggregate;

G_{mm} = maximum specific gravity (ASTM D2041) of paving mixture (no air voids);

P_{mm} = percent by mass of total loose mixture = 100;

P_b = asphalt content at which ASTM D2041 test was performed, percent by total mass of mixture; and

G_b = specific gravity of asphalt.

- **Asphalt Absorption**

Absorption is expressed as a percentage by mass of aggregate rather than as a percentage of total mixture. Absorption (P_{ba}) is determined by Equation 4.4:

$$P_{ba} = 100 * \frac{G_{se} - G_{sb}}{G_{sb} G_{se}} * G_b \qquad (4.4)$$

where

P_{ba} = absorbed asphalt, percent by mass of aggregate and

G_{se}, G_{sb}, and G_b have their usual meanings.

- **Effective Asphalt Content**

Effective asphalt content P_{be} is the total asphalt content minus the amount of asphalt lost to absorption in the aggregates. It is this portion that remains as a coating on the outside of aggregate particles and it is this that governs the performance of an asphalt paving mixture. It is expressed as in Equation 4.5:

$$P_{be} = P_b - \frac{P_{ba}}{100} * P_s \qquad (4.5)$$

where

P_{be} = effective asphalt content, percent by total mass of mixture;

P_s = aggregate content, percent by total mass of mixture and P_b and P_{ba} have their usual meanings.

Maximum Theoretical Specific Gravity of Mixtures

The maximum theoretical specific gravity of mixtures (G_{mm}) was determined using ASTM D2041. Samples for the determination of the maximum specific gravity were prepared as outlined in Section 4.3.2. This value was used to calculate the values for the percent of air voids in the compacted mixtures.

Bulk Specific Gravity of Compacted Mixtures

The bulk specific gravity (G_{mb}) of compacted mixtures was measured using ASTM D2726 after compaction and prior to structural testing. This test is normally performed by placing the mix samples into water and comparing the submerged weight and the dry weight in the air. This value is used to determine the volumetric properties of the compacted asphalt mixtures. It is expressed in Equation 4.6:

$$G_{mb} = \frac{A}{B - C} \qquad (4.6)$$

where

A = mass of the compacted mixture in the air, g;
B = mass of the saturated surface - dry compacted mixture in the air, g; and
C = mass of the compacted mixture in the water, g.

Percent VMA in Compacted Paving Mixture

The intergranular void space between aggregates in a compacted mixture, which includes air voids and effective asphalt content, is considered to be very important for the durability of a compacted paving mixture. The voids are calculated from

bulk specific gravity of the aggregate and are expressed as a percentage of the bulk volume of the compacted mixture. Thus, the voids in the mineral aggregate (VMA) can be calculated by subtracting the volume of the aggregate determined by its bulk specific gravity from the bulk volume of the compacted paving mixture. The calculations are performed as in Equation 4.7:

$$VMA = 100 - \frac{G_{mb} * P_s}{G_{sb}} \qquad (4.7)$$

If the mix composition is determined as percent by mass of total mixtures,

VMA = voids in the mineral aggregates (percent of bulk volume);
G_{mb} = bulk specific gravity of compacted mixture (ASTM D2726) and
G_{sb} and P_s have their usual meanings.

If the mix composition is determined as percent by mass of aggregate, then from Equation 4.8:

$$VMA = 100 - \frac{G_{mb}}{G_{sb}} * \frac{100}{100 + P_b} * 100 \qquad (4.8)$$

where the symbols have their usual meanings.

- **Percent Air Voids in a Compacted Mixture**

The air voids in a compacted mixture is the small air spaces between the coated particles. It is determined using Equation 4.9 below:

$$V_a = 100 * \frac{G_{mm} - G_{mb}}{G_{mm}} \qquad (4.9)$$

where

V_a = air voids in compacted mixture, percent of total volume and G_{mm} and G_{mb} have their usual meanings.

- **Percent VFA in Compacted Mixture**

The percentage of the voids in the mineral aggregate that are filled with asphalt, VFA, not including absorbed asphalt, is determined using Equation 4.10:

$$VFA = 100 * \frac{VMA - V_a}{VMA} \qquad (4.10)$$

where

VFA = voids fillled with asphalt;

VMA and V_a have their usual meanings.

4.4.5 Resilient Modulus Test

The resilient modulus (M_R) of asphalt mixtures is used in the mechanistic pavement design procedures to evaluate the ability of a mixture to carry load in the pavement structure. It is also used as an index for evaluating stripping, fatigue and low temperature cracking of asphalt mixtures. It can be determined by the repeated load indirect tensile test. This test method is simple, fast, and economical and can be performed on standard size ($\Phi 100mm \times 63.5mm$) cylindrical asphalt specimens. During the course of the test, a dynamic load was applied and total deformation was recorded. In the computation of M_R, Poisson's ratio was assumed to be 0.35.

The repeated load indirect tensile test was conducted on the Material Testing Apparatus (MATTA), which is an Australian piece of equipment that was based on the Nottingham Asphalt Tester (NAT) developed in the UK. Figures 4.10 and 4.11 show the MATTA apparatus and the set up for the repeated load indirect tensile test, respectively. The MATTA is a top loading closed-loop pneumatic testing machine with the capability of applying a haversine or other shapes of load pulse over a

range of load duration, load levels and rest period. The test is specified by the ASTM D4123. A modified technique involving five-pulse loading was used as described in the Australian Standard Methods (AS Method 13.1, 1995).

The resilient modulus of each mixture is measured at 25 °C. A compression load with a haversine waveform is applied in the vertical diametric plane of a 63.5 mm by 100 mm cylindrical specimen through a loading strip. The resulting total recoverable diametral strain under each load is measured from perpendicular at 90° to the applied force and the resilient modulus is calculated. The equation used for calculating resilient modulus is:

$$M_R = P(\upsilon + 0.2734)/\delta t \qquad (4.11)$$

where

P is the magnitude of the dynamic load;

υ is the Poisson's ratio;

δ is the total recoverable deformation; and

t is the specimen thickness.

Figure 4.10 Material Testing Apparatus (MATTA)

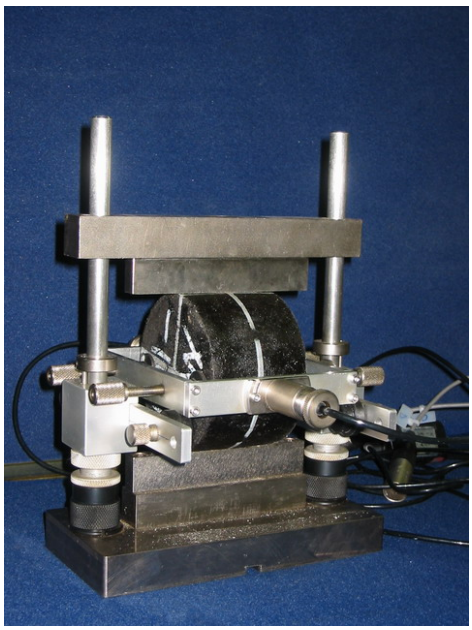

Figure 4.11 MATTA Set Up for Repeated Load Indirect Tensile Test

4.4.6 Repeated Load Uniaxial Test

The repeated load uniaxial test aims to measure the permanent deformation characteristics of SMA mixtures typically through several thousand load repetitions. During the test, the cumulative permanent deformation as a function of the number of load cycles is recorded. It provides the ability to characterise the time dependent response, and the stress dependent response of the material.

The repeated load uniaxial test is conducted on the Material Testing Apparatus (MATTA). Figure 4.12 shows the MATTA set up for the test. The Standard Method of Sampling and Testing Asphalt (AS Method 12.1, 1995) has recommended a set of the test conditions. However, in this study, based on trial tests conducted for the SMA specimens by past projects carried out within Nanyang Technological University (Lau, 1999), a modified set of test conditions was adopted for the test,

which is as follows:

- Test temperature: 50 ± 0.5 °C ;
- Compressive stress: 300 ± 5 KPa ;
- Loading period: 0.5 ± 0.05 s ;
- Pulse repetition period (sinusoidal pulse): 1.0 ± 0.05 s ; and
- Test terminal pulse count: 20,000.

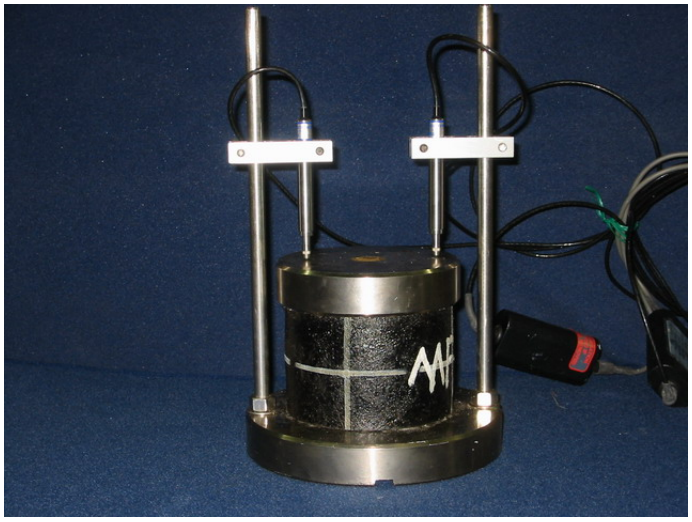

Figure 4.12 MATTA Set Up for Repeated Load Uniaxial Test

4.4.7 Wheel Tracking Test

Wheel tracking test is to simulate the application of the actual wheel loads onto the road pavement. It directly estimates the internal resistance of asphalt mixtures in terms of rutting depth. The specimens were tested in accordance with BS 598: Part 110 (1998).

However, BS 598: Part 110 (BSI, 1998) does not specify a reference temperature in contrast to the superseded standard BS 598: Part 110 (BSI, 1996) that recommends

a test temperature of 45°C. The reason for the choice of temperature in the revised standard is to obtain results that will produce a reasonable ranking, and need not be truly representative of the extreme road conditions. For example, a temperature of 45°C is used for lesser traffic roads and 60°C is used for heavily traffic roads in the UK. The choice of higher temperature for heavily traffic roads is not because heavily traffic roads are somehow exposed to greater temperatures but because the materials necessary for heavily traffic roads would have such limited deformations at 45°C to be effectively all identical while materials adequate for lesser roads would not be able to complete the 45 min at 60°C. In view of this, an appropriate temperature of 50 °C was used.

In this investigation the wheel tracking test will be conducted on the Wessex Wheel Tracker (WWT). Figures 4.13 and 4.14 show WWT apparatus and the set up for the wheel tracking test, respectively. The WWT is capable of testing asphalt beam or cylindrical specimens. Beam dimensions are generally 300 mm wide, 300 mm long, and 50 mm high (300 mm×300 mm×50 mm). Cylindrical specimens generally have diameter 200 mm and height 50 mm (Φ 200 mm×50 mm).

In this experiment, cylindrical specimens were tested to investigate SMA mixture rutting resistance. They were cored from the slabs compacted by rolling compactor. Testing of samples within the WWT generally consists of applying a 520 N load onto a weighted cantilever arm. The load is applied through a rubber wheel onto the specimens. Test specimens are tracked back and forth under the applied stationary loading. Testing is typically accomplished for a total of 45 minutes with a frequency of 21 load cycles (one cycle is defined as the backward and forward movement over sample by the wheel) per minute and a 230 mm travel in each direction. At the end of each minute, permanent deformation (rutting) is measured. Rut depths are obtained from computer record by the average difference in specimen surface

before and after testing.

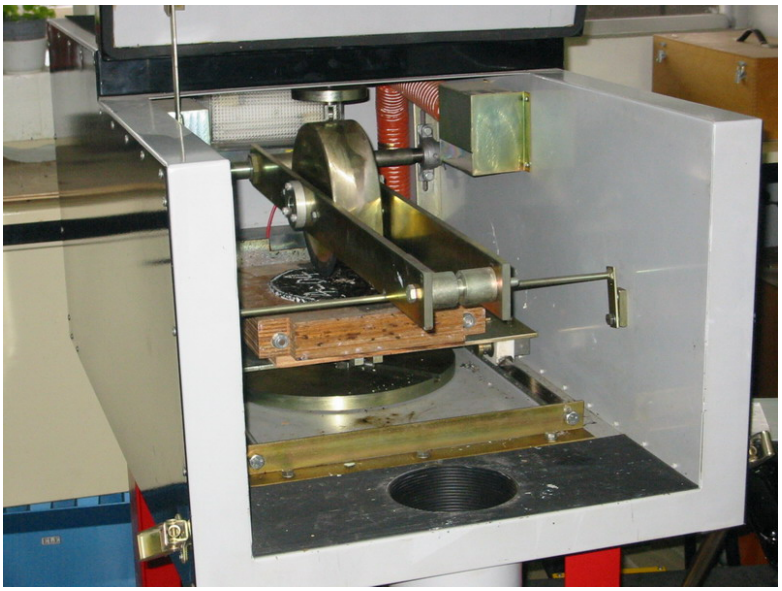

Figure 4.13 Wessex Wheel Tracker

Figure 4.14 WWT Set Up for the Wheel Tracking Test

4.5 SUMMARY

The experimental design and procedures evaluating aggregate properties and

aggregate combinations would provide a backbone for a comprehensive mixture design of SMA. The testing of dry aggregates, both coarse and fine, should characterise packing of the individual components for use in the aggregate blend. These aggregates are then combined to produce SMA mixtures.

A comprehensive testing matrix using fractional factorial experimental method was developed to study the effect of change in gradation of the coarse and fine aggregate portions of an aggregate blend while changing the volume of coarse and fine aggregates and the effect of change in asphalt binder content. Table 4.5 shows this fractional factorial experimental design. Through this test matrix and the proposed mixture testing, 195 individual specimens and 7 rolling compacted slabs were produced in the SGC and rolling compactor, respectively, for volumetric and mechanical property tests.

The proposed testing equipment and methodology would provide insight into the properties of SMA mixtures (volumetric, modulus, permanent deformation and rutting depth, etc.). The analysis of volumetric properties would provide a direct indication of the volumetric changes with a change in aggregate gradation, degree of aggregate stone-to-stone contact, and asphalt binder content. The repeated load uniaxial test and wheel tracking test would provide an evaluation of the rutting potential of the SMA mixtures, while the resilient modulus would provide valuable inputs for pavement design.

It is expected that the physical test results will correlate with the volume of coarse aggregate and the aggregate ratios used to develop the gradations. The mechanical property tests may provide an indication of the structural characteristics achievable through the use of these aggregate ratios.

CHAPTER FIVE

TEST RESULTS AND ANALYSIS

This chapter presents the results of aggregate and mixture tests. The first part of the chapter (Section 5.1) summarises the aggregate test results. Section 5.2 develops the different aggregate gradations for the mixture testing according to the results of aggregate test. The rest of the chapter describes the analysis of the volumetric properties of mixtures and the engineering performance test results. A standard statistical procedure, ANOVA has been used to test if the mean values of the fundamental engineering properties are significantly different among the mixtures. A 95-perent confidence level has been utilised to test its significance. A multiple regression analysis has been performed to fit a quantitative model relating the variables with the resulting engineering properties.

5.1 AGGREGATE TEST RESULTS AND ANALYSIS

Aggregate test results provide the information to understand the change in the

aggregate packing properties with changes in aggregate gradation and provide the information necessary for SMA mixture design procedure.

5.1.1 Aggregate Specific Gravity Test Results

Loose and rodded unit weights for both coarse and fine aggregates were determined through the Uncompacted Void Content of Aggregate Test as described in Chapter 4. However, the aggregate specific gravity plays an important role in the determination of these two unit weights. In the study, it was deemed more efficient to measure specific gravity on each sieve size separately (AASHTO, 2004) and then compute the specific gravity for each gradation. The single size sieve results for specific gravity and absorption are listed in Table 5.1.

Table 5.1 Specific Gravity and Absorption Capacity Results for Individual Sieve Sizes

Sieve Size	Specific Gravity	Absorption Capacity (%)
9.5 mm – 14 mm*	2.683	1.024
6.3 mm – 9.5 mm*	2.673	1.066
3.35 mm – 6.3 mm*	2.643	1.107
0.075 mm – 3.35 mm*	2.536	2.250
P 0.075 mm**	2.78	-

* Bulk specific gravity

** Apparent specific gravity

In Table 5.1, the bulk specific gravity of mineral filler is rather difficult to determine accurately so the apparent specific gravity is generally used. The absorption capacity of single sieve size can be used in the determination of volumetric properties. The specific gravity of coarse and fine aggregate gradations for

aggregate testing can be calculated from the single size sieve results. The results are listed in Table 5.2.

Table 5.2 Specific Gravity of Coarse and Fine Aggregate Gradations

Aggregate Type		Specific Gravity
Coarse Aggregate	**Upper**	2.669
	Medium	2.661
	Lower	2.653
Fine Aggregate	**Upper**	2.536
	Medium	2.536
	Lower	2.536

5.1.2 Coarse Aggregate Test Results and Analysis

Coarse aggregate is considered the primary deformation resisting component in SMA mixtures. The loose and rodded unit weights for the coarse aggregate characterise the aggregates and provide the limits for aggregate stone-to-stone contact in SMA mixtures.

5.1.2.1 Test Results

Only one aggregate source which is typically used for Singapore roads was selected and sampled for testing in the modified UVCATA under the loose, 10 rods, and 25 rods conditions. The aggregate source and aggregate type are given in Table 5.3.

Table 5.3 Aggregate Source and Aggregate Type for Coarse Aggregate Testing

Aggregate Name	Aggregate Source	Aggregate Type	Characteristic Size
Granite	Indonesia	Crushed Granite	14 mm

Coarse aggregates for the upper, medium, and lower limits of the specification were tested. The results for unit weight and the voids in the coarse aggregate for all of the tested aggregates are given in Table 5.4 and Figure 5.1. The reported values for the test were the average results of 10 repeated tests.

Table 5.4 Unit Weight and Voids in the Coarse Aggregate for Coarse Aggregate Testing

Test Item		Unit Weight (g/cm^3)			Voids in the Coarse Aggregate (VCA) (%)		
		Loose	10 Rod	25 Rod	Loose	10 Rod	25 Rod
Coarse Aggregate	Lower	1.28	1.52	1.56	48.73	42.70	41.2
	Medium	1.42	1.55	1.59	46.63	41.64	40.25
	Upper	1.38	1.58	1.62	48.35	40.92	39.48

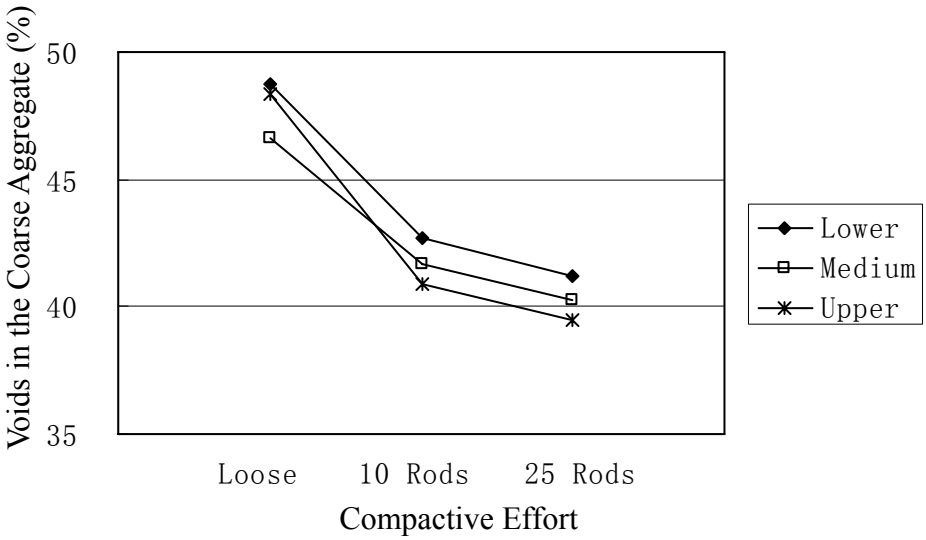

Figure 5.1 Voids in the Coarse Aggregate for Coarse Aggregate Testing

Uncompacted void content of aggregate test is rather quantitative in nature. Large samples reduce variation caused by segregation, but some degree of subjectivity is involved in striking off excess aggregate from the top of the mould for coarse aggregate. ASTM D3398 recommends placing or removing particles by hand to make the surface of the aggregate even with the rim of the mould. Additionally, the repeated testing of aggregates can cause degradation of the aggregate material resulting in varying the test results. This aggregate degradation can be especially prominent with an increase in compactive effort.

The coefficient of variation, standard deviation and the analysis of residuals are common measures of test variability. Standard deviation and coefficient of variations for the uncompacted voids, 10 rods voids, and 25 rods voids testing are summarised in Table 5.5. The analysis of residuals with the tests taken in order is used to identify the existence of any change in the test value after repeating the tests. It is a visual identification of trends in the ordered test residual output. Figures 5.2, 5.3, and 5.4 give the residual analysis for the uncompacted voids, 10 rods voids, and 25 rods voids testing, respectively.

Table 5.5 Standard Deviation and Coefficient of Variation for Voids in the CA

Test Item		Standard Deviations (%)			Coefficients of Variation (%)		
		Loose	10 Rod	25 Rod	Loose	10 Rod	25 Rod
Coarse Aggregate	Lower	0.360	0.513	0.476	0.7	1.2	1.2
	Medium	0.333	0.124	0.275	0.7	0.3	0.7
	Upper	0.171	0.133	0.197	0.4	0.3	0.5

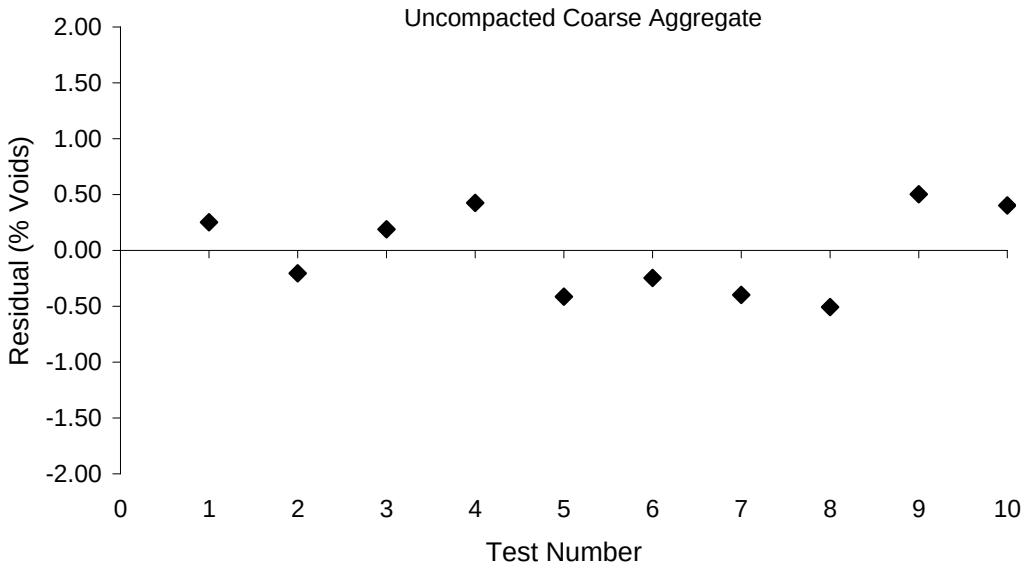

Figure 5.2 Residual Analysis for Uncompacted Voids of Coarse Aggregate

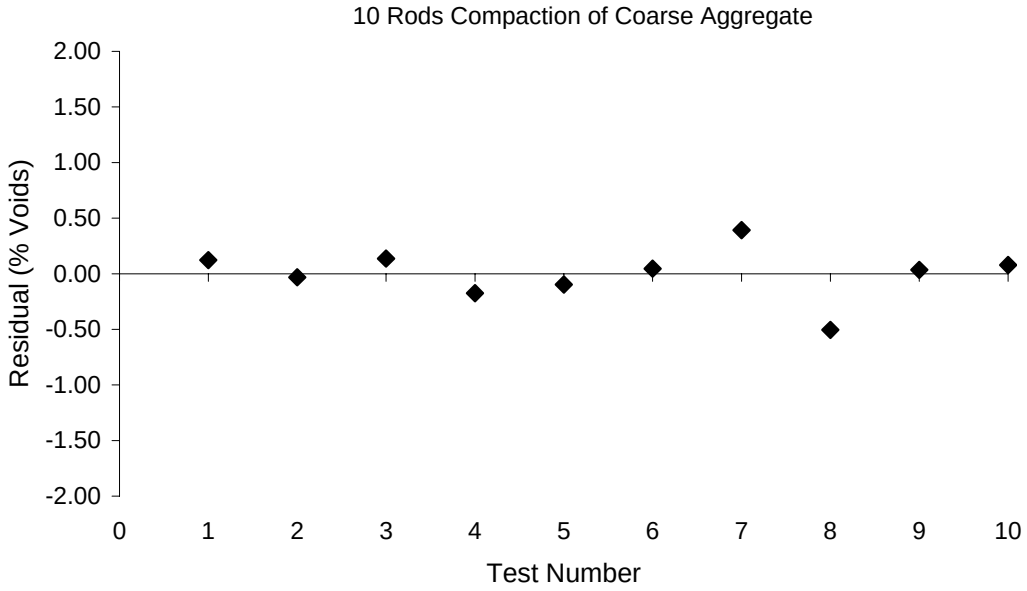

Figure 5.3 Residual Analysis for 10 Rods Compaction Voids of Coarse Aggregate

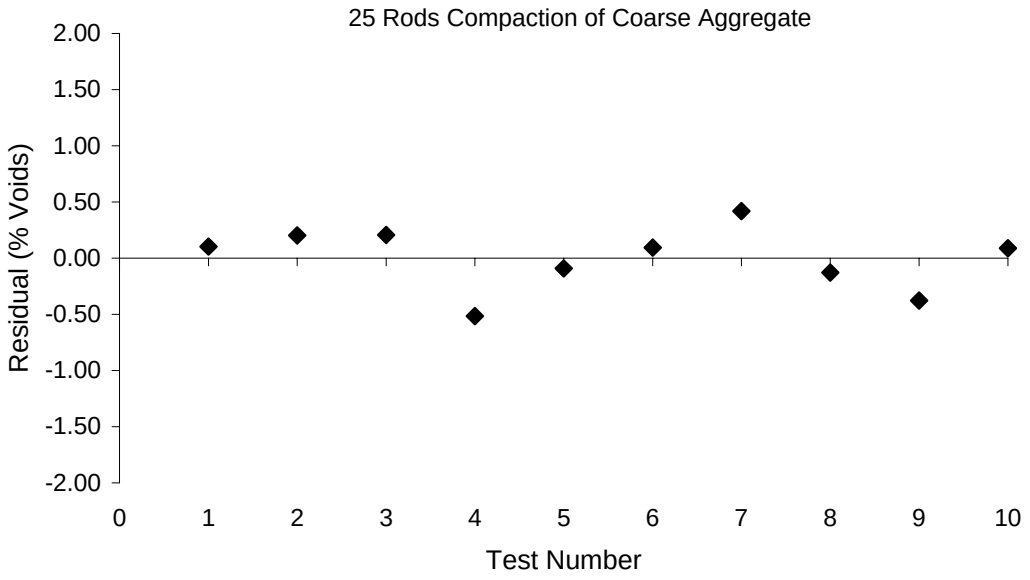

Figure 5.4 Residual Analysis for 25 Rods Compaction Voids of Coarse Aggregate

Table 5.5 shows that the maximum standard deviation of the test was 0.513. The average standard deviation for the test was 0.287 for all samples tested. Alternatively, the coefficient of variation (COV) ranged from 0.3% to 1.2%. The analysis of residuals is based on visual identification of trends in the ordered test residual output. This analysis of ordered test residuals from Figures 5.2 to 5.4 did not show any large change in the test value with the repeated testing of the aggregate materials. The unit weight tests were normally scattered about the mean (0-value on the Y axis of the residual plot) with no apparent trend in the scatter plot, which signifies the normality of the testing method. There was also no apparent effect in the change in unit weight after several tests that can be seen in the test data. This is not to say that no breakdown is taking place, but rather the breakdown that did occur with the repeated testing was rather limited.

5.1.2.2 Result Analysis

The unit weight and voids in the coarse aggregate are related through the aggregate specific gravity. The use of voids in the coarse aggregate is the first piece of information required in the proposed aggregate blending procedures. Therefore, the analysis of coarse aggregate is based on the comparison of voids in the coarse aggregates.

The compactive effort applied to the aggregate sample has a significant effect on the resulting voids in the coarse aggregate. Since all aggregates used in the experimental study were from the same aggregate type and source, different compactive efforts would result in different coarse aggregate contact and thus, a different void content. Examination of the percent change in voids in the aggregate for all cases from uncompacted to 10 rods of compaction showed an average decrease of 12.8%. The additional change in voids from 10 rods to 25 rods of compaction was 3.5% on average, giving an average change in voids of 15.8% from the uncompacted voids to the 25 rods compaction. This indicated that much more densification would be realised in the first 10 rods of the coarse aggregate than the next 15 rods necessary to reach 25 rods total.

The reduction in voids of the coarse aggregate has provided details on the relative amount of fine aggregate required to fill those voids. With the limits for coarse aggregate interlock near the uncompacted condition of the coarse aggregate and the maximum practical limit near 25 rods of compaction, the mix designer can easily recognise the amount of change in coarse aggregate needed in the mixture while maintaining coarse aggregate interlock in the mixture.

The change in aggregate gradation was examined using the upper, medium, and

lower limit of the appropriate specification. The data in Table 5.4 showed that there was a difference from the upper to lower limit gradation for the majority of the aggregates tested. The results indicated that changing from the upper to lower limit gradation did change the volume of voids in the uncompacted state. The voids of the 10 rods and 25 rods of compaction for these aggregates showed that less difference was observed between the upper and lower limit gradation. The addition of compactive effort reduced the difference in compacted voids between the aggregate gradations, but did not change the significance of the change in gradation.

5.1.3 Fine Aggregate Test and Analysis

Fine aggregate is used as a filler material in the asphalt mixture and therefore must be packed into the voids created by the coarse aggregate. As the primary deformation resistance is derived from the coarse aggregate, for the design of SMA mixture, the fine aggregate packing was not investigated in the testing of dry aggregates.

5.1.3.1 Test Results

The aggregates from the same source as coarse aggregate were sampled, sieved into component aggregate sizes, and recombined for aggregate voids testing. This aggregate was prepared to the lower, medium, and upper limit gradation specification. Testing of this aggregate was performed in the UVCATA.

The results for unit weight and the voids in the fine aggregates for all of the tested aggregates are given in Table 5.6 and Figure 5.5. The reported values for the test were the average results of 10 repeated tests.

Table 5.6 Unit Weight and Voids in the Fine Aggregate for Fine Aggregate Testing

Test Item		Unit Weight (g/cm^3)			Voids in the Fine Aggregate (%)		
		Loose	10 Rod	25 Rod	Loose	10 Rod	25 Rod
Fine Aggregate	Lower	1.49	1.78	1.84	39.2	29.72	27.43
	Medium	1.56	1.79	1.85	38.47	29.54	27.07
	Upper	1.60	1.83	1.89	36.77	27.91	25.62

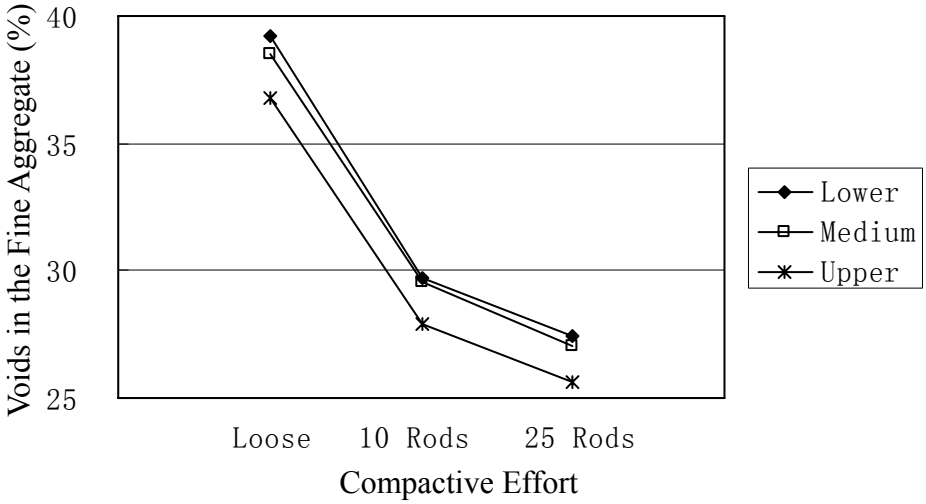

Figure 5.5 Voids in the Fine Aggregate for Fine Aggregate Testing

Similarly, some degree of subjectivity is involved in striking off the excess aggregates from the top of the mould for fine aggregate as the repeated testing of aggregates can cause degradation of the aggregate material, which results in changing the test results.

In order to measure the test variability, standard deviation and the coefficient of variation for the uncompacted voids, 10 rods voids, and 25 rods voids are calculated and shown in Table 5.7. The analysis of residuals with the tests taken in order for the uncompacted voids, 10 rods voids, and 25 rods voids testing are plotted in Figures 5.6, 5.7, and 5.8, respectively.

Table 5.7 Standard Deviations and Coefficients of Variation for Voids in the FA

Test Item		Standard Deviations (%)			Coefficients of Variation (%)		
		Loose	10 Rod	25 Rod	Loose	10 Rod	25 Rod
Fine Aggregate	Lower	0.275	0.181	0.460	0.7	0.6	1.7
	Medium	0.588	0.653	0.451	1.5	2.2	1.7
	Upper	0.444	0.840	0.399	1.2	3.0	1.6

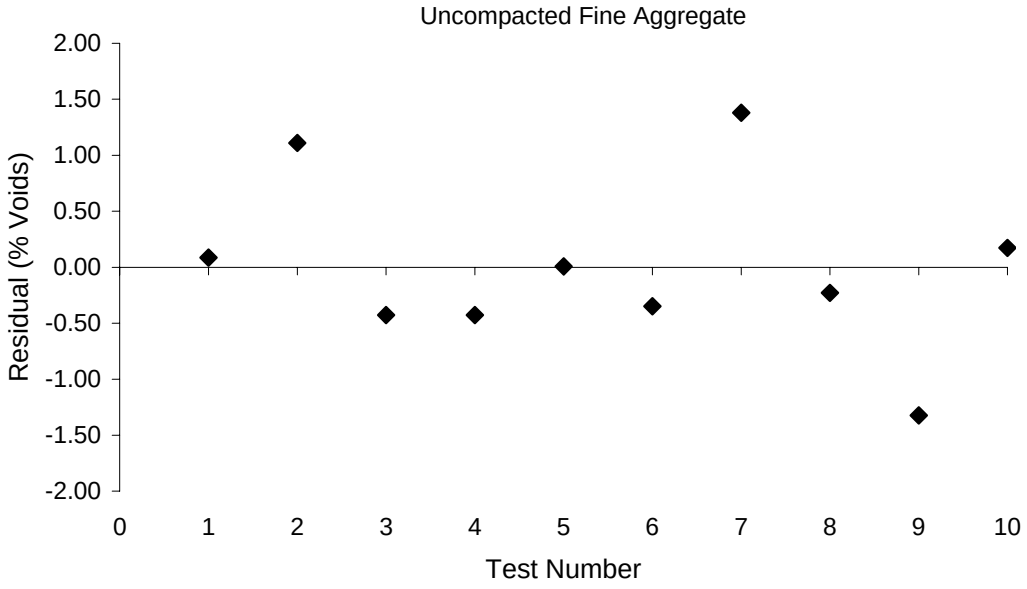

Figure 5.6 Residual Analysis for Uncompacted Voids of Fine Aggregate

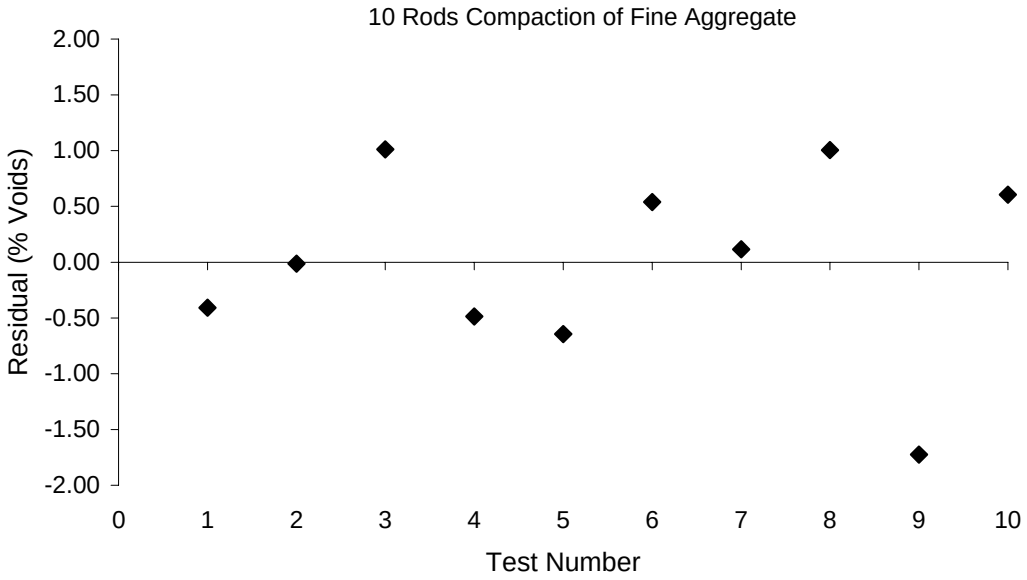

Figure 5.7 Residual Analysis for 10 Rods Compaction Voids of Fine Aggregate

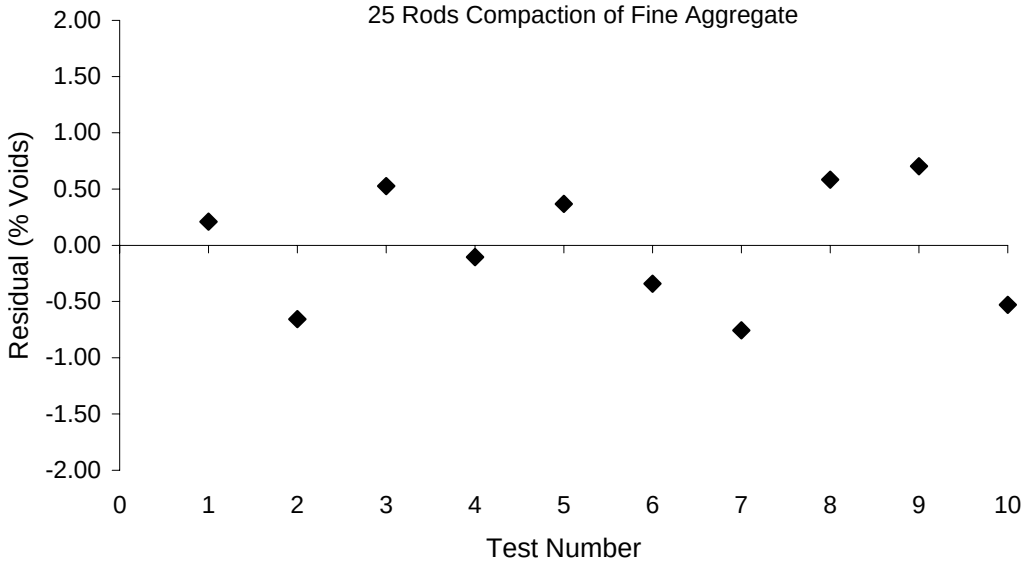

Figure 5.8 Residual Analysis for 25 Rods Compaction Voids of Fine Aggregate

From Table 5.7, the results showed that the maximum standard deviation of the test was 0.840. The average standard deviation for the test was 0.477 for all samples tested. Alternatively, the coefficient of variation (COV) ranged from 0.6% to 3.0%. The analysis of residuals is based on visual identification of trends in the ordered test residual output. This analysis of ordered test residuals from Figures 5.2 to 5.4 did not show any large change in the test value with the repeated testing of the aggregate materials. The unit weight tests were normally scattered about the mean (0-value on the Y axis of the residual plot) with no apparent trend in the scatter plot, which signifies the normality of the testing method. There was also no apparent effect in the change in unit weight after several tests that can be seen in the test data.

5.1.3.2 Result Analysis

Comparison of change in compactive effort and change in gradation will provide details on the volume of aggregate necessary to fill the voids created in the coarse aggregate. The change in the unit weight of the fine aggregate was significant when applying compactive effort. Similar results with coarse aggregate test can be obtained as more densification was noted in the first 10 rods of the fine aggregate than the next 15 rods necessary to reach 25 rods total for all cases studied. Changing the gradation of the fine aggregate affected both the unit weight and the change in unit weight with compaction. The difference of unit weight between upper, medium, and lower limit gradation became lesser with the increase in compactive effort.

5.1.4 Summary of Aggregate Test Results

Examination of aggregate packing for coarse and fine aggregates validated that the packing of an aggregate to fill a unit volume is dependent on the characteristics of the aggregate material and the test method. The results from this testing showed that

aggregate gradation and compactive energy affected the resulting voids of dry aggregate testing.

The testing methods utilised in this experiment are acceptable for the evaluation of coarse and fine aggregates. The use of the UVCATA and the modified UVCATA is appropriate for determining the voids in an aggregate in the uncompacted and rodded conditions. Repeated testing of the same sample did not change the test result and the results of ten tests were used to determine the average unit weight. Changing gradation will change the voids in an aggregate structure. This result has provided the basis for the continued evaluation of aggregate gradation in SMA mixtures.

5.2 AGGREGATE GRADATION ANALYSIS

With the selection and testing of the individual dry coarse and fine aggregate components completed, the aggregates were combined in precise percentages to produce SMA mixtures which should exhibit controlled levels of coarse aggregate stone-to-stone contact. Utilising the proposed procedure for the blending of aggregates outlined in Chapter 3 and the test matrix given in Table 4.5, 27 aggregate gradations for the six blocks (Blocks 1.1 to 1.3 have the same aggregate gradations and Blocks 1.1, 2.2, and 3.2 are the same asphalt mixtures, thus, there were 27 aggregate gradations altogether.) were developed. These gradations contained varied relative percentages of coarse and fine aggregate while keeping the material passing the 0.075 mm sieve constant.

As discussed and shown in Table 4.5, the design unit weight of each coarse aggregate can be expressed by the percentage of rodded and loose unit weight of

coarse aggregate. Table 5.8 provides the loose unit weight, rodded unit weight, and design unit weight for the coarse aggregate for each block in the test scheme (Blocks 1.1 to 1.3, Block 2.2, and Block 3.2 have the same design unit weight.). Table 5.8 also gives the rodded unit weight of the fine aggregate for each block. These loose and rodded unit weights were gotten from aggregate testing results.

Using the concepts as outlined in Chapter 3 and the test values given above, the blending percentages for the coarse aggregate, fine aggregate and mineral filler were calculated. These calculated blending percentages are presented in Table 5.9.

The gradations for each block were developed using the blending percentages and the designed gradations for the coarse and fine aggregates as described in Chapter 4. These gradations are tabulated in Table 5.10 using standard sieve sizes and are plotted in Figure 5.9.

Figure 5.9 shows all 27 aggregate gradations in one figure, which gives an overview on the difference between the blocks and levels of coarse aggregate in the experiment. Figure 5.10 through Figure 5.15 showed the plots for each block of the experiment, thereby allowing a more individual comparison of the change of the gradation for each individual block of the experiment.

Table 5.8 Loose, Rodded, and Design Unit Weight of Aggregates in Mixture Testing

Sample Name	Coarse Aggregate (g/cm^3)			Fine Aggregate (g/cm^3)
	LUW	RUW	DUW	RUW
Block 1.1-90% RUW	1.42	1.59	1.43	1.85
Block 1.1-95% RUW	1.42	1.59	1.51	1.85
Block 1.1- RUW	1.42	1.59	1.59	1.85
Block 1.1-105% RUW	1.42	1.59	1.67	1.85
Block 1.1-110% RUW	1.42	1.59	1.75	1.85
Block 2.1-90% RUW	1.38	1.62	1.45	1.85
Block 2.1-95% RUW	1.38	1.62	1.53	1.85
Block 2.1- RUW	1.38	1.62	1.62	1.85
Block 2.1-105% RUW	1.38	1.62	1.70	1.85
Block 2.1-110% RUW	1.38	1.62	1.78	1.85
Block 2.3-90% RUW	1.28	1.56	1.40	1.85
Block 2.3-95% RUW	1.28	1.56	1.48	1.85
Block 2.3- RUW	1.28	1.56	1.56	1.85
Block 2.3-105% RUW	1.28	1.56	1.64	1.85
Block 2.3-110% RUW	1.28	1.56	1.72	1.85
Block 3.1-90% RUW	1.42	1.59	1.43	1.89
Block 3.1-95% RUW	1.42	1.59	1.51	1.89
Block 3.1- RUW	1.42	1.59	1.59	1.89
Block 3.1-105% RUW	1.42	1.59	1.67	1.89
Block 3.1-110% RUW	1.42	1.59	1.75	1.89
Block 3.3-90% RUW	1.42	1.59	1.43	1.84
Block 3.3-95% RUW	1.42	1.59	1.51	1.84
Block 3.3- RUW	1.42	1.59	1.59	1.84
Block 3.3-105% RUW	1.42	1.59	1.67	1.84
Block 3.3-110% RUW	1.42	1.59	1.75	1.84
Block 4- LUW	1.42	1.59	1.42	1.85
Block 4-80% LUW	1.42	1.59	1.14	1.85

Note: Blocks 1.1 to 1.3, Block 2.2, and Block 3.2 have the same design unit weight;
LUW – loose unit weight;
DUW – design unit weight;
RUW – rodded unit weight.

Table 5.9 Blending Percentages of Each Aggregate Component in Mixture Testing

Sample Name	Coarse Aggregate (%)	Fine Aggregate (%)	Mineral Filler (%)
Block 1.1-90% RUW	62.60	27.40	10
Block 1.1-95% RUW	65.38	24.62	10
Block 1.1- RUW	68.11	21.89	10
Block 1.1-105% RUW	70.78	19.22	10
Block 1.1-110% RUW	73.40	16.60	10
Block 2.1-90% RUW	63.32	26.68	10
Block 2.1-95% RUW	66.13	23.87	10
Block 2.1- RUW	68.87	21.13	10
Block 2.1-105% RUW	71.56	18.44	10
Block 2.1-110% RUW	74.19	15.81	10
Block 2.3-90% RUW	61.72	28.28	10
Block 2.3-95% RUW	64.48	25.52	10
Block 2.3- RUW	67.19	22.81	10
Block 2.3-105% RUW	69.83	20.17	10
Block 2.3-110% RUW	72.43	17.57	10
Block 3.1-90% RUW	62.14	27.86	10
Block 3.1-95% RUW	64.93	25.07	10
Block 3.1- RUW	67.68	22.32	10
Block 3.1-105% RUW	70.37	19.63	10
Block 3.1-110% RUW	73.01	16.99	10
Block 3.3-90% RUW	62.71	27.29	10
Block 3.3-95% RUW	65.49	24.51	10
Block 3.3- RUW	68.22	21.78	10
Block 3.3-105% RUW	70.88	19.12	10
Block 3.3-110% RUW	73.49	16.51	10
Block 4- LUW	62.22	27.78	10
Block 4-80% LUW	51.74	38.26	10

Note: Blocks 1.1 to 1.3 have the same aggregate gradations;
Blocks 1.1, 2.2, and 3.2 are the same asphalt mixtures;
LUW – loose unit weight;
DUW – design unit weight;
RUW – rodded unit weight.

Table 5.10 Blended Aggregate Gradations in Mixture Testing

Sample Name	Percent Passing (%) at Various Sieve Size									
	14	9.5	6.3	3.35	2.36	1.18	0.6	0.3	0.15	0.075
Block 1.1-90% RUW	94	81	56	40	31	26	20	17	13	10
Block 1.1-95% RUW	93	80	54	37	28	24	19	16	13	10
Block 1.1- RUW	93	80	52	34	26	23	18	15	13	10
Block 1.1-105% RUW	93	79	50	32	24	21	17	15	12	10
Block 1.1-110% RUW	93	78	49	29	22	20	16	14	12	10
Block 2.1-90% RUW	87	72	49	37	30	25	20	16	13	10
Block 2.1-95% RUW	87	70	47	34	28	24	19	16	13	10
Block 2.1- RUW	86	69	45	31	26	22	18	15	13	10
Block 2.1-105% RUW	86	68	43	28	24	21	17	14	12	10
Block 2.1-110% RUW	85	67	41	26	22	19	16	14	12	10
Block 2.3-90% RUW	100	91	63	43	31	26	20	17	13	10
Block 2.3-95% RUW	100	90	61	40	29	25	19	16	13	10
Block 2.3- RUW	100	90	60	38	27	23	18	15	13	10
Block 2.3-105% RUW	100	90	58	35	25	22	17	15	12	10
Block 2.3-110% RUW	100	89	57	33	23	20	17	14	12	10
Block 3.1-90% RUW	94	81	57	40	28	26	19	16	13	10
Block 3.1-95% RUW	94	81	55	37	27	25	18	15	13	10
Block 3.1- RUW	93	80	53	35	25	23	17	14	12	10
Block 3.1-105% RUW	93	79	51	32	23	21	16	14	12	10
Block 3.1-110% RUW	93	78	49	30	21	20	16	13	12	10
Block 3.3-90% RUW	94	81	56	39	33	26	21	18	14	10
Block 3.3-95% RUW	93	80	54	37	30	24	20	17	13	10
Block 3.3- RUW	93	80	52	34	28	23	19	16	13	10
Block 3.3-105% RUW	93	79	50	32	26	21	18	15	13	10
Block 3.3-110% RUW	93	78	49	29	24	20	17	15	12	10
Block 4- LUW	94	81	56	40	31	26	20	17	13	10
Block 4-80% LUW	95	84	64	50	39	32	24	19	15	10

Note: Blocks 1.1 to 1.3 have the same aggregate gradations;
Blocks 1.1, 2.2, and 3.2 are the same asphalt mixtures;
LUW – loose unit weight;
DUW – design unit weight;
RUW – rodded unit weight.

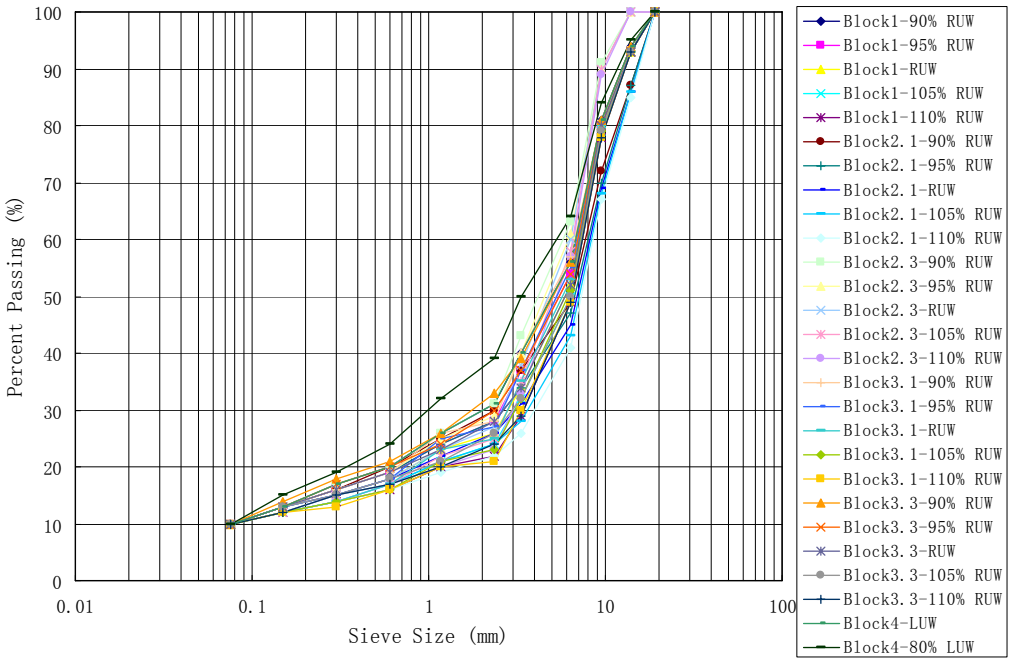

Figure 5.9 Aggregate Gradation Plot for All Asphalt Mixtures

As stated in the literature review, SMA mixes utilise a gap-graded gradation that is also coarse-graded. National Stone, Sand and Gravel Association (NSSGA) (1991) defined gap-graded gradation as a gradation that contains only a small percentage of aggregate particles in the mid-size range and defined coarse-graded gradation as a gradation that, when plotted on the 0.45 power gradation graph, falls mostly below the 0.45 power maximum density line. The 0.45 power maximum density curve is used as a standard gradation graph in the hot mix asphalt (HMA) industry and is convenient for determining the maximum density line and adjusting gradation (Roberts et al., 1996). It is also plotted in Figures 5.10 to 5.15.

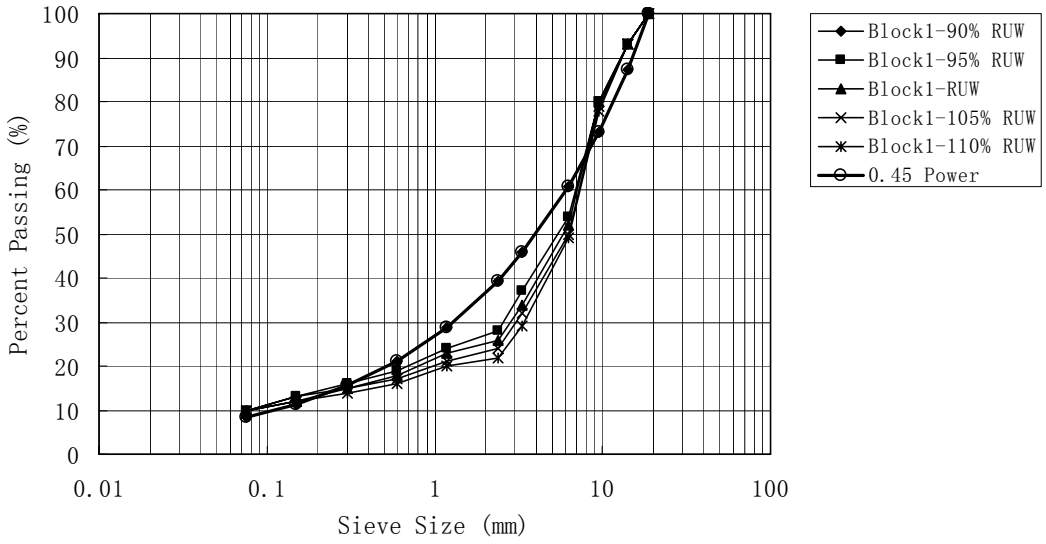

Figure 5.10 Blocks 1, 2.2, and 3.2 Aggregate Gradation Plot

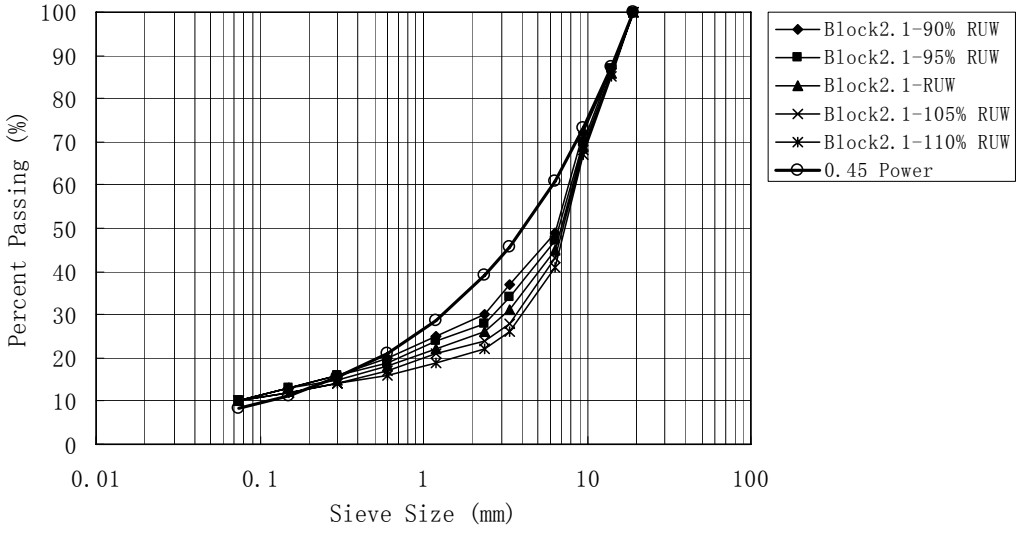

Figure 5.11 Block 2.1 Aggregate Gradation Plot

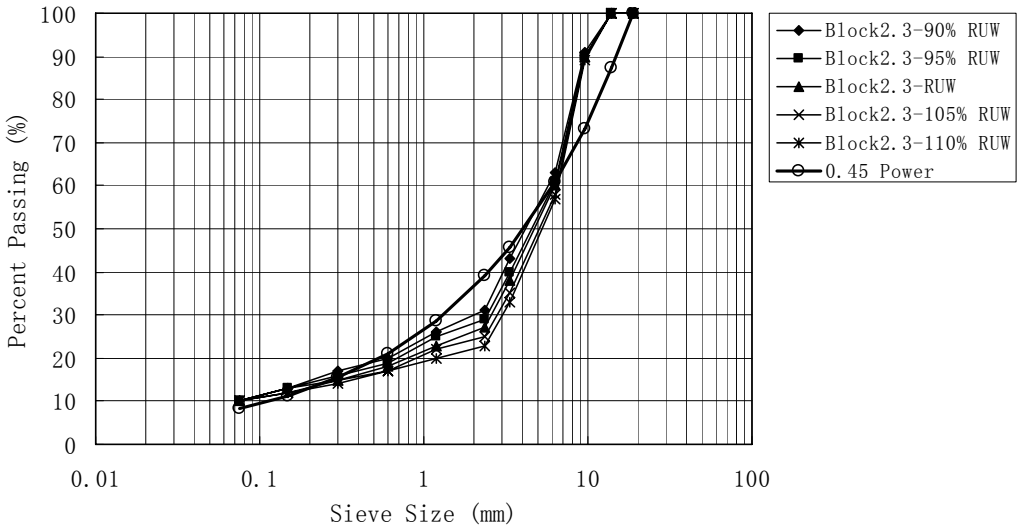

Figure 5.12 Block 2.3 Aggregate Gradation Plot

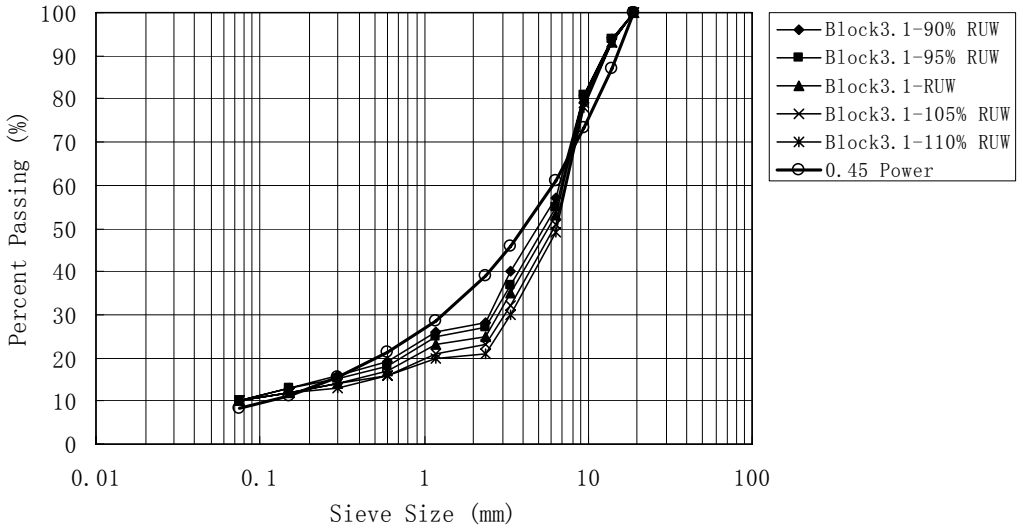

Figure 5.13 Block 3.1 Aggregate Gradation Plot

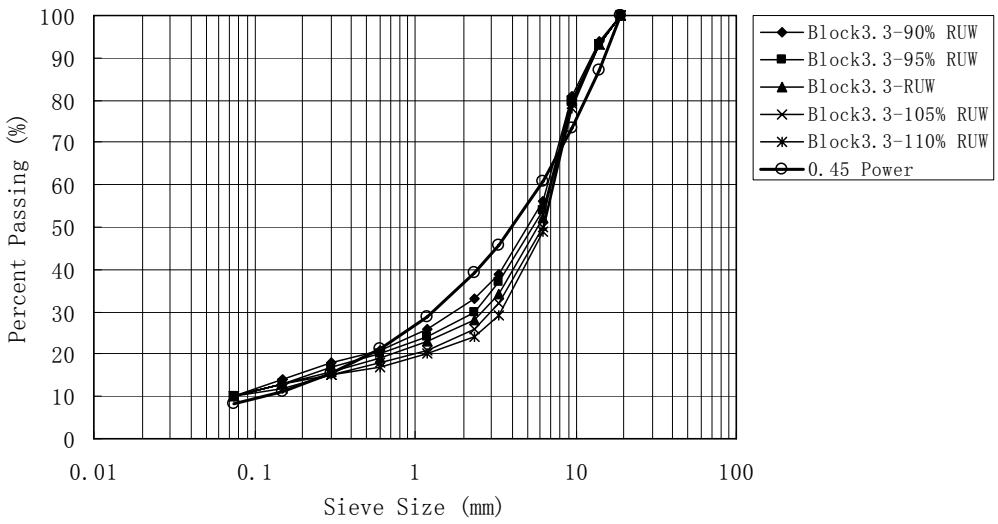

Figure 5.14 Block 3.3 Aggregate Gradation Plot

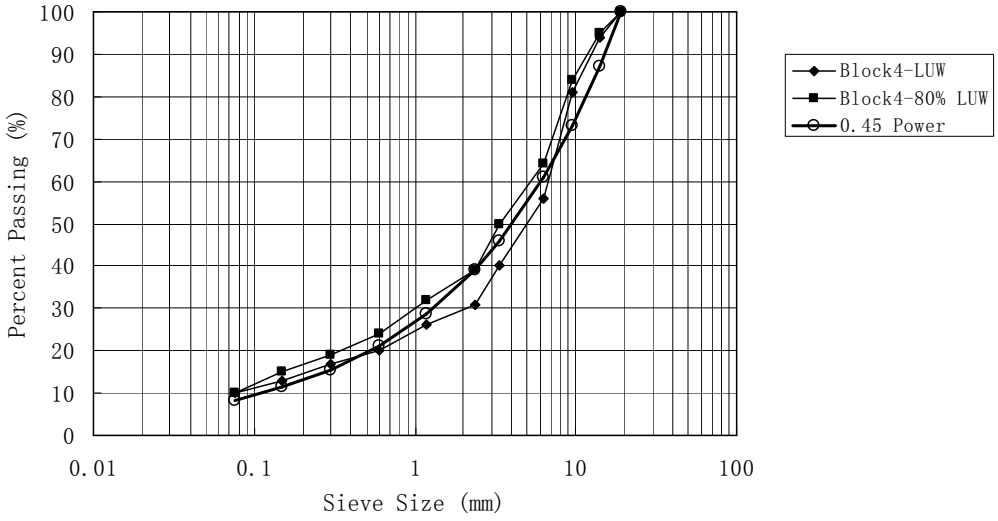

Figure 5.15 Block 4 Aggregate Gradation Plot

From Figures 5.10 to 5.15, the curves showed that all gradations were mostly below the 0.45 power maximum density line (from 9.5 mm sieve to 0.6 mm sieve), with the gradation with 80% LUW above the 0.45 power maximum density line, which indicated that the gradation with 80% LUW is a dense-graded gradation. This

complete coverage of aggregate gradations provided a detailed study of aggregate gradation and mixture volumetric properties and mechanical properties.

Chapter 3 has presented concepts for the analysis of aggregate gradations with the use of ratios for the coarse and fine aggregates. These ratios were developed from aggregate packing principles and allowed the gradation to be proportioned from the upper to the lower limit of the aggregate blend. The ratios calculated for the analysis of gradation are given in Table 5.11. These ratios will be used in the analysis of the volumetric test results and the mechanical property test results.

5.3 DRAINDOWN TEST RESULTS AND ANALYSIS

Draindown test results provide the information to determine whether the use of polymer (used in polymer modified binder) is enough to minimise asphalt binder to drain from the coarse aggregate structure.

To evaluate the effect of polymer, fifteen mixtures with three different binder contents and five different aggregate gradations (Blocks 1.1 to 1.3) were tested in the draindown test. The amount of draindown for each test was measured at 200 °C and 210 °C , and the results are shown in Table 5.12.

From Table 5.12, one can see that the draindown potential increased with an increase of asphalt binder content. However, the draindown values of all samples were far less than the maximum draindown limit of 0.3 percent. Some samples did not have draindown at all. The results indicated that the use of PMB was good enough to prevent the draindown problem of SMA at three different asphalt binder contents. Therefore, no cellulose fibre will be added in the study.

Table 5.11 Aggregate Ratios for the Evaluation of Aggregate Gradation

Sample Name	CA Ratio	FA_c Ratio	FA_f Ratio
Block 1.1-90% RUW	0.36	0.50	0.65
Block 1.1-95% RUW	0.37	0.51	0.68
Block 1.1- RUW	0.38	0.53	0.72
Block 1.1-105% RUW	0.36	0.53	0.71
Block 1.1-110% RUW	0.39	0.55	0.75
Block 2.1-90% RUW	0.24	0.54	0.65
Block 2.1-95% RUW	0.25	0.56	0.68
Block 2.1- RUW	0.25	0.58	0.72
Block 2.1-105% RUW	0.26	0.61	0.71
Block 2.1-110% RUW	0.25	0.62	0.75
Block 2.3-90% RUW	0.54	0.47	0.65
Block 2.3-95% RUW	0.54	0.48	0.68
Block 2.3- RUW	0.55	0.47	0.72
Block 2.3-105% RUW	0.55	0.49	0.71
Block 2.3-110% RUW	0.56	0.52	0.71
Block 3.1-90% RUW	0.40	0.48	0.68
Block 3.1-95% RUW	0.40	0.49	0.72
Block 3.1- RUW	0.38	0.49	0.71
Block 3.1-105% RUW	0.39	0.50	0.75
Block 3.1-110% RUW	0.37	0.53	0.75
Block 3.3-90% RUW	0.39	0.54	0.67
Block 3.3-95% RUW	0.37	0.54	0.65
Block 3.3- RUW	0.38	0.56	0.68
Block 3.3-105% RUW	0.36	0.56	0.72
Block 3.3-110% RUW	0.39	0.59	0.71
Block 4- LUW	0.36	0.50	0.65
Block 4-80% LUW	0.39	0.48	0.63

Note: Blocks 1.1 to 1.3 have the same aggregate gradations;
Blocks 1.1, 2.2, and 3.2 are the same asphalt mixtures;
CA Ratio – coarse aggregate ratio;
FA_C – fine aggregate coarse portion ratio;
FA_f – fine aggregate fine portion ratio.

Table 5.12 Draindown Test Data for Asphalt Mixtures

Sample Name		Draindown Value (%)					
		200 °C			210 °C		
		1	2	Avg.	1	2	Avg.
Block 1.1	90% RUW	0.02	0	0.01	0.02	0.01	0.02
	95% RUW	0	0.01	0.01	0.02	0	0.01
	RUW	0.01	0.02	0.02	0.03	0.01	0.02
	105% RUW	0.03	0.01	0.02	0.03	0.03	0.03
	110% RUW	0.04	0.05	0.05	0.05	0.05	0.05
Block 1.2	90% RUW	0.04	0.03	0.04	0.05	0.04	0.05
	95% RUW	0.04	0.02	0.03	0.06	0.04	0.05
	RUW	0.05	0.05	0.05	0.06	0.07	0.07
	105% RUW	0.03	0.06	0.05	0.05	0.07	0.06
	110% RUW	0.06	0.06	0.06	0.07	0.08	0.08
Block 1.3	90% RUW	0.06	0.08	0.07	0.08	0.09	0.09
	95% RUW	0.08	0.09	0.09	0.07	0.09	0.08
	RUW	0.09	0.10	0.10	0.09	0.10	0.10
	105% RUW	0.08	0.10	0.09	0.09	0.11	0.10
	110% RUW	0.11	0.09	0.10	0.11	0.12	0.12

5.4 VOLUMETRIC TEST RESULTS AND ANALYSIS

For SMA mixture design, stone-to-stone contact of coarse aggregate is a very important factor; on the other hand, it must fulfill the requirement of the volumetric properties. In this study, volumetric test results would provide an understanding on the effect of the change in coarse and fine aggregate gradations, design unit weight

of coarse aggregates, and asphalt binder content on the resulting mixture volumetric properties. It would also provide an indication of the mixture's probable pavement service performance.

Voids in the total mix (VTM), voids in the mineral aggregate (VMA), voids in the coarse aggregate (VCA), and the voids filled with asphalt (VFA) are the volumetric properties significantly affecting the durability and stability of mixtures. However, there are some other fundamental volumetric properties forming the basis for the previous four volumetric properties, which include bulk specific gravity of the combined aggregate (G_{sb}), percentage of absorbed asphalt (P_{ba}), percentage of effective asphalt (P_{be}), aggregate surface area factor (SA), asphalt film thickness (f_t), maximum theoretical specific gravity of mixtures (G_{mm}), and bulk specific gravity of compacted mixtures (G_{mb}). These fundamental volumetric properties are given in Tables 5.13 and 5.14. The volumetric properties of VTM, VMA, VCA, and VFA are given in Table 5.15.

Table 5.13 Fundamental Volumetric Properties of Combined Aggregate

Sample Name	G_{sb}	P_{ba} (%)	P_{be} (%)	SA (m^2/Kg)
Block 1.1-90% RUW	2.639	1.31	4.259	7.75
Block 1.1-95% RUW	2.642	1.28	4.288	7.59
Block 1.1- RUW	2.646	1.25	4.318	7.42
Block 1.1-105% RUW	2.649	1.22	4.346	7.26
Block 1.1-110% RUW	2.652	1.19	4.374	7.11
Block 1.2-90% RUW	2.639	1.31	4.765	7.75
Block 1.2-95% RUW	2.642	1.28	4.795	7.59
Block 1.2- RUW	2.646	1.25	4.824	7.42
Block 1.2-105% RUW	2.649	1.22	4.852	7.26
Block 1.2-110% RUW	2.652	1.19	4.880	7.11
Block 1.3-90% RUW	2.639	1.31	5.272	7.75
Block 1.3-95% RUW	2.642	1.28	5.301	7.59
Block 1.3- RUW	2.646	1.25	5.330	7.42
Block 1.3-105% RUW	2.649	1.22	5.359	7.26
Block 1.3-110% RUW	2.652	1.19	5.386	7.11
Block 2.1-90% RUW	2.645	1.27	4.295	7.70
Block 2.1-95% RUW	2.648	1.24	4.327	7.53
Block 2.1- RUW	2.652	1.21	4.357	7.37
Block 2.1-105% RUW	2.656	1.18	4.387	7.21
Block 2.1-110% RUW	2.659	1.15	4.417	7.05
Block 2.3-90% RUW	2.633	1.35	4.221	7.81
Block 2.3-95% RUW	2.636	1.32	4.249	7.65
Block 2.3- RUW	2.639	1.29	4.277	7.49
Block 2.3-105% RUW	2.642	1.27	4.304	7.33
Block 2.3-110% RUW	2.645	1.24	4.331	7.18
Block 3.1-90% RUW	2.638	1.32	4.254	7.59
Block 3.1-95% RUW	2.642	1.29	4.284	7.44
Block 3.1- RUW	2.645	1.26	4.313	7.30
Block 3.1-105% RUW	2.648	1.23	4.342	7.16
Block 3.1-110% RUW	2.652	1.20	4.370	7.02
Block 3.3-90% RUW	2.639	1.31	4.260	7.93
Block 3.3-95% RUW	2.642	1.28	4.290	7.75
Block 3.3- RUW	2.646	1.25	4.319	7.56
Block 3.3-105% RUW	2.649	1.22	4.347	7.39
Block 3.3-110% RUW	2.652	1.19	4.375	7.21
Block 4-LUW	2.638	1.32	4.254	7.78
Block 4-80% LUW	2.625	1.44	4.142	8.40
Note: Blocks 1.1, 2.2, and 3.2 are the same asphalt mixtures.				

Table 5.14 Fundamental Volumetric Properties of Asphalt Mixtures

Sample Name	G_{mm}	G_{mb}	f_t (μm)
Block 1.1-90% RUW	2.508	2.420	7.06
Block 1.1-95% RUW	2.509	2.417	7.21
Block 1.1- RUW	2.511	2.415	7.53
Block 1.1-105% RUW	2.512	2.413	7.54
Block 1.1-110% RUW	2.513	2.408	7.70
Block 1.2-90% RUW	2.490	2.408	7.74
Block 1.2-95% RUW	2.491	2.406	7.91
Block 1.2- RUW	2.492	2.406	8.09
Block 1.2-105% RUW	2.493	2.404	8.27
Block 1.2-110% RUW	2.494	2.402	8.45
Block 1.3-90% RUW	2.472	2.395	8.43
Block 1.3-95% RUW	2.473	2.391	8.61
Block 1.3- RUW	2.474	2.388	8.81
Block 1.3-105% RUW	2.475	2.386	9.00
Block 1.3-110% RUW	2.476	2.386	9.20
Block 2.1-90% RUW	2.511	2.418	7.11
Block 2.1-95% RUW	2.512	2.423	7.27
Block 2.1- RUW	2.514	2.431	7.43
Block 2.1-105% RUW	2.515	2.428	7.60
Block 2.1-110% RUW	2.516	2.421	7.77
Block 2.3-90% RUW	2.505	2.405	7.00
Block 2.3-95% RUW	2.506	2.397	7.15
Block 2.3- RUW	2.508	2.403	7.30
Block 2.3-105% RUW	2.509	2.387	7.47
Block 2.3-110% RUW	2.510	2.396	7.62
Block 3.1-90% RUW	2.508	2.415	7.21
Block 3.1-95% RUW	2.509	2.407	7.35
Block 3.1- RUW	2.510	2.403	7.50
Block 3.1-105% RUW	2.511	2.404	7.65
Block 3.1-110% RUW	2.513	2.410	7.80
Block 3.3-90% RUW	2.508	2.411	6.90
Block 3.3-95% RUW	2.509	2.410	7.06
Block 3.3- RUW	2.511	2.410	7.24
Block 3.3-105% RUW	2.512	2.404	7.41
Block 3.3-110% RUW	2.513	2.408	7.60
Block 4-LUW	2.508	2.403	7.03
Block 4-80% LUW	2.504	2.398	6.50
Note: Blocks 1.1, 2.2, and 3.2 are the same asphalt mixtures.			

Table 5.15 Four Volumetric Properties of Asphalt Mixtures

Sample Name	VTM	VMA	VCA	VFA
Block 1.1-90% RUW	3.51	13.32	47.99	73.67
Block 1.1-95% RUW	3.70	13.57	45.55	72.72
Block 1.1- RUW	3.79	13.72	43.06	72.37
Block 1.1-105% RUW	3.94	13.93	41.47	71.69
Block 1.1-110% RUW	4.16	14.19	39.08	70.72
Block 1.2-90% RUW	3.28	14.21	48.53	76.91
Block 1.2-95% RUW	3.42	14.41	46.08	76.27
Block 1.2- RUW	3.48	14.53	43.59	76.08
Block 1.2-105% RUW	3.58	14.69	41.99	75.64
Block 1.2-110% RUW	3.70	14.86	39.55	75.12
Block 1.3-90% RUW	3.09	15.12	49.07	79.57
Block 1.3-95% RUW	3.33	15.40	46.70	78.36
Block 1.3- RUW	3.49	15.61	44.30	77.66
Block 1.3-105% RUW	3.61	15.79	42.74	77.12
Block 1.3-110% RUW	3.64	15.88	40.27	77.09
Block 2.1-90% RUW	3.70	13.59	45.56	72.81
Block 2.1-95% RUW	3.55	13.54	42.94	73.83
Block 2.1- RUW	3.28	13.37	40.23	75.46
Block 2.1-105% RUW	3.46	13.60	37.79	74.58
Block 2.1-110% RUW	3.76	13.94	36.32	73.07
Block 2.3-90% RUW	4.01	13.68	50.80	70.95
Block 2.3-95% RUW	4.38	14.08	48.45	68.99
Block 2.3- RUW	4.16	13.95	46.65	70.25
Block 2.3-105% RUW	4.83	14.61	44.50	67.04
Block 2.3-110% RUW	4.52	14.40	42.65	68.66
Block 3.1-90% RUW	3.71	13.49	48.10	72.66
Block 3.1-95% RUW	4.07	13.89	45.75	70.69
Block 3.1- RUW	4.27	14.14	44.19	69.83
Block 3.1-105% RUW	4.30	14.23	41.68	69.93
Block 3.1-110% RUW	4.07	14.10	39.87	71.15
Block 3.3-90% RUW	3.89	13.67	47.34	71.57
Block 3.3-95% RUW	3.95	13.79	45.69	71.41
Block 3.3- RUW	4.02	13.94	43.20	71.12
Block 3.3-105% RUW	4.28	14.23	41.68	69.93
Block 3.3-110% RUW	4.15	14.19	39.08	70.73
Block 4-LUW	4.20	13.93	48.36	69.88
Block 4-80% LUW	4.22	13.68	56.84	69.15
Note: Blocks 1.1, 2.2, and 3.2 are the same asphalt mixtures.				

5.4.1 Fundamental Volumetrics

Fundamental volumetric properties form the basis of the main volumetric properties. Bulk specific gravity of the combined aggregate, percentage of absorbed asphalt, percentage of effective asphalt, combined with different aggregate gradations and asphalt binder contents for all experimental blocks, can be calculated from the single size sieve results listed in Table 5.1. Aggregate surface area is calculated from the aggregate gradation using the procedure outlined in the Asphalt Institute's MS-2 (1993). It was used in calculating asphalt film thickness.

Studies have shown that asphalt mix durability is directly related to asphalt film thickness (Kandhal et al., 1998). It is highly unlikely that all the particles in a mix have the same film thickness of asphalt coating. Fine aggregate particles may have a much thicker coating as compared to the coarse aggregate particles, and in fact, for all practical purpose, some very fine particles might simply be embedded in the asphalt cement/filler mortar system. Therefore, the term 'film thickness' in this study is assumed to the 'average film thickness' for the purpose of calculation. The gradation of the aggregate determines the aggregate surface area, and together with asphalt content and absorption determines the asphalt film thickness, which is the amount of free asphalt available to cover the aggregates. For the same aggregate gradation, different film thickness reflects different asphalt binder content. With the volume of coarse aggregate in the mixtures increased, the film thickness would increase too. This trend is observed in all of the blocks as shown in Table 5.14.

The maximum theoretical specific gravity of an asphalt mixture (G_{mm}) is used as the point where the complete volume is taken by aggregate and asphalt and forms the basis for many volumetric properties. It is expected that the trend for all G_{mm} measurements would be consistent with a change in the volume of coarse aggregate.

As coarse aggregate has a higher specific gravity than fine aggregate, samples with increased coarse aggregate would have increased G_{mm} for the mixture. This trend is observed in all of the blocks of the experiment as shown in Table 5.14. The amount of change in G_{mm} with a change in gradation is important in the quality control of asphalt mixtures. Changes in G_{mm} affect the volumetric properties measured in the lab for quality control, and affect the resulting measured in place density of the compacted pavement.

The bulk specific gravity of the compacted mixtures (G_{mb}) in this study shows the compactability of the mixtures. At the same asphalt content, preparation technique, and compactive effort, different G_{mb} indicates different resistance to densification of the mixture. Because the G_{mb} are to calculate the mixture air voids and the air voids are used as a mixture design criterion, the analysis of G_{mb} data is given through a discussion of mixture air voids.

5.4.2 Voids in the Total Mix (VTM)

The design of asphalt mixtures specifies the control of air voids in the laboratory compacted sample, therefore, an understanding on the change of air voids with change in aggregate gradation and asphalt content is essential. The air voids in an asphalt mixture allow void space for the expanding asphalt binder during temperature increase. A properly designed asphalt mixture will contain enough air voids to allow for the expansion of the asphalt.

If the total air void structure in a mixture is not sufficient for the total expansion of the asphalt cement, the mixture will be lubricated by the additional asphalt binder and will flow. This flow in the asphalt material is reflected as rutting. If the total

voids in the asphalt mixture is greater than necessary, problems can develop with permeability, stripping, and rutting. With an increase in the volume of the air voids in the mixture, the voids will become interconnected. Interconnected air voids would allow water to permeate through the material. With water trapped in the compacted asphalt mixture, stripping of the asphalt binder can occur, thus, creating durability problems. Laboratory study indicated that air voids between 3-4% are considered to be applicable for SMA mixture (Bellin, 1997 and Brown and Mallick, 1994).

As air voids is a fundamental property in the design of asphalt mixtures, an understanding of the relationship between aggregate gradation and air voids is important in the development of asphalt mixture design. The air void data for the 37 mixtures of this experiment are given in Table 5.15. Figure 5.16 gives a plot of the air void data for each experimental block.

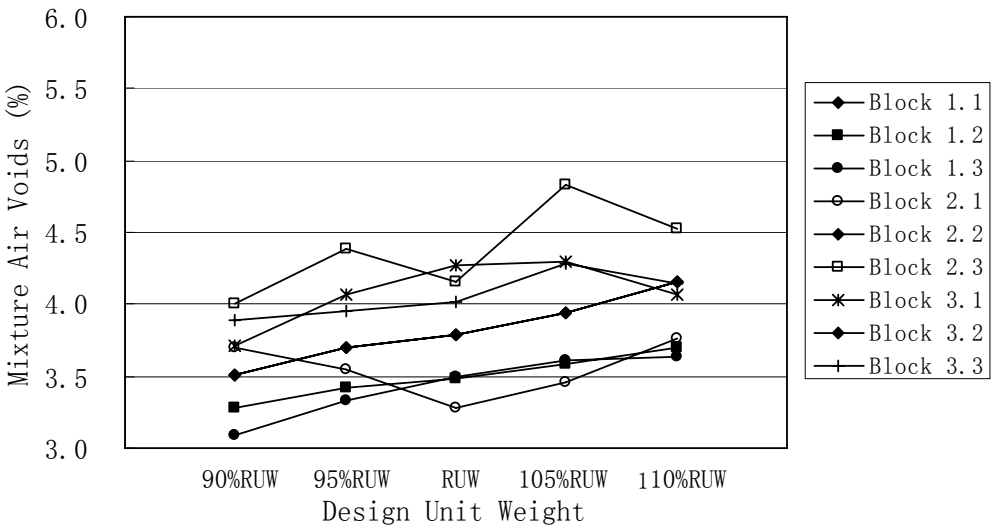

Figure 5.16 Air Void Plot for Asphalt Mixtures by Experimental Blocks

5.4.2.1 Discussion of Asphalt Content, Design Unit Weight of Coarse Aggregate, Aggregate Gradation and Air Voids

The experimental blocks in the testing scheme showed a similar, but not identical trend with an increase in the volume of coarse aggregate (Figure 5.16). The air voids in all experimental blocks showed a minimum at 90% RUW except Block 2.1 in which the minimum point occurred when the design unit weight is equal to RUW.

Figure 5.16 plotted all air voids of 37 asphalt mixtures in one figure, which gave an overview on the difference between the blocks and levels of coarse aggregate design unit weight. Figure 5.17 through Figure 5.19 showed the plots for each block of the experiment, thereby allowing individual comparison of the change of asphalt content, coarse aggregate gradation, and fine aggregate gradation for each individual block.

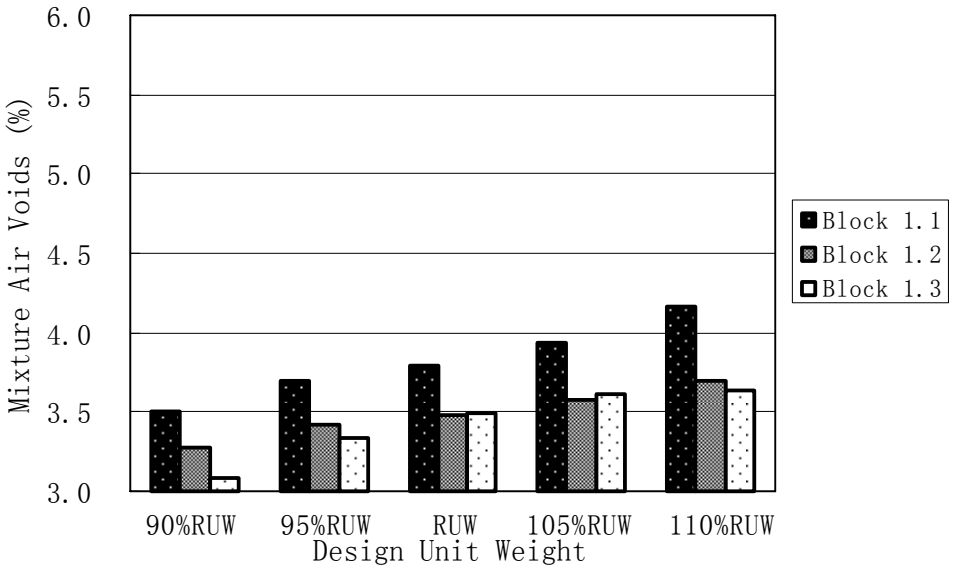

Figure 5.17 Air Void Plot for Experimental Block 1 Mixtures

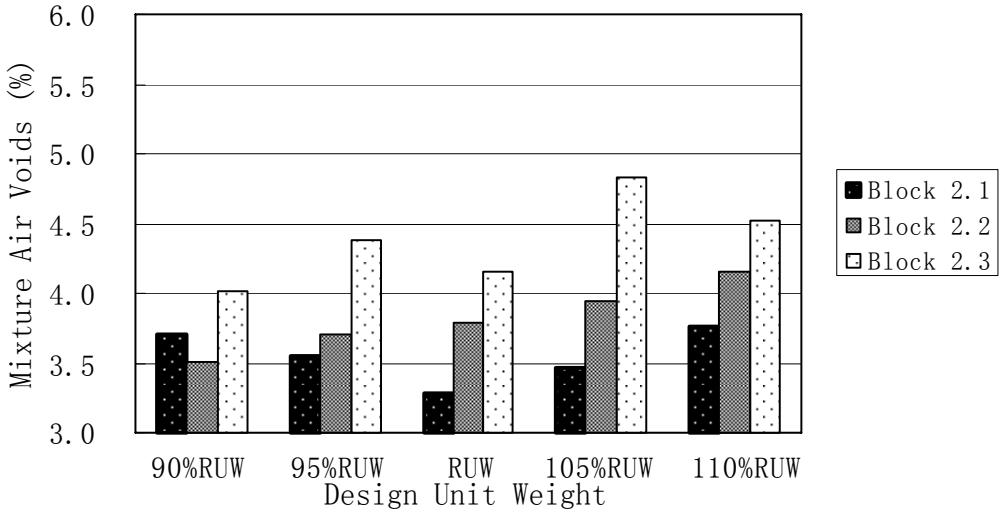

Figure 5.18 Air Void Plot for Experimental Block 2 Mixtures

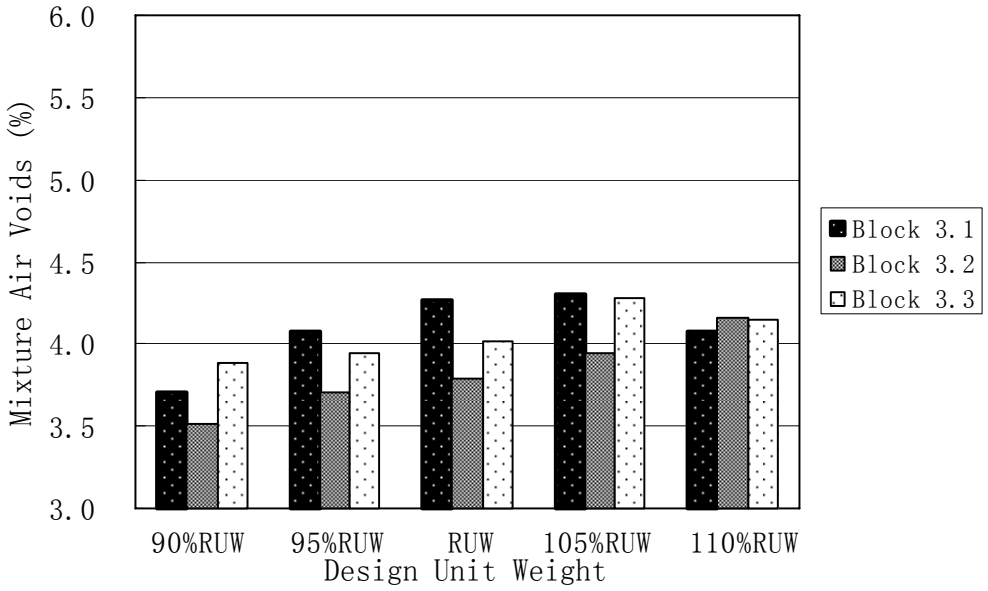

Figure 5.19 Air Void Plot for Experimental Block 3 Mixtures

Figure 5.17 showed the change in air voids with an increase of asphalt content in Block 1 mixtures. The change in asphalt binder content changes the asphalt film

thickness available to coat the aggregate, which changes the amount of asphalt binder filled in the void space. From Figure 5.17, it is noted that the air voids decreased with an increase in asphalt binder content for all levels of design unit weight. Since all mixtures were prepared under the same compactive effort, higher asphalt binder content means more void space is occupied by asphalt binder and results in lower air voids for the mixtures having the same aggregate gradation.

Figure 5.18 showed the change in air voids with different coarse aggregate gradations in Block 2 mixtures. The air voids increased for which design unit weight of coarse aggregate equals to or larger than 95% RUW when the coarse aggregate gradation changed from upper limit to lower limit. The change in the gradation of coarse aggregate changes the void structure in the coarse aggregate, which changes the way of the fine aggregate orientation. It is also noted from Figure 5.18 that the effect of coarse aggregate gradation limit on the air voids of mixtures with different design unit weights (coarse aggregate volume) showed a different trend. The medium gradation limit of coarse aggregate (Block 2.2) contains a balanced gradation of coarse aggregate, which allows the coarse aggregate to compact the fine aggregate in the mix. With an increase in the coarse aggregate design unit weight, the coarse aggregate developed stone-to-stone contact and is no longer able to compact the fine aggregate, yielding an increase of air voids. While the mixtures using an upper gradation limit of coarse aggregate (Block 2.1) produces lesser voids in the coarse aggregates that are larger in size. This larger void size in the coarse aggregates and fewer “interceptor” aggregates would give a larger space for the fine aggregates to occupy. With the larger void space in the coarse aggregates and fewer “interceptor” aggregates, it appears that the fine aggregates are compacted because appreciable coarse aggregate stone-to-stone contact develops until the design unit weight is the rodded unit weight and the air voids begin to increase, indicating an increase of resistance to compaction. Using a

lower gradation limit of coarse aggregate, in Block 2.3, the amount of "interceptor" aggregates is increased, thus, an increase in the voids in the coarse aggregate. This increase in coarse aggregate voids is apparent in the greater voids in the mixture. The average voids for Block 2.1 is 3.55% and for Block 2.3 is 4.38%. The change in the volume of coarse aggregate for Block 2.3 produces a more sensitive response of air voids than in other blocks. A lower gradation limit of coarse aggregate appears to accentuate the change in coarse aggregate volume when analysed by the resulting air voids.

Block 3 is used in the comparison of fine aggregate gradation. Figure 5.19 showed the air void data of it. When the fine aggregate gradation changed from medium limit to upper (Block 3.1) or lower limit (Block 3.3), the air voids in each level of the design unit weight both increased. However, this change in the air voids is much smaller than other blocks. Similar to the results of Block 3.2, the influence of coarse aggregate design unit weight is observed by an increase of the air voids in Blocks 3.1 and 3.3 with an increase in the volume of coarse aggregate up to 105% RUW.

An analysis of variance (ANOVA) using data from all experimental blocks was performed to study the effect of changing coarse aggregate gradation (CA), fine aggregate gradation (FA), design unit weight (DUW), and asphalt binder content (AC) on the resulting air voids of the mixture. The results from the ANOVA are given in Table 5.16. The ANOVA results showed that statistical differences ($p \leq 0.05$) in the air voids exist with a change in the gradation of the component aggregates, change in the design unit weight of coarse aggregate and change in the asphalt binder content. Changing the gradation of the coarse aggregate, design unit weight, and asphalt content have significant effect on changing the air voids. The change in the fine aggregate gradation was also significant, but its effect is not as

dominating as compared to other variables. The relevant effect of each of the treatments is reflected by the magnitude of the F value.

Table 5.16 ANOVA for Air Voids

Source	DF	Sum of Square	Mean of Square	F value	P > F
Model	9	2.30661111	0.25629012	23.15	<0.0001
Error	8	0.08855000	0.01106875		
Corrected Total	17	2.39516111			
R-Square	**Coeff. Var.**		**Root MSE**	**VTM Mean**	
0.963030	2.752138		0.105208	3.822778	
Source	**DF**	**Type III SS**	**Mean of Square**	**F value**	**P > F**
DUW	3	0.50021667	0.16673889	15.06	0.0012
CA	1	0.25215000	0.25215000	22.78	0.0014
FA	1	0.06000000	0.06000000	5.42	0.0483
AC	1	0.25626667	0.25626667	23.15	0.0013

The ANOVA of the entire data set showed the variables that affect the air voids in an asphalt mixture. This analysis is taken on the entire data set in order to understand the overall trend. Additional analysis, through the use of ANOVA, on the data points from each individual block (Blocks 1, 2, and 3) gave the same result as the ANOVA using the entire data.

Taking the mean values from the ANOVA, the general trend in air voids is established for a change in design unit weight. This general trend is shown in Figure 5.20. The general trend showed that with an increase in the volume of coarse aggregate, the air voids in the mixture increase until the design unit weight is 105% RUW. After that, the air voids decreased gradually. This increase in voids is derived from aggregate interlock. With an increase in the volume of coarse aggregate, the

large aggregate particles interlock and resist deformation, thereby giving an increase of voids in the mixture.

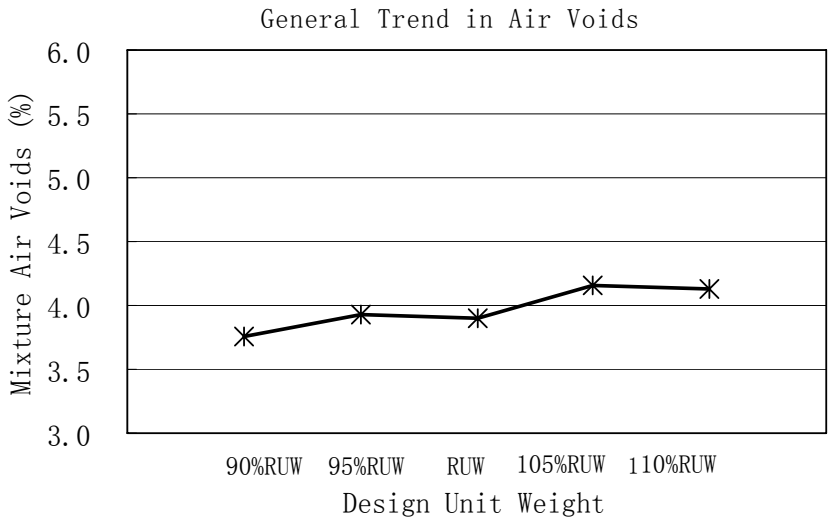

Figure 5.20 General Trend in Air Voids for Asphalt Mixtures

5.4.2.2 Evaluation of Aggregate Ratios for Air Voids

The use of aggregate ratios for the analysis of gradation is proposed as a method for understanding the aggregate packing and resulting voids. The asphalt film thickness reflects the asphalt binder content and is directly related to asphalt mix durability. A multiple regression was performed using the aggregate ratios and film thickness to fit a model with the resulting air voids. All 35 mixtures (not including the mixtures with LUW and 80% LUW) were used in the development of the models. Table 5.17 summarises the results of the regression analyses. The model with the CA, FA_c, FA_f ratio, and asphalt film thickness f_t gives a good result with an R-Square value of 0.74. However, the estimation of the coefficient of FA_c in the model was not significant at 95% confidence level ($P>0.05$). It should be excluded from the predicted model. An additional model was developed using the CA ratio, FA_f, and f_t.

This model described the air voids with a better R-Square of 0.75 and the p values of all coefficients are much smaller than 0.05. Equation 5.1 shows this relationship of air voids with aggregate ratios and asphalt film thickness:

$$VTM=1.27+2.75CA+6.17FA_f-0.37f_t \quad (5.1)$$

The predicted air voids and measured air voids from the model are shown in Figure 5.21. The model was developed using a multiple regression optimisation routine that will display the order that variables were allowed into the model.

Table 5.17 Regression Analysis Results of Air Voids

Independent Variables	DF	Estimated Parameter	Standard Error (SE)	R-Square	t value	P > |t|
Intercept	1	0.64799	1.00820		4.64	<.0001
CA	1	3.22749	0.63345		5.10	<.0001
FA_c	1	1.59642	1.49202	0.74	1.07	0.2932
FA_f	1	5.49310	1.36848		4.01	0.0004
f_t	1	-0.35765	0.06943		-5.15	<.0001

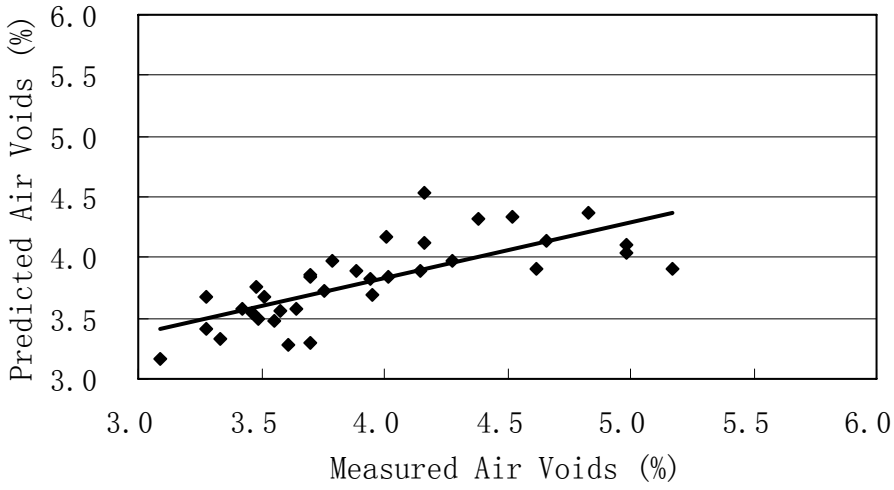

Figure 5.21 Measured and Predicted Air Voids Using Regression Model

5.4.3 Voids in the Mineral Aggregate (VMA)

Voids in the mineral aggregate are desired in an asphalt mixture to ensure durability. A requirement for adequate VMA will ensure that a mixture contains the asphalt binder content necessary to form a thick film of asphalt over the aggregate particles that will resist environmental effects and develop a durable material.

The calculation of VMA is based on the bulk specific gravity of compacted mixture, the maximum theoretical specific gravity of the mixture, and the percentage of asphalt binder in the mixture. A change in aggregate gradation would affect VMA. This, in turn, would affect the workability, compaction and cohesion of the mixture. Since the percentage of asphalt binder in the mixture for Blocks 2 and 3 was kept the same in the experiment, the analysis of the effect of coarse aggregate gradation, fine aggregate gradation, and design unit weight on VMA showed the same trend as that of the VTM. The factors that change the air voids are the same factors that change the VMA of these mixtures in the design of the experiment.

The change in the asphalt binder content has a significant effect on the VMA of the mixtures. With the increase of the percentage of asphalt binder, the VMA increased too. Figure 5.22 shows the change in VMA with an increase of asphalt binder content in Block 1 mixtures. It can be seen that the mixtures with 6.5% asphalt content have the highest VMA. For a fixed design void content, higher VMA means higher asphalt content, and higher asphalt content would be more rut susceptible. Since the air voids of the mixtures in Block 1 were mostly between 3-4%, which can fulfil the requirement of SMA mixture design, the 5.5% asphalt binder content seems to be enough for the designed aggregate gradation of SMA mixture. This would be further studied in the mechanical property tests.

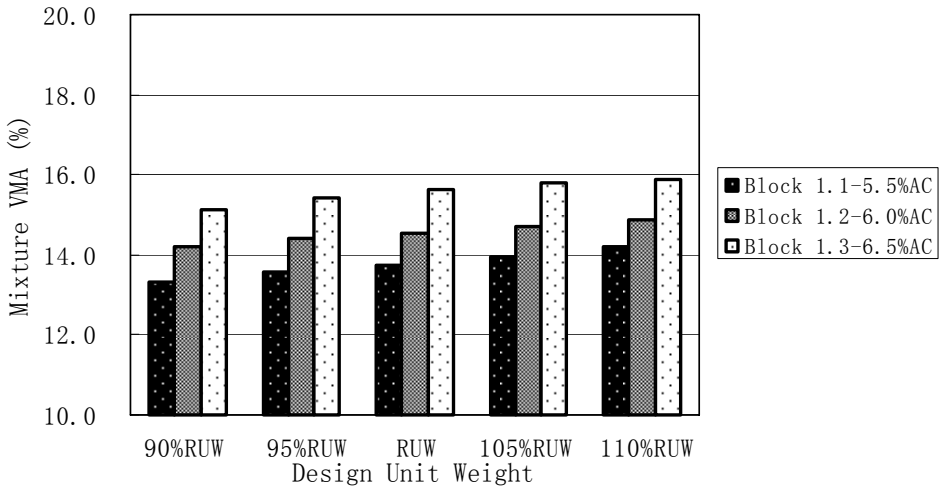

Figure 5.22 VMA Plot for Experimental Block 1 Mixtures

5.4.4 Voids in the Coarse Aggregate (VCA)

Voids of the coarse aggregate in the mixture (VCA_{mix}) are determined for the coarse portion of the aggregate blend as a property that identifies the existence of a coarse aggregate skeleton with stone-to-stone contact. A coarse aggregate skeleton is developed when the VCA_{mix} in the mixture is equal to or less than the VCA_{dry} of the coarse aggregate in the dry rodded condition (Brown and Mallick, 1995). VCA_{dry} can be tested in accordance with ASTM C29. It is used as a design criterion in SMA mixtures as an identifier of coarse aggregate skeleton when compared with the design unit weight of coarse aggregate.

Figures 5.23 to 5.25 show the relationship between VCA_{mix} and VCA_{dry} for Blocks 1, 2, and 3, respectively. One can infer that coarse aggregate stone-to-stone contact is developed when the design unit weight of coarse aggregate is equal to or above 95% RUW of the coarse aggregate (for Block 2.1, it is equal to 90% RUW). Above this level, less amount of fine aggregate was likely to be contained within the coarse

aggregate structure. VCA_{mix} values gradually decreased as stone-to-stone contact increased. When the packing mechanism between stones takes place, the coarse aggregates become closely packed and cannot be moved any closer resulting in stone-to-stone contact being fully developed. At this point, one can infer that the mixtures have the maximum internal resistance. Additionally, from Figures 5.23 and 5.25, it is noted that the change of asphalt binder content and fine aggregate gradation did not change the development of coarse aggregate stone-to-stone contact. When the design unit weight of coarse aggregate is equal to or above 95% RUW, one can infer that coarse aggregate stone-to-stone contact begins to develop. However, when the coarse aggregate gradation was changed, the development of coarse aggregate stone-to-stone contact was affected. The mixtures in Block 2.1 using an upper gradation limit of coarse aggregate produced fewer "interceptor" aggregates, which make the "larger" coarse aggregate (size is larger than the half sieve of NMAS) develop stone-to-stone contact in the early stage. In Figure 5.24, this is expressed as the value of VCA_{mix} which is smaller than VCA_{dry} when the design unit weight is equal to 90% RUW for Block 2.1. For the mixtures using a lower gradation limit of coarse aggregation (Block 2.3), the stone-to-stone contact of coarse aggregate was still not developed at 95% RUW.

In order to compare the relationship of SMA mixtures and dense-graded mixtures with VCA, Figure 5.26 gives a plot of VCA_{mix} and VCA_{dry} from the mixture with 80% LUW (dense-graded mixture) to the mixture with 110% RUW (SMA mixture). For the design unit weight of coarse aggregate that is near to or below the loose unit weight, which is dense-graded mixture, fine aggregate controlled the aggregate skeleton and coarse aggregate is "floating" between the fine aggregates (VCA_{mix} above VCA_{dry}). It means that the coarse aggregate was not touching each other as the fine aggregate pushed for more "space" within the asphalt mixture. Thus, stone-to-stone contact was not formed and the mixture would have lower internal

resistance.

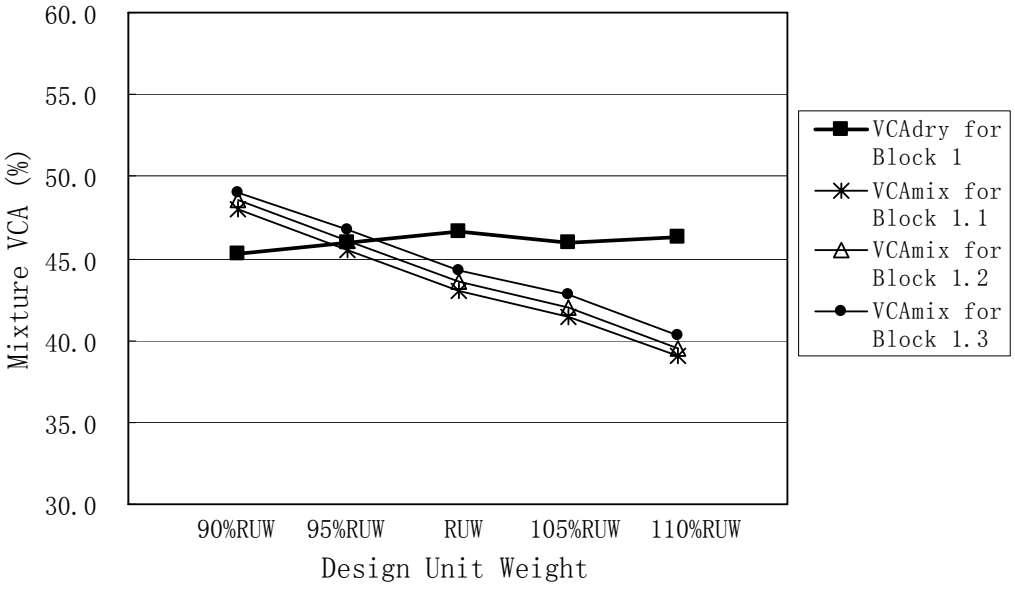

Figure 5.23 VCA Plot for Experimental Block 1 Mixtures

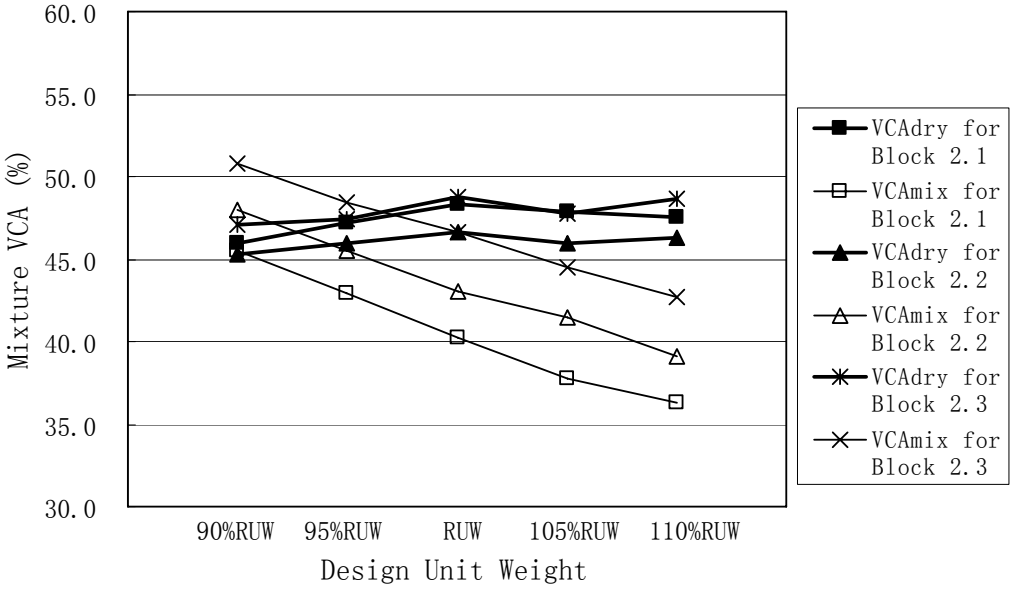

Figure 5.24 VCA Plot for Experimental Block 2 Mixtures

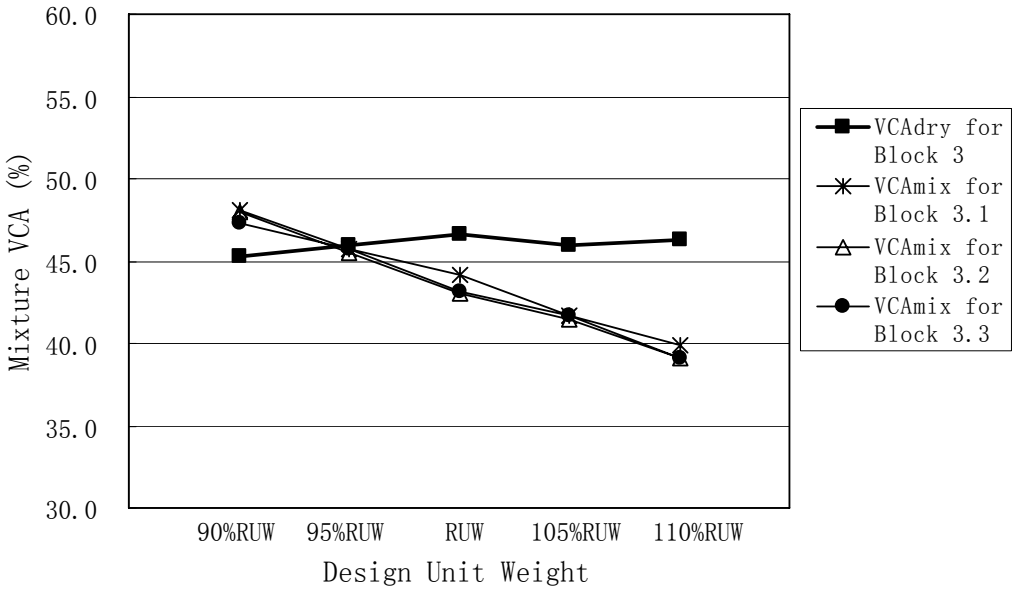

Figure 5.25 VCA Plot for Experimental Block 3 Mixtures

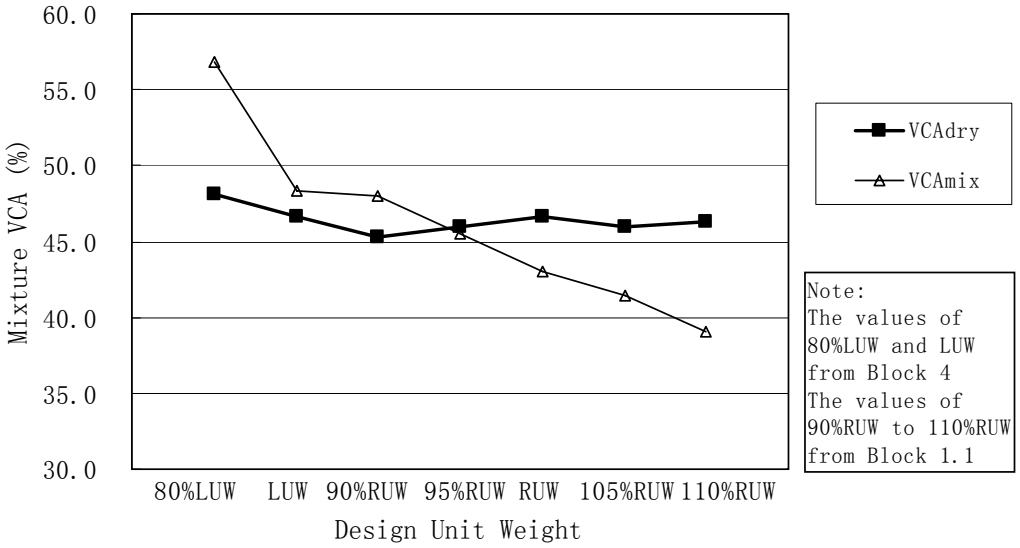

Figure 5.26 VCA Plot for Comparison of SMA and Dense-Graded Mixtures

5.4.5 Summary of Volumetric Test Results

Voids in an asphalt mixture, which are fundamental in mixture design, are highly influenced by change in the volume of coarse aggregate in the mixture. With mixtures controlled by the concepts as presented in this study, this volume change in aggregate can be designed by changing the design unit weight of the coarse aggregate in the mixture.

Changing the gradation of coarse aggregate changes the size of the voids in the coarse aggregates, which in turn, affects the resulting voids in the mixture. Mixtures with an upper limit gradation of coarse aggregates, indicated by a low CA ratio, are able to provide a larger void space in the coarse aggregates. The fine aggregates in this void space are compacted more by the coarse aggregates than that of the mixtures with a higher CA ratio. Mixtures with a high CA ratio would contain interceptor size aggregates. These interceptors would change the void structure in the coarse aggregates that may result in lesser compaction of the fine aggregates by the coarse aggregates.

The gradation of the fine aggregates will change the resulting voids in the mixture. The change in the fine aggregate gradation would change the degree to which the fine aggregate compacts, thereby changing the resulting air voids. However, this change is very small compared to other variables.

The change in asphalt binder content changes the air voids in the mixture. Since all mixtures were prepared under the same compactive effort, a higher asphalt binder content would mean more void space being occupied by asphalt binder and would result in lower air voids for the mixtures having the same aggregate gradation.

Taken collectively, with an increase in the volume of coarse aggregate, the large aggregate particles interlock and resist deformation, thereby giving an increase of voids in the mixture.

VCA_{dry} and VCA_{mix} can be used as a design criterion in SMA mixtures as an identifier of coarse aggregate skeleton when compared with the design unit weight of coarse aggregate. In this study, coarse aggregate stone-to-stone contact is developed when the design unit weight of coarse aggregate is equal to or above 95% RUW of coarse aggregate. The change of coarse aggregate gradation had significant effect on the development of coarse aggregate skeleton. It can result in varying degree stone-to-stone contact under the lower or higher design unit weight. The ratios (CA ratio and FA_f ratio) used for the analysis of gradation and the asphalt film thickness used for the analysis of asphalt binder are good tools for understanding the voids in an asphalt mixture. Based on the data from this experiment, it is possible to develop an adequate prediction model (Equation 5.1), based on the aggregate ratios and asphalt film thickness, to describe the resulting air voids in the mixture. This model is confined within the range of data set, but shows potential for expansion to the larger set of asphalt mixtures.

5.5 MECHANICAL PROPERTY TEST RESULTS AND ANALYSIS

The mechanical properties of an asphalt mixture will indicate the performance of the mixture under traffic. The measurement of the engineering properties, including strength and modulus, is used to determine indices that can rank the performance of asphalt materials.

A testing scheme, as outlined in Chapter 4, was proposed to investigate the mechanical properties of the SMA mixtures. This testing scheme includes resilient modulus test, repeated load uniaxial test, and wheel tracking test. The mechanical property test results would provide the information to determine the effect of changing the design unit weight of coarse aggregate, coarse aggregate gradation, fine aggregate gradation, and the asphalt binder content on the mechanical properties of the resulting mixtures.

5.5.1 Resilient Modulus Test Results and Analysis

The resilient modulus test is designed to measure the stiffness or load bearing capacity of asphalt stabilised aggregate mixtures. The resilient modulus of 37 mixtures for all blocks was measured at 25 °C . The test results are shown in Table 5.18. The reported values for the test were the average results of 30 (6 samples × 5 replicates) repeated tests in each case.

An analysis of variance (ANOVA) was performed to study the effect of changing coarse aggregate gradation (CA), fine aggregate gradation (FA), design unit weight (DUW), and asphalt binder content (AC) on the resulting resilient modulus of the mixtures. The results are given in Table 5.19. The ANOVA results showed that changing the gradation of the coarse aggregate and asphalt content have a significant effect on the resilient modulus. The effect of changing in the fine aggregate gradation and design unit weight is not significant as compared to other variables. The relevant effect of each of the treatments is revealed by the magnitude of the F value.

Table 5.18 Resilient Modulus Test Results for Asphalt Mixtures

Sample Name	Resilient Modulus (MPa)	Standard Deviation (MPa)
Block 1.1-90% RUW	2629	510
Block 1.1-95% RUW	2417	266
Block 1.1- RUW	2235	251
Block 1.1-105% RUW	2059	168
Block 1.1-110% RUW	1992	180
Block 1.2-90% RUW	1912	365
Block 1.2-95% RUW	1855	386
Block 1.2- RUW	2015	228
Block 1.2-105% RUW	2060	219
Block 1.2-110% RUW	1863	330
Block 1.3-90% RUW	1780	236
Block 1.3-95% RUW	1637	256
Block 1.3- RUW	1555	174
Block 1.3-105% RUW	1574	202
Block 1.3-110% RUW	1477	299
Block 2.1-90% RUW	2046	636
Block 2.1-95% RUW	1854	328
Block 2.1- RUW	1970	424
Block 2.1-105% RUW	2108	534
Block 2.1-110% RUW	2293	449
Block 2.3-90% RUW	1810	310
Block 2.3-95% RUW	1761	507
Block 2.3- RUW	1726	504
Block 2.3-105% RUW	1790	303
Block 2.3-110% RUW	2006	434
Block 3.1-90% RUW	1657	560
Block 3.1-95% RUW	2029	378
Block 3.1- RUW	1903	534
Block 3.1-105% RUW	1996	480
Block 3.1-110% RUW	1738	439
Block 3.3-90% RUW	2046	571
Block 3.3-95% RUW	2109	425
Block 3.3- RUW	1871	337
Block 3.3-105% RUW	2000	330
Block 3.3-110% RUW	2171	521
Block 4-LUW	1657	352
Block 4-80% LUW	1974	308
Note: Blocks 1.1, 2.2, and 3.2 are the same asphalt mixtures.		

Table 5.19 ANOVA for Resilient Modulus

Source	DF	Sum of Square	Mean of Square	F value	P > F
Model	9	888293.944	98699.327	2.98	0.0693
Error	8	264706.500	33088.313		
Corrected Total	17	1153000.444			
R-Square	**Coeff. Var.**		**Root MSE**	**M_R Mean**	
0.770419	9.301803		181.9019	1955.556	
Source	**DF**	**Type III SS**	**Mean of Square**	**F value**	**P > F**
DUW	3	132006.5000	44002.1667	1.33	0.3310
CA	1	287766.0000	287766.0000	8.70	0.0185
FA	1	98304.0000	98304.0000	2.97	0.1231
AC	1	696322.6667	696322.6667	21.04	0.0018

Figure 5.27 shows the effect of change in asphalt binder content on the resilient modulus for the asphalt mixtures (Block 1). With an increase of asphalt binder content, the resilient modulus decreased greatly in each level of design unit weight. The resilient modulus of the mixtures with 5.5% asphalt binder content was much higher than that of the mixtures with 6.5% asphalt binder content. Since the asphalt cement has much lower stiffness than that of aggregate, higher asphalt binder content would have a greater effect on the resilient modulus of the mixtures and would result in lower resilient modulus for the mixtures with the same aggregate gradation.

Figure 5.28 showed the change in resilient modulus with different coarse aggregate gradations in Block 2 mixtures. Although the change in coarse aggregate gradation has a significant effect on the resilient modulus, no clear trend can be observed,

which may be primarily due to the high variability.

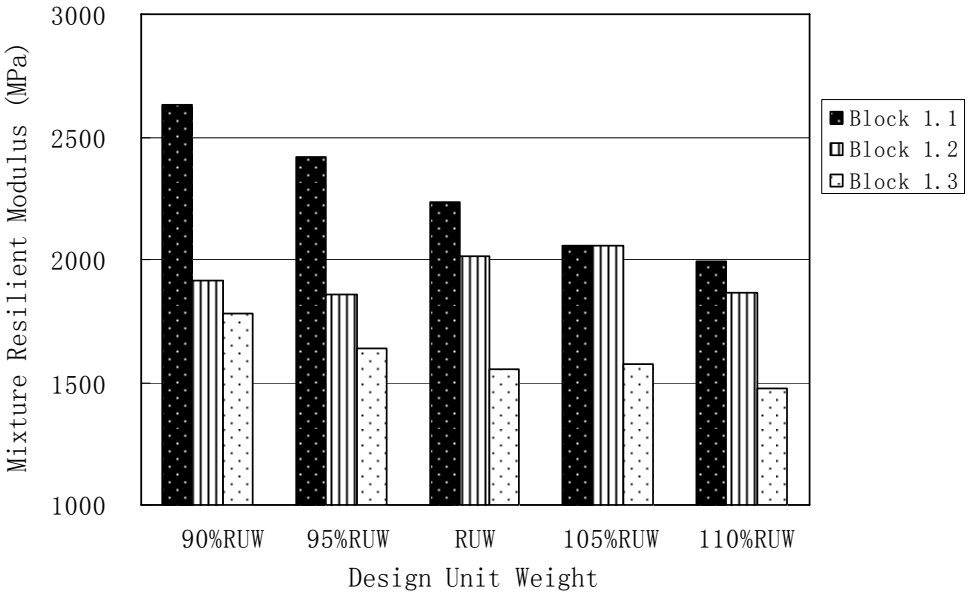

Figure 5.27 Resilient Modulus Plot for Experimental Block 1 Mixtures

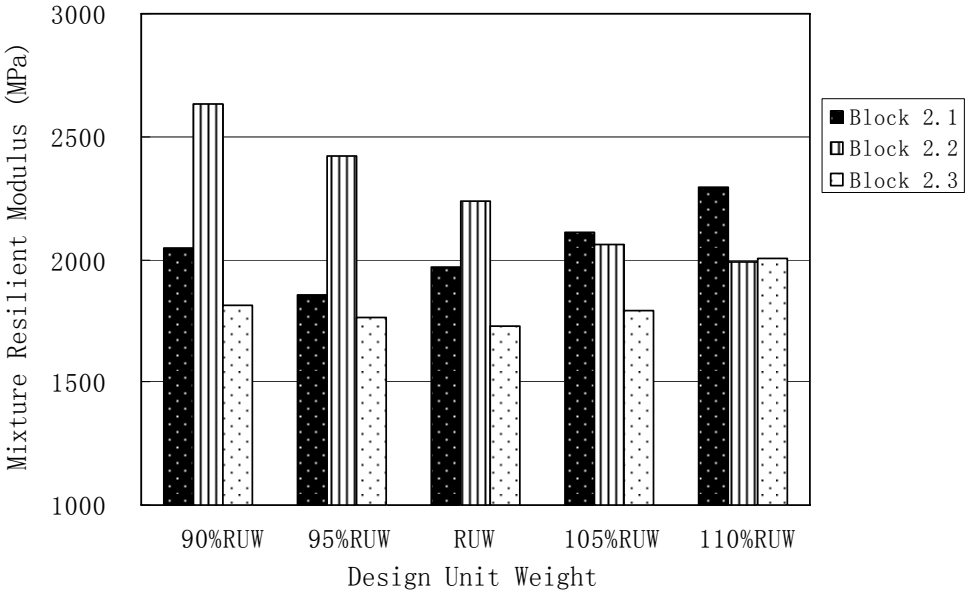

Figure 5.28 Resilient Modulus Plot for Experimental Block 2 Mixtures

The study by Brown (1993a) indicated that the resilient modulus is a highly variable test and has not been shown to be related to the performance of SMA mixtures. In order to study whether the resilient modulus is related to coarse aggregate stone-to-stone contact, the effect of a change in the design unit weight was analysed. Figure 5.29 shows the effect of change in the design unit weight (from 80% LUW to 110% DUW) on the resilient modulus for the asphalt mixtures in Blocks 1.1 and 4, which have the same coarse and fine aggregate gradation and asphalt binder content. No clear trend can be observed with a change in the design unit weight. In examining the data from 80% LUW to 110% RUW, where mixtures were typically designed under the proposed concepts, the change in design unit weight would cause a decrease or an increase in the resilient modulus. According to the analysis in Section 5.4.4 (Figure 5.26), coarse aggregate stone-to-stone contact is developed gradually when the design unit weight of coarse aggregate increased from 80% LUW. However, from Figure 5.29, it is noted that the resilient modulus did not increase with the development of coarse aggregate stone-to-stone contact. The highest value of resilient modulus is found in mixture with 90% RUW, which did not develop coarse aggregate stone-to-stone contact. The analysis of the mixtures in other blocks gives similar results as that in Figure 5.29. Figure 5.30 shows the interaction of resilient modulus with the VCA_{mix}. One can see there is little or no trend between resilient modulus and VCA_{mix}. This indicated that there is no insight that the resilient modulus is related to coarse aggregate stone-to-stone contact of SMA mixtures.

The inconclusive resilient modulus results could be partly explained by the following reasons:

- The resilient modulus value obtained is based on the elastic and recoverable portion of the stress-strain curve. In this regard, the applied load is usually limited to about 10% of its failure load. With such low loading, the significance

of coarse aggregate stone-to-stone contact may not have been mobilised to its fully potential.

- Coarse aggregate stone-to-stone contact is mainly effective against rutting or permanent deformation. As discussed above, resilient modulus which is based on the recoverable strain may not be relevant in the context of permanent deformation.
- The resilient modulus test was conducted at 25 °C . This temperature may not be high enough to fully exploit the true potential of coarse aggregate stone-to-stone contact.

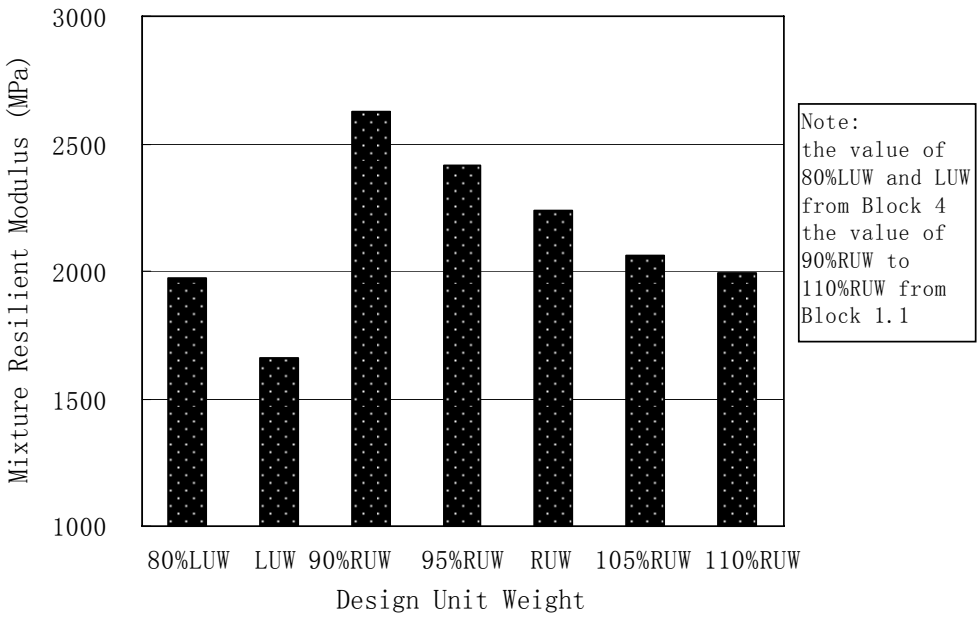

Figure 5.29 Resilient Modulus Plot for Different Design Unit Weight

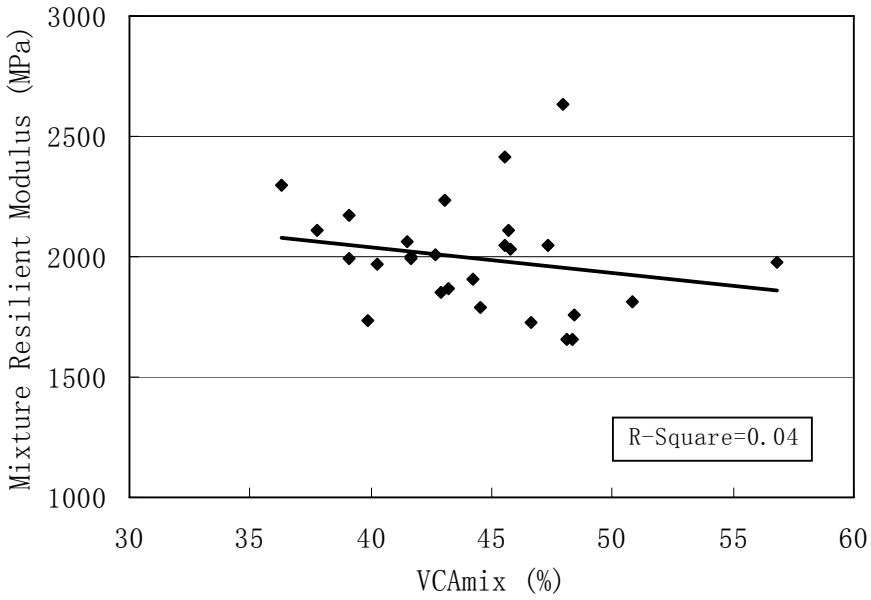

Figure 5.30 Resilient Modulus Interaction with VCA_{mix}

5.5.2 Repeated Load Uniaxial Test Results and Analysis

The repeated load uniaxial test assesses the resistance to permanent deformation of the asphalt mixtures. Six specimens compacted with Servopac Gyratory Compactor (SGC) of each mixture for all blocks were tested at 50°C using MATTA. Test results of the accumulated micro-strain from 0 to 20,000 cycles of repeated load are plotted on the curves as shown in Figure 5.31. Additionally, the final accumulated micro-strain for each block is listed in Table 5.20.

Figure 5.31 plots all 37 asphalt mixtures of Block 1 to Block 4 in one figure, which gives an overall picture on the difference of asphalt content and the change in the volume of coarse aggregates between the blocks in the experiments. Figure 5.32 through Figure 5.39 shows the plots for each block of the experiment. They reflected the effect of change in design unit weight, coarse aggregate gradation, fine aggregate gradation, and asphalt binder content on the permanent deformation for the SMA mixtures.

Table 5.20 Repeated Load Uniaxial Test Results for Asphalt Mixtures

Sample Name	Final Accumulated Micro-strain	Standard Deviation
Block 1.1-90% RUW	24156	1614
Block 1.1-95% RUW	19199	1389
Block 1.1- RUW	17560	1747
Block 1.1-105% RUW	12683	1326
Block 1.1-110% RUW	19465	1269
Block 1.2-90% RUW	36096	1117
Block 1.2-95% RUW	25018	603
Block 1.2- RUW	22853	1729
Block 1.2-105% RUW	21761	381
Block 1.2-110% RUW	33159	1721
Block 1.3-90% RUW	46060	1057
Block 1.3-95% RUW	35309	1027
Block 1.3- RUW	29249	1329
Block 1.3-105% RUW	25690	328
Block 1.3-110% RUW	37464	1784
Block 2.1-90% RUW	22787	1037
Block 2.1-95% RUW	18863	948
Block 2.1- RUW	13484	1647
Block 2.1-105% RUW	15620	1265
Block 2.1-110% RUW	17152	1220
Block 2.3-90% RW	26063	263
Block 2.3-95% RUW	20657	1459
Block 2.3- RUW	19855	1624
Block 2.3-105% RUW	15536	1436
Block 2.3-110% RUW	14197	1176
Block 3.1-90% RUW	23722	727
Block 3.1-95% RUW	18915	1057
Block 3.1- RUW	17717	1269
Block 3.1-105% RUW	12974	1610
Block 3.1-110% RUW	18644	1612
Block 3.3-90% RUW	24793	139
Block 3.3-95% RUW	19901	1055
Block 3.3- RUW	18184	1277
Block 3.3-105% RUW	13204	1444
Block 3.3-110% RUW	18652	1002
Block 4-LUW	24465	1054
Block 4-80% LUW	28530	1300
Note: Blocks 1.1, 2.2, and 3.2 are the same asphalt mixtures.		

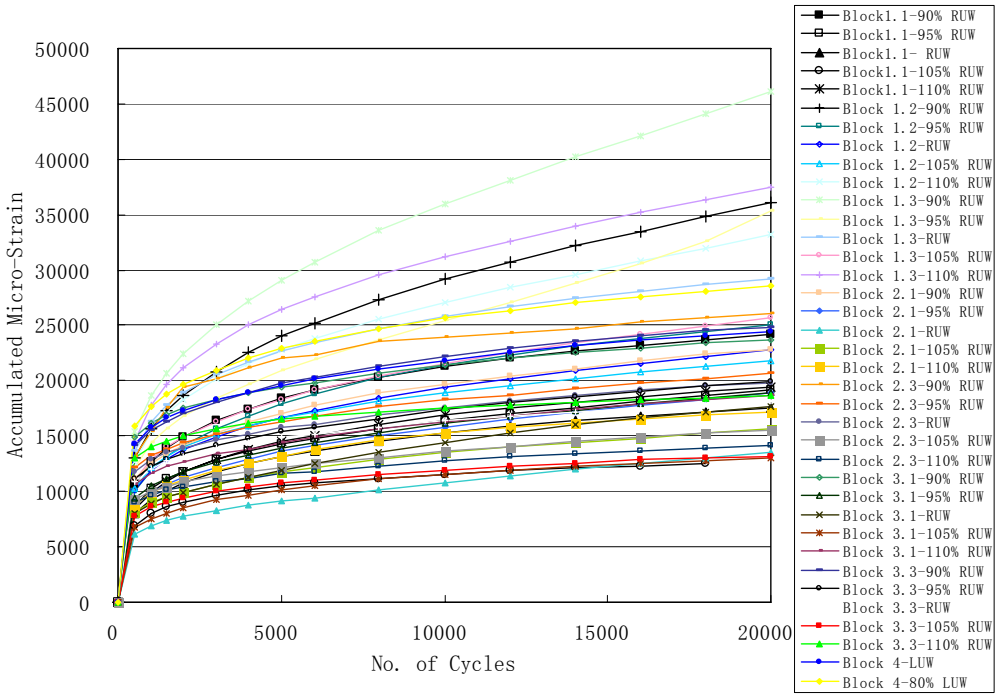

Figure 5.31 Permanent Deformation for Asphalt Mixtures by Experimental Blocks

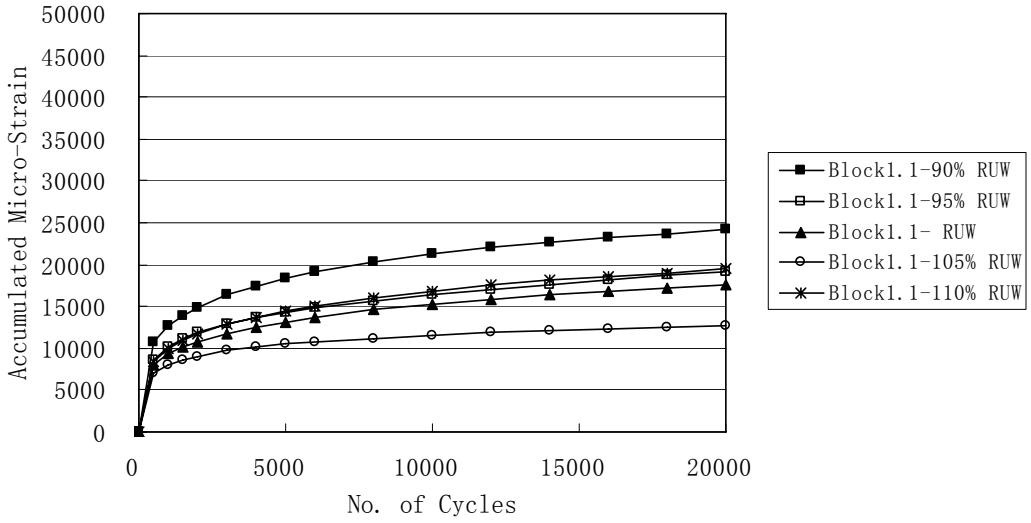

Figure 5.32 Permanent Deformation for Experimental Block 1.1 Mixtures

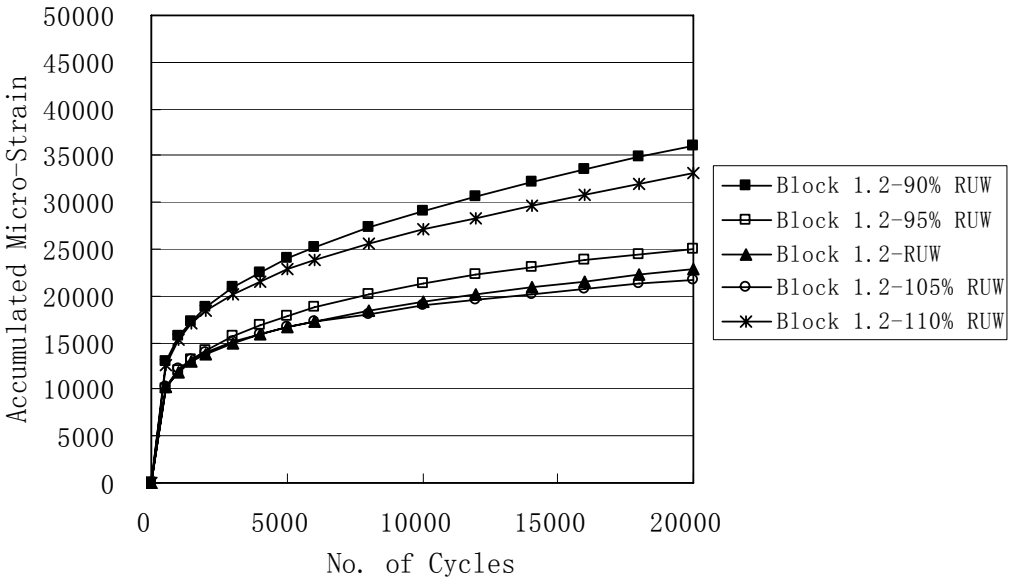

Figure 5.33 Permanent Deformation for Experimental Block 1.2 Mixtures

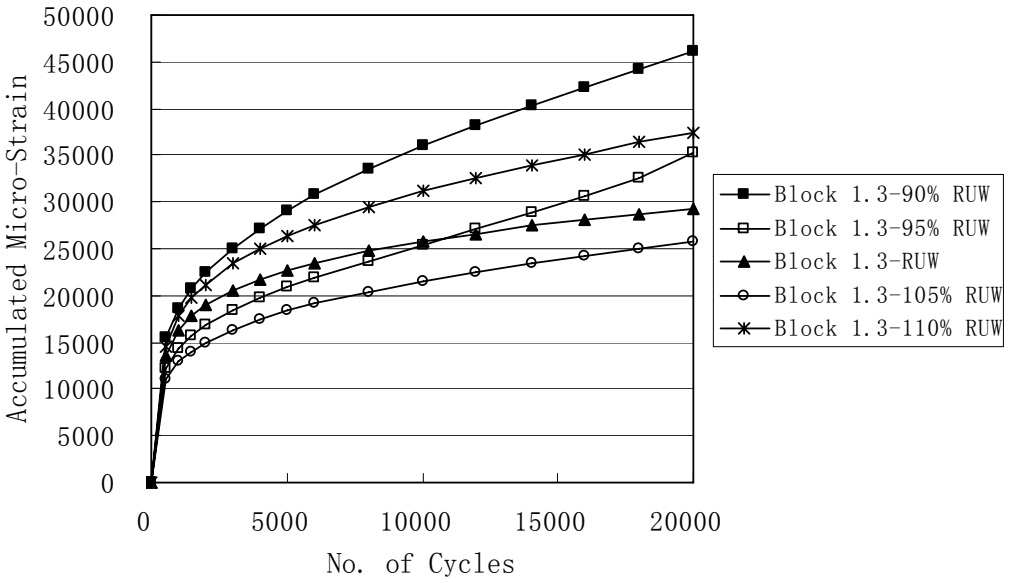

Figure 5.34 Permanent Deformation for Experimental Block 1.3 Mixtures

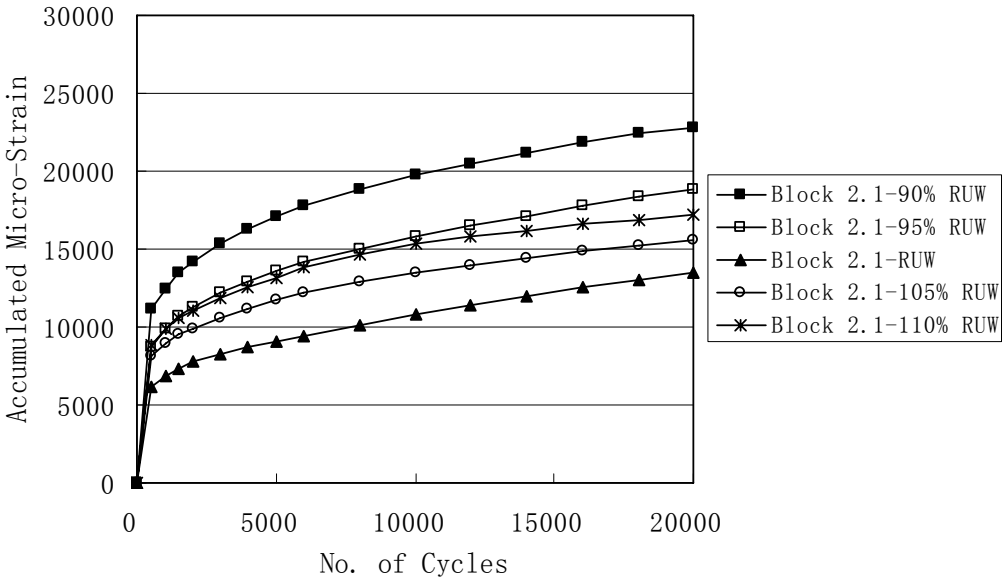

Figure 5.35 Permanent Deformation for Experimental Block 2.1 Mixtures

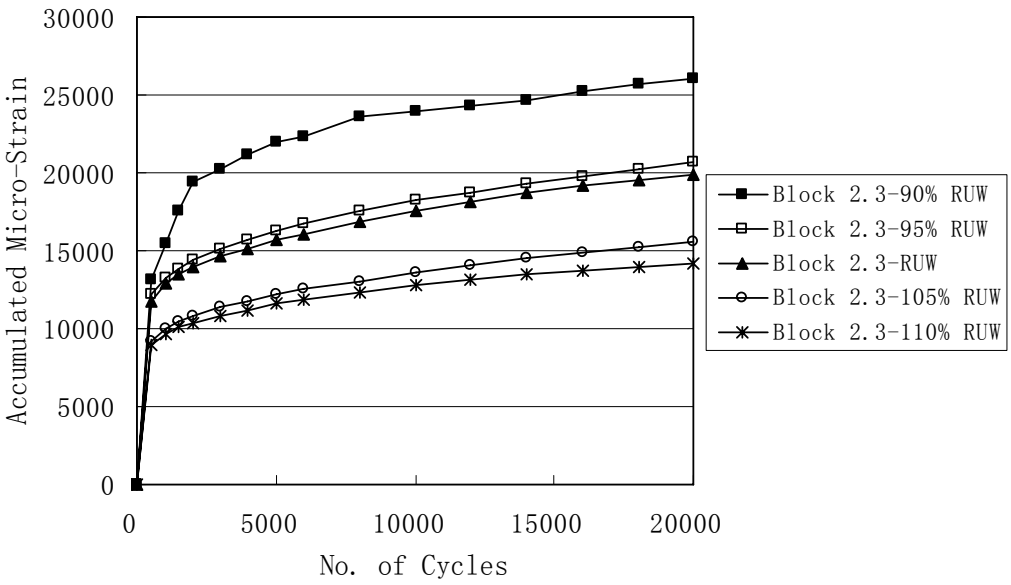

Figure 5.36 Permanent Deformation for Experimental Block 2.3 Mixtures

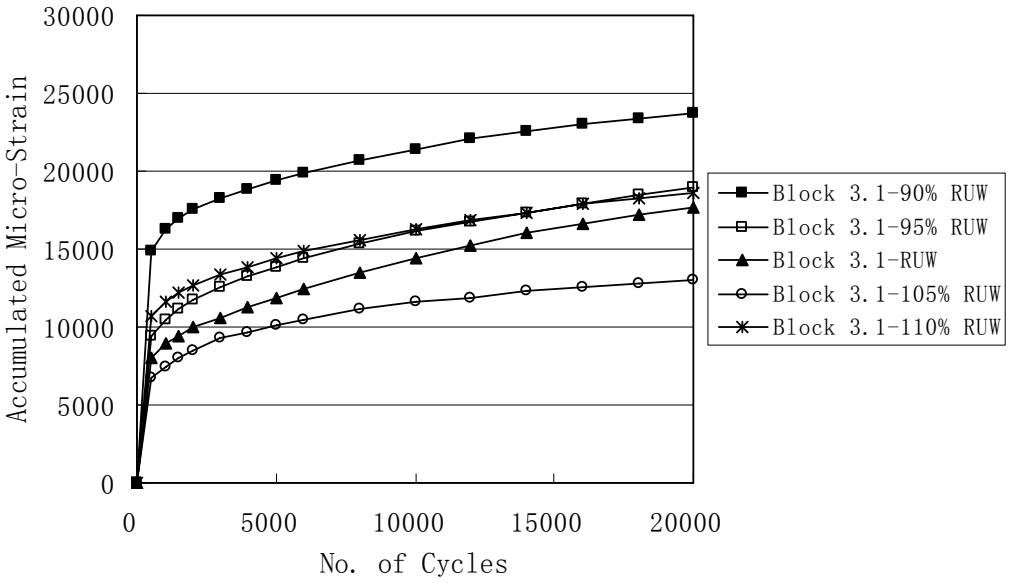

Figure 5.37 Permanent Deformation for Experimental Block 3.1 Mixtures

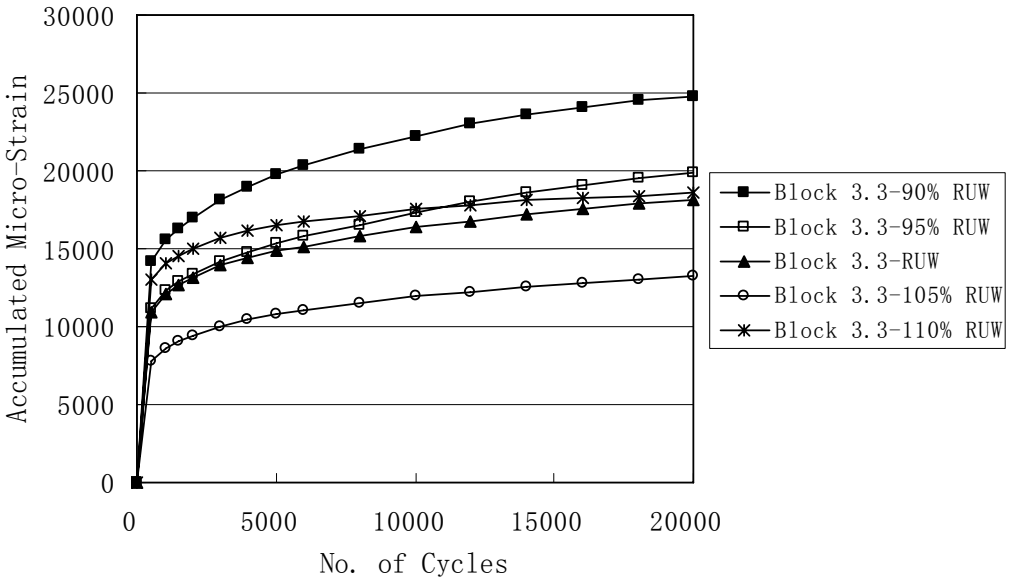

Figure 5.38 Permanent Deformation for Experimental Block 3.3 Mixtures

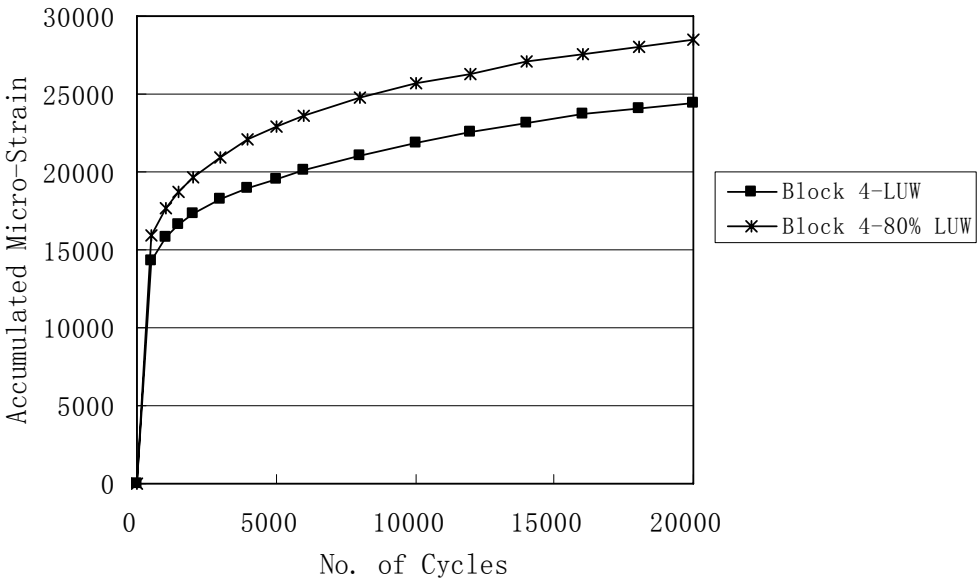

Figure 5.39 Permanent Deformation for Experimental Block 4 Mixtures

5.5.2.1 Discussion of Asphalt Content, Design Unit Weight of Coarse Aggregate, Aggregate Gradation and Permanent Deformation

An ANOVA analysis of the entire data set for the test was performed to identify the significance and the influence of the effect of changing coarse aggregate gradation, fine aggregate gradation, design unit weight of coarse aggregate, and asphalt binder content on the resulting micro-strain of the mixture. As shown in Table 5.21, the results indicated that two factors (DUW and AC) were significant at the 95% confidence level. There exists a statistical difference in the permanent deformation of mixtures with a change in the design unit weight of coarse aggregate or a change in the asphalt binder content. However, through the magnitude of the F value, one can notice that asphalt binder content is a much more significant variable as compared with other variables in explaining the permanent deformation of the asphalt mixtures. Additional analyses, through the use of ANOVA, on the data points from each individual block (Blocks 1, 2, and 3) gave the same results as the

ANOVA using the entire data.

Table 5.21 ANOVA for Permanent Strain

Source	DF	Sum of Square	Mean of Square	F value	P > F
Model	9	1086985439	120776160	13.52	0.0006
Error	8	71461701	8932713		
Corrected Total	17	1158447141			
R-Square	**Coeff. Var.**		**Root MSE**	**Micro-strain Mean**	
0.938313	13.15834		2988.764	22713.83	
Source	**DF**	**Type III SS**	**Mean of Square**	**F value**	**P > F**
DUW	3	218779539.5	72926513.2	8.16	0.0081
CA	1	189392.7	189392.7	0.02	0.8878
FA	1	33450.7	33450.7	0.00	0.9527
AC	1	443622410.7	443622410.7	49.66	0.0001

Figure 5.40 shows the final accumulated micro-strain for different asphalt binder contents (Blocks 1.1 to 1.3). Obviously, asphalt binder content had much effect on the permanent deformation of asphalt mixtures. With an increase of asphalt binder content, the accumulated micro-strain increased greatly for each level of design unit weight. When asphalt binder content was 5.5%, minimum permanent deformation was observed for the same design unit weight of coarse aggregate. This result confirmed the conclusion in the analysis of volumetric properties that the 5.5% asphalt binder content is enough for the designed aggregate gradation of SMA mixture. Although asphalt binder content had a significant effect on the permanent deformation of the asphalt mixtures, it did not change the trend of the change of micro-strain with the change in design unit weight of coarse aggregate. The minimum permanent deformation can be found in the mixtures with 105% RUW.

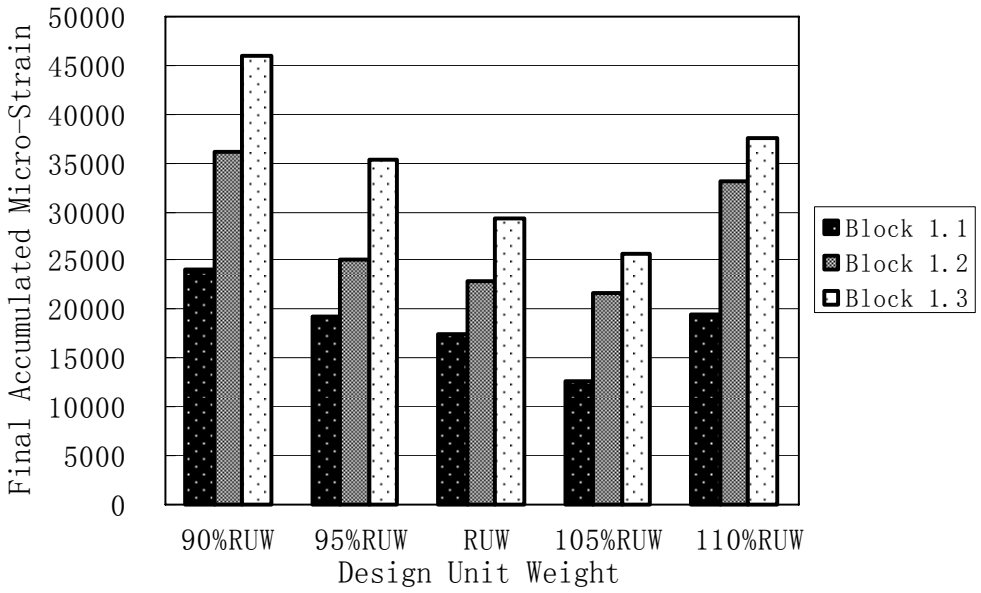

Figure 5.40 Permanent Deformation for Experimental Block 1 Mixtures

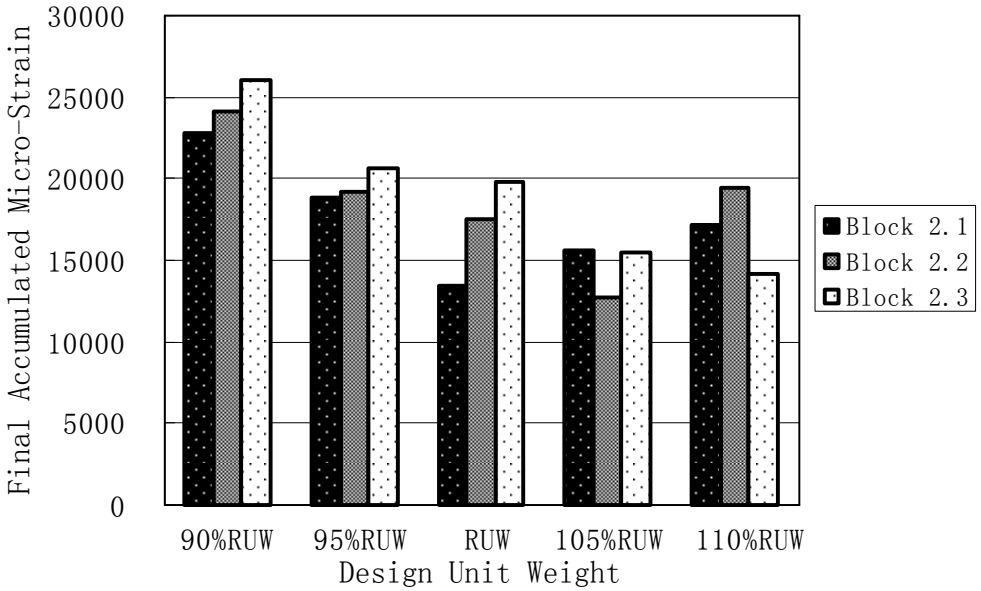

Figure 5.41 Permanent Deformation for Experimental Block 2 Mixtures

The change in design unit weight had a significant effect on the permanent deformation of SMA mixtures since the quantity of coarse aggregate stone-to-stone contact is controlled by the different design unit weight of coarse aggregates in this study. Figure 5.41 gives a plot of the micro-strain data in different design unit weight for experimental Block 2.

Clear trend can be observed with a change in the design unit weight of coarse aggregate. In Block 2.2, with the increase of the volume of coarse aggregates, the permanent deformation of asphalt mixtures decreased until the design unit weight is 105% RUW. After that, the permanent strain increased again with the increase of the volume of coarse aggregates. The same trend also can be observed for Blocks 1 and 3, which have the same coarse aggregate gradation. This result can be explained by coarse aggregate stone-to-stone contact. As the volume of coarse aggregate increases, stone-to-stone contact is gradually initiated. From the analysis in Section 5.4.4 (Figure 5.26), it is known that a coarse aggregate skeleton will be developed when the VCA_{mix} in the mixture is equal to or less than the VCA of the coarse aggregate in the dry rodded condition. When coarse aggregate starts to develop stone-to-stone contact (95% RUW), the internal resistance within SMA starts to increase. On the other hand, any further increase in the volume of coarse aggregate would not increase the internal resistance when coarse aggregate stone-to-stone is fully developed (105% RUW). In fact, the reduction of fine aggregate did little to help to consolidate the coarse aggregate structure within the SMA. The increase in voids within the mineral aggregates may further lead to the loss of internal resistance.

For Blocks 2.1 and 2.3, although the change in coarse aggregate gradation had no significant effect on the permanent strain of each level of design unit weight, and the trend of the change in permanent strain was similar to Block 2.2, it had a

different minimum permanent deformation. The minimum value of permanent strain in Blocks 2.1 and 2.3 was when the design unit weight is equal to RUW and 110% RUW, respectively. This can be explained by the relationship between VCA_{mix} and VCA_{dry} shown in Figure 5.24. When the coarse aggregate gradation is changed, the development of coarse aggregate stone-to-stone contact was affected. The mixtures in Block 2.1 using an upper gradation limit of coarse aggregate produced fewer "interceptor" aggregates; while the amount of "interceptor" coarse aggregate in Block 2.3, using a lower gradation limit of coarse aggregate, increased. This decrease or increase in the amount of "interceptor" aggregates appeared to affect the development of coarse aggregate stone-to-stone contact. Fewer "interceptor" aggregates make the "larger" coarse aggregate (size is larger than the half sieve of NMAS) develop stone-to-stone contact in the early stage (90% RUW in Figure 5.24). Therefore, the mixtures in Block 2.1 have the higher resistance to permanent deformation at the lower design unit weight (equal to or lower than rodded unit weight) compared with mixtures with medium and lower gradation limits. At the rodded unit weight, the stone-to-stone contact of the mixtures in Block 2.1 developed fully that resulted in a minimum permanent deformation. For the mixtures with medium limit gradation, in Block 2.2, the stone-to-stone contact was fully developed at 105% RUW. With the increase of "interceptor" aggregate, voids in the coarse aggregate increased. The development of "larger" coarse aggregate fraction packing (stone-to-stone contact) needs the higher design unit weight (RUW in Figure 5.24). Therefore the mixtures in Block 2.3 resulted in a higher micro-strain value at the lower design unit weight (equal to or lower than rodded unit weight) but had a higher resistance at 110% RUW.

5.5.2.2 Evaluation of Aggregate Ratios for Permanent Deformation

The use of ratios for the analysis of gradation is proposed as a method for

understanding the aggregate packing and resulting permanent deformation. The asphalt film thickness reflects the asphalt binder content and is directly related to asphalt mix durability. A multiple regression analysis was used to develop a model that predicted the permanent deformation in a SMA mixture based on the aggregate ratios and asphalt film thickness. All 35 mixtures (not including the mixtures with LUW and 80% LUW) were used in the development of the models. Table 5.22 summarises the results of the regression analyses. Since the estimation of the coefficient of FA_c in the model is not significant at 95% confidence level ($p>0.05$), it was excluded from the predicted model. An additional model was developed using the CA ratio, FA_f, and f_t. This model describes the air voids with a better R-Square of 0.71 and the p values of all coefficient are much smaller than 0.05. Equation 5.2 shows this relationship of permanent strain with aggregate ratios and asphalt film thickness:

$$Strain=42281+7585CA-154452FA_f+11104f_t \quad (5.2)$$

The predicted micro-strain and measured micro-strain from this developed model are shown in Figure 5.42.

Table 5.22 Regression Analysis Results of Permanent Strain

Independent Variables	DF	Estimated Parameter	Standard Error (SE)	R-Square	t value	P > |t|
Intercept	1	54393	21379		2.54	0.0163
CA	1	-1719.42672	13432		-0.13	<.0001
FA_c	1	-31046	31638	0.70	-0.98	0.3343
FA_f	1	-141378	29018		-4.87	<.0001
f_t	1	10932	1472.25523		7.43	<.0001

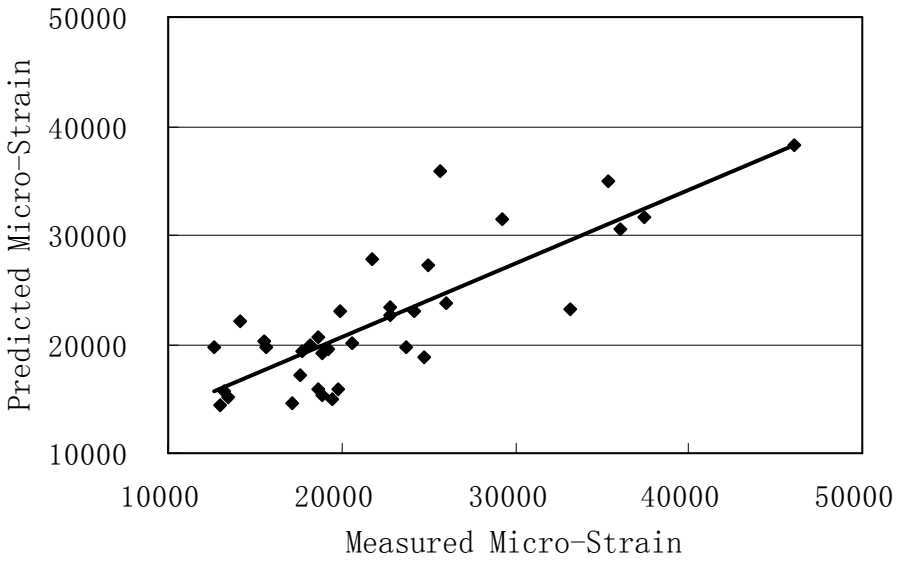

Figure 5.42 Measured and Predicted Micro-Strain Using Regression Model

5.5.3 Wheel Tracking Test Results and Analysis

Wheel tracking test directly estimates the internal resistance of asphalt mixtures in terms of rutting depth. The slabs were produced for each mix having the respective design unit weight of coarse aggregate and design binder content as outlined in Table 4.6 of Chapter 4. Each slab was compacted to the design air void level (i.e. 4.0 ± 1.0 percent) and a final height of 50 mm. This was accomplished by varying the amount of mixture placed into the slab mould. Compaction was then carried out to the specified height. The intent of these procedures was to produce slabs having densities representative of those pavements after two or three years of densification due to traffic and to produce slabs having similar air voids in order to make comparisons between the mixtures with the different design unit weight of coarse aggregates.

For each asphalt mixture, four specimens cored from slabs were subjected to rutting using the Wessex Wheel Tracker. Test results of the rut depth with time are shown in Figure 5.43. The results of the final rut depth at 45 minutes for these test mixtures are illustrated graphically by the column charts shown in Figure 5.44. These two figures showed the effect of changing the coarse aggregate gradation and the design unit weight of coarse aggregate on the rutting performance of SMA mixtures.

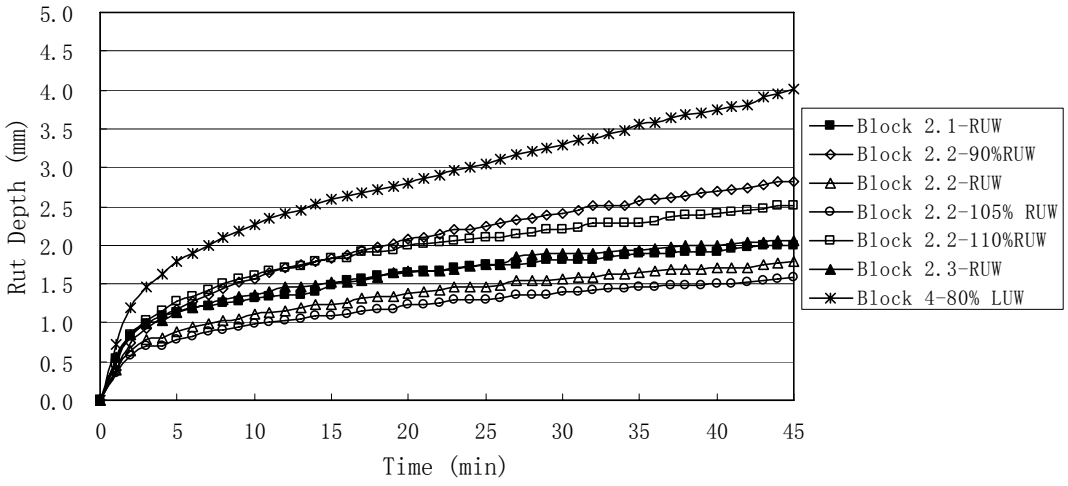

Figure 5.43 Rut Depth with Time Plot for Asphalt Mixtures

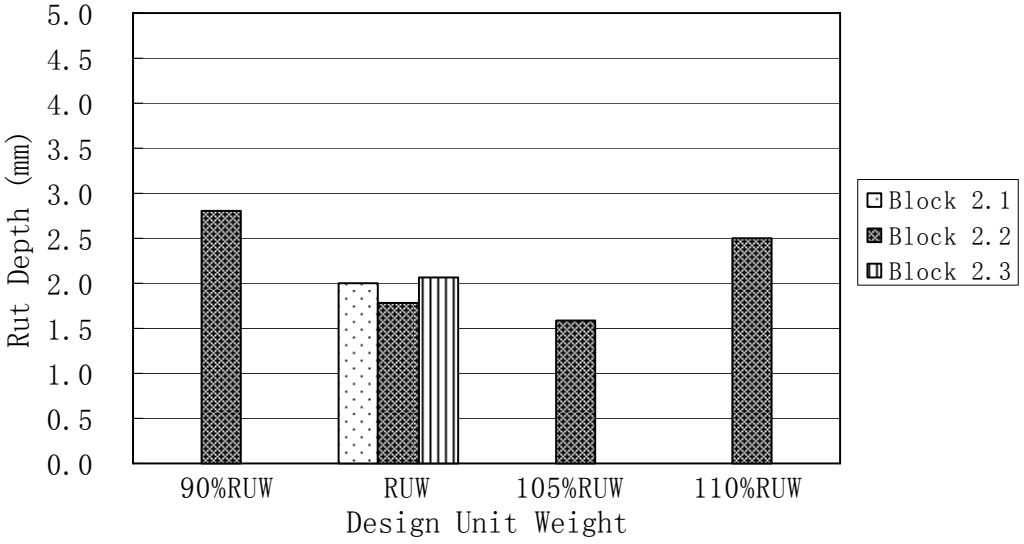

Figure 5.44 Final Rut Depth for Asphalt Mixtures

No specimen reached a rut depth of 5 mm, which is the limiting value used by the National Centre for Asphalt Technology (Kandhal and Mallick, 1999), and all specimens were tested for 45 minutes of test time. This result served to indicate that all the slabs had a good resistance against rutting. Hence, one would expect good in-service performance from these mixtures based on this established performance criterion (Kandhal and Mallick, 1999).

Identical trend to the results in the repeated load uniaxial test was observed for the effect of the change in design unit weight on the rutting of SMA mixtures. It is noted that SMA mixtures with RUW and 105 % RUW showed a lower wheel-tracking rate and lower rut depth as compared to other mixtures. This is because their volume of the coarse aggregate was at the range between 95 and 105% RUW, which formed coarse aggregate stone-to-stone contact. At the point of 105% RUW, where the coarse aggregate stone-to-stone contact was fully developed, the rutting depth was the minimum.

Changing the gradation limit of coarse aggregate from the lower to the upper band, one can see the increase or decrease of "interceptor" aggregates in the coarse aggregate did change the rutting resistance of SMA mixtures. The mixtures with the medium limit gradation had the minimum rut depth at the rodded unit weight (shown in Figure 5.44). However, this change was not significant compared to the change in the design unit weight.

5.5.4 Comparisons between SMA and Dense-Graded Mixtures

SMA develops coarse aggregate stone-to-stone skeleton and provides a high

resistance to rutting as compared with dense-graded asphalt mixtures. Figures 5.45 and 5.46 give a plot of the permanent strain and rut depth, respectively, to show the comparison of rutting resistance between SMA and dense-graded mixtures which have the same asphalt binder content and the same medium gradation limit of coarse and fine aggregates.

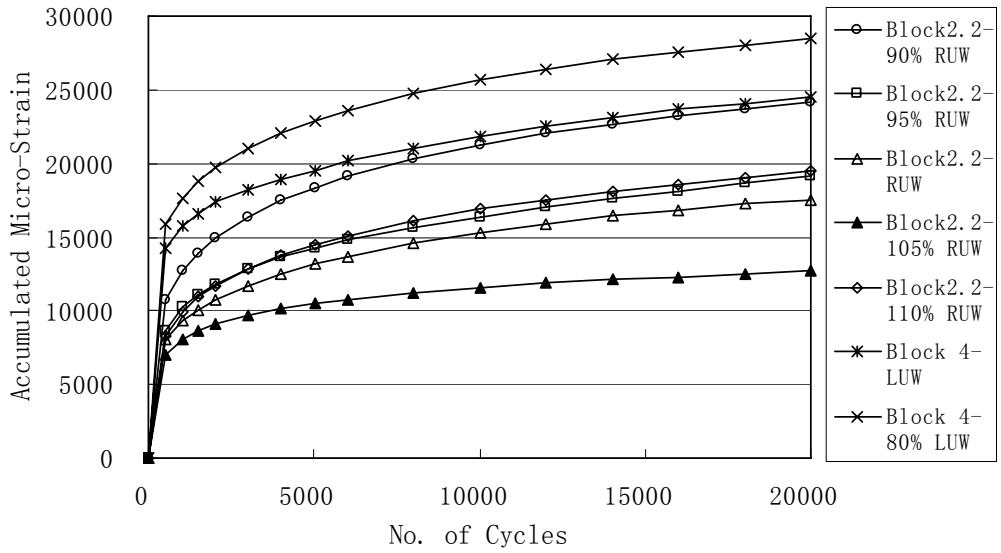

Figure 5.45 Permanent Strain for Comparison of SMA and Dense-Graded Mixtures

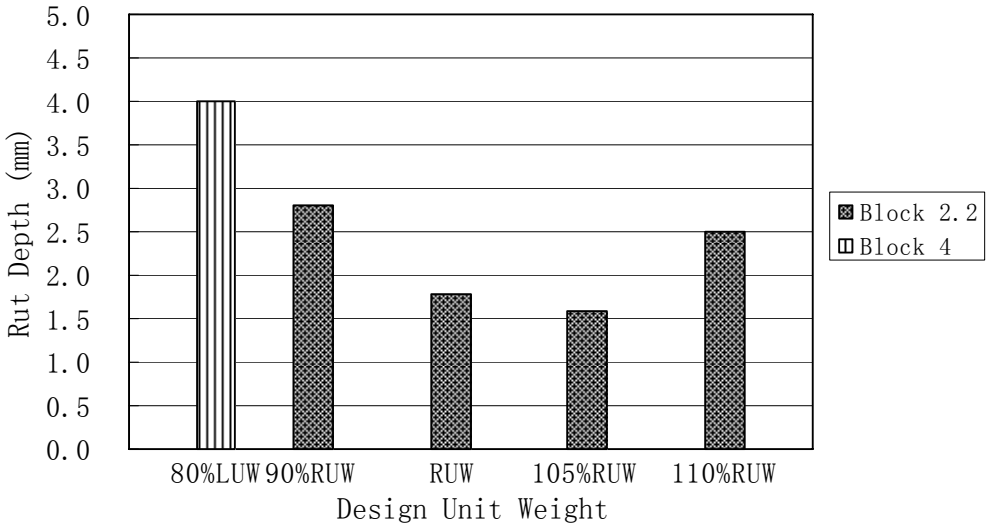

Figure 5.46 Rut Depth for Comparison of SMA and Dense-Graded Mixtures

It is evident that SMA mixtures with 95 to 105% RUW (Block 2.2) exhibited higher rut resistance than the dense-graded mixtures (Block 4). Additionally, it is also noted that SMA mixtures showed a lower permanent deformation rate as compared to dense-graded mixtures. Thus, one may infer that the proposed method to combine aggregates by volume for SMA mixtures will develop aggregate stone-to-stone contact and enhance the rutting resistance of SMA.

5.5.5 Relationship among Different Mechanical Property Tests

In this study, three main mechanical properties were tested: resilient modulus, permanent deformation, and the rut depth. The study by Brown (1993a) has shown that the resilient modulus is a highly variable test and has not been shown to be related to the performance for SMA mixtures. It is a measure of stiffness which allows one to calculate stresses and strains in a pavement structure. It is also a tensile test and therefore is not related to permanent deformation and rutting. Ideally, a good asphalt mixture would have high stiffness in shear and low stiffness in tension. The study in Section 5.5.1 also showed that there is no insight that the resilient modulus is related to coarse aggregate stone-to-stone contact of SMA mixtures.

Wheel tracking test and repeated load uniaxial test were both used to assess the resistance of SMA mixture to permanent deformation. Test results of them showed similar trend against rutting. Therefore, a relationship of each of these two tests with performance was studied and the trend plotted as shown in Figure 5.47. Table 5.23 shows the results of regression analysis. The relationship of these two test data indicates a good correlation (R^2=0.82). Hence, it seems valid that a positive

correlation existed between the rut depth obtained from wheel tracking test and the uniaxial strain obtained from the repeated load uniaxial test.

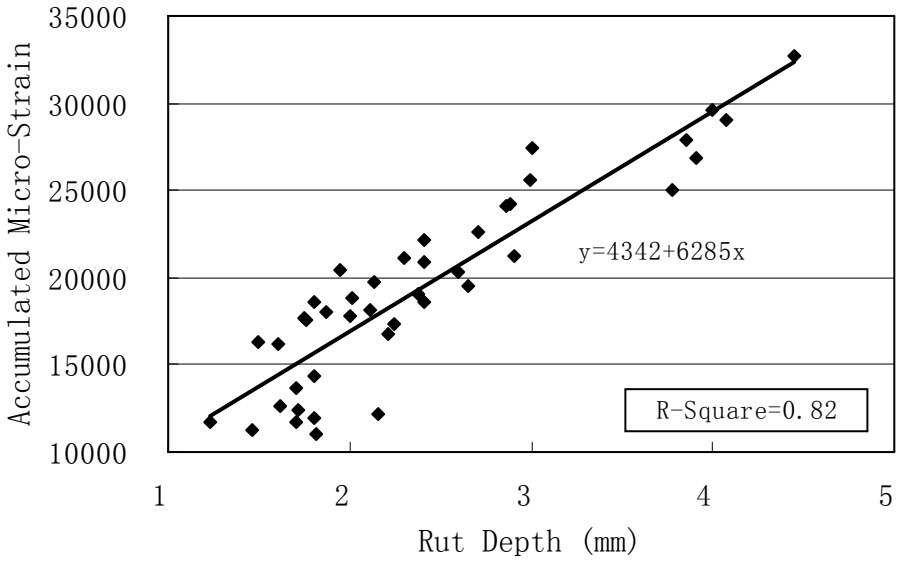

Figure 5.47 Relationship between Permanent Deformation and Rut Depth

Table 5.23 Regression Analysis Results for Permanent Strain and Rut Depth

Independent Variables	DF	Estimated Parameter	Standard Error (SE)	R-Square	t value	P > |t|
Intercept	1	4342.14252	1165.12808	0.82	3.73	0.0006
Rut Depth	1	6285.06378	461.88007		13.61	<.0001

5.5.6 Summary of Mechanical Property Test

Thirty-seven mixtures were characterised through a series of asphalt mixture performance tests. Twenty-seven different aggregate gradations and 3 different asphalt binder contents were employed to study the effect of changing the design

unit weight of coarse aggregates, coarse aggregate gradation, fine aggregate gradation, and the asphalt binder content on the mechanical properties of the resulting mixtures. The results of laboratory mixture characterisation can be summarised as follows:

- The resilient modulus was found not to be related to the coarse aggregate stone-to-stone contact of SMA mixtures;
- The change in asphalt binder content has a significant effect on the resilient modulus since the asphalt cement has much lower stiffness than that of aggregate and higher asphalt binder content affects the resilient modulus of the mixtures more readily and results in a lower resilient modulus for the mixtures with the same aggregate gradation;
- The results of the repeated load uniaxial test indicated that asphalt binder content and the design unit weight of coarse aggregate had a significant effect on the permanent deformation of SMA mixtures;
- Asphalt content of 5.5% was found to be sufficient for the designed aggregate gradation of SMA mixture since the minimum permanent deformation in each level of design unit weight was observed in the mixtures with this asphalt content. In addition, asphalt binder content was a more significant variable as compared with aggregate gradation in explaining the permanent deformation of asphalt mixtures;
- SMA designed with the unit weight of the coarse aggregate between 95 and 105% RUW performed with better rut resistance than those SMA with other percentages of RUW. Also, the higher the degree of stone-to-stone contact, the higher would be the rutting resistance;
- The change in the gradation limit of coarse aggregate and fine aggregate has no significant effect on the permanent strain at all levels of design unit weight. However, the change of coarse aggregate gradation affected the development of aggregate stone-to-stone contact since the decrease or increase of the amount of

"interceptor" in the coarse aggregates changes the aggregate packing;

- A quantitative prediction model (Equation 5.2), based on the aggregate ratios and asphalt film thickness, to describe the resulting permanent strain in the mixture was developed. This model can be used to predict the rutting performance of SMA mixtures for the used crushed granite aggregate in this study;
- The overall mixture conducted in the wheel tracking test showed very similar pattern of overall rut resistance with that in the repeated load uniaxial test;
- The mixture properties of permanent deformation and rutting indicated that the SMA mixture had significantly higher rut resistance when compared with the dense-graded mixture. This significant effect was attributed to coarse aggregate stone-to-stone contact;
- The linear regression analysis indicated that the resilient modulus is a highly variable test and has not been shown to be related to the performance for SMA mixtures; and
- Taken collectively, there seems to have a positive correlation between the rut depth obtained from wheel tracking test and the permanent strain obtained from the repeated load uniaxial test.

5.6 APPLICATION OF MIX CHARACTERISTICS TO PERFORMANCE PREDICTION

The overall purpose of SMA mixture design and laboratory mix characterisation is to produce an improved SMA mixture. Therefore, it is necessary to correlate mixture performance to the fundamental engineering properties. One way to correlate material properties to mixture performance is to establish empirical relationship based on the laboratory experiments. The other approach is to apply the

material engineering properties into certain material models and predict the mixture performance structural analysis.

In this chapter, regression analysis that predicted the SMA performance based on the fundamental engineering properties has been conducted and the empirical equations which described the relationships between mixture performance and material properties had been proposed. However, the meaning and limitations of these predictive equations must be understood. They predict the magnitude of the performance for the mixtures tested mainly based on Singapore conditions (only crushed granite aggregate was used.) and compacted at 100 gyrations of the SGC or rolling compaction. They provide a means by which the performance of an asphalt mixture may be estimated based on aggregate ratios and film thickness, which controlled aggregate stone-to-stone contact and the durability of SMA mixtures. From Figure 5.42, there is a good fit between the predicted and measured performance for the data set studied. However, the relationship needs to be validated with field and laboratory data prior to being used as design criteria.

The latter part of this study involved the development of 2-D dynamic finite element analysis, in which visco-elastic material model was applied for the asphalt mixtures. After the material model which explicitly considered the aggregate microstructure and the linear visco-elastic behaviour of the binder is validated, the 2-D finite element procedure was used to predict SMA mixture permanent deformation. During the finite element analysis of mixture performance prediction, the following results from the material characterisation were used:

- Resilient modulus for the elastic properties; and
- Repeated load uniaxial test for permanent deformation (rutting).

CHAPTER SIX

NUMERICAL SIMULATION OF SMA IN CONNECTION WITH PERMANENT DEFORMATION

The purpose of a pavement is to carry traffic safely, conveniently, and economically throughout its design life. There are several reasons why a pavement may cease to fulfil this purpose. The most common forms of structural failure are permanent deformation (rutting) and fatigue cracking. This requires a mechanistic pavement design procedure that should be able to correctly predict pavement response. A numerical simulation procedure with realistic material performance models would be ideal to achieve such a goal.

The development of a model that explains the rutting of flexible pavements relies, at least in part, on the understanding of the constitutive behaviour of bituminous mixes that are used in the upper layers. Bituminous mixes are complex multi-phase

materials consisting of a gradation of aggregate, air voids, and asphalt binder. The constitutive behaviour is defined by the interaction between these three phases, especially by the drastic differences in stiffness between the aggregates and the binder. A further complication arises from the visco-elastic nature of the asphalt binder and the dependency of its stiffness on temperature, loading frequency and strain magnitude. Studying the complex constitutive behaviour of bituminous mixes requires the understanding of their microstructure and the modelling of the stress-strain behaviour of the binder.

This chapter presents a micromechanical model for the deformation of asphalt mixtures that would give a simple analytical constitutive relation in terms of measurable mix parameters like volume fractions of aggregate. The basic approach generally involves a methodology for combining the measured performance of the bitumen with some simple assumptions on the behaviour of the aggregate to give a constitutive relation for the bituminous mix.

6.1 PAST RESEARCH ON FINITE ELEMENT MODELLING

Constitutive modelling on the deformation behaviour of bituminous mixes using continuum mechanics has been the focus of research among paving technologists for over 50 years. Most of the existing models on the deformation behaviour of bituminous mixes are continuum models or empirical equations (Cheung, 1995). Very complicated continuum models have been proposed to understand the complex deformation behaviour of these materials. However, the main limitation of these approaches is that the deformation mechanism was not understood because the microstructure of the materials has not been considered. There may also be a large

number of empirical model parameters to be determined experimentally. Furthermore, extrapolation of empirical models will generally not give reliable results. The structure, applicability, and limitations of various existing models are discussed in Deshpande (1997).

An early attempt to model the elastic behaviour of bituminous mixes using an assumed microstructure was reported by Van der Poel (1958). His model calculated the rigidity of a concentrated solution of elastic spheres in an elastic medium, using a method developed for dilute dispersions by Frohlich and Sack (1946). Another attempt to model the viscous behaviour of bituminous mixes was reported by Hills (1973). He developed a creep model for asphalt with micro-structural variables such as bitumen film thickness between aggregate particles as input variables. The imposed macroscopic strain on the bituminous mix was assumed to be accommodated on the microscopic scale by the displacements of adjacent aggregate particles in both shear and compression. Employing this assumption, Hills calculated the effective elastic stiffness of the bituminous mix. The model provides a mode for the constitutive equations but depends entirely on curve fitting to experimental data to obtain numerical data. In the spirit of the Hills's model, Cheung et al. (1999) used the isolated contact modelling approach originally developed from the analysis of powder compaction to rigorously analyse the deformation behaviour of asphalt idealised as a random distribution of rigid spheres separated by thin films of bitumen. The predictions of the model agreed qualitatively with experimental measurements but the isolated contact model substantially under-predicted the "stiffening" effect of the aggregate. An attempt was reported by Rothenburg et al. (1992), who proposed a micromechanical model of bituminous mixes (originally developed to model granular materials), in which the material was represented by a set of discrete elastic particles bounded by a linear visco-elastic bitumen. Although the proposed microstructure and the constitutive

behaviour of bitumen were rather rudimentary, the simulation yielded many revealing results concerning the fundamental mechanism of deformation in bituminous mixes.

Deshpande (1995) conducted a literature review on the current understanding of the deformation mechanics of particulate composite materials. He concluded that no existing models of random particulate composites were suitable, because of the very high volume fraction of particulates in typical paving mixes. The most suitable existing theories are based on variational methods which yield bounding solutions for the deformation properties of the material. However, more specific assumptions regarding the microstructure of the composite and its evolution with loading are required if the deformation properties peculiar to bituminous mixes are to be understood.

One approach towards modelling the deformation behaviour of mixes with high volume fractions of rigid inclusions in a deformable matrix is to consider the microstructure of the composite as consisting of a randomly distributed, rigid aggregate particle, separated by thin films of bitumen. [The thin films could also be assumed to have the properties of a material which is itself a composite (e.g. filled bitumen), enabling a wide range of materials to be modelled by this approach.] The deformation behaviour of each "contact" is primarily controlled by the mechanical properties of the bitumen film. Using this approach, a bounding solution to the macroscopic behaviour can be obtained by a set of variational arguments involving the microscopic behaviour of individual contacts and an assumed compatible displacement field in the mix (Cocks, 1994).

Recently, a uniaxial constitutive model of asphalt-aggregate mixtures has been developed by Kim et al. (1997a and 1997b) and Lee and Kim (1998). The model

employed the elastic-viscoelastic correspondence principle and Schapery's work (1987) on potential theory to model the mechanical behaviour of asphalt concrete under cyclic loading. It has been proven that this model is able to predict the hysteretic stress-strain behaviour of asphalt concrete under different loading histories (monotonic and cyclic), varying rates of loading, different models-of-loading (controlled-stress and controlled-strain), various stress/strain amplitudes, and random rest periods. Some contact-based analysis of asphalt performance had been reported by Zhu (1998). Zhu and Nodes (2000) used the contact-based mechanism to analyse the behaviour of asphalt pavement with the effect of aggregate angularity. In their study, the contact mechanism was defined such that the execution of load/force transmission was mainly characterised by the contact-based force-displacement interaction of particles adjacent to each other.

6.2 OBJECTIVES AND SCOPE

The intent of the study is to attempt both approaches, i.e. simulation of asphalt concrete in conditions of repeated load uniaxial test and in problems that involved a wheel-pavement interaction leading to rutting. The emphasis of the study is to develop a numerical model capable of modelling the visco-elastic behaviour of asphalt concrete by explicitly considering the aggregate microstructure and the visco-elastic behaviour of the binder. The primary objective is to study, based on numerical simulations, the relationship between material properties and permanent deformation of SMA, and to gather some aspects of creep behaviour that influences the susceptibility of pavement materials to rutting.

According to past study stated in Section 6.1, modelling the asphalt concrete microstructure has been possible through either the Finite Element Method (FEM)

or the Discrete Element Method (DEM). This study involved the FEM technique. In order to develop a numerical approach to analyse the permanent deformation of SMA, geometric models for simulating asphalt-aggregate system, which are suitable for finite element analysis, are proposed. Visco-elastic micromechanical model was applied for the asphalt concrete. Different material parameters of the visco-elastic model were used in the finite element analysis and were compared to determine the optimal material parameters used in numerical simulation of SMA. Finally, different finite element analyses were performed for numerical comparisons and different aggregate size, shape, and elongation were simulated to expand the numerical results. The commercial finite element software, ANSYS was selected for the numerical simulation. Figure 6.1 shows a schematic of the numerical simulation.

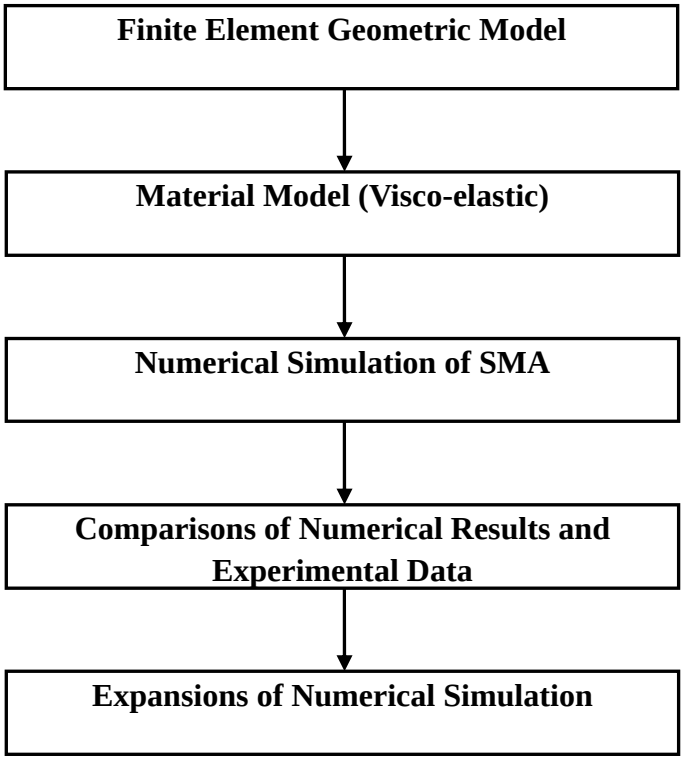

Figure 6.1 Overview of the Numerical Simulation

6.3 GEOMETRIC MODELS FOR THE FINITE ELEMENT ANALYSIS

Asphalt concretes are composite three-phase materials consisting of aggregate, asphalt binder, and air voids. The cemented particulate system of asphalt concrete is schematically shown in Figure 6.2. The aggregate material is much stiffer than the binder, thus it can be considered as rigid particles. On the other hand, bitumen is a visco-elastic binder material. Thus, its behaviour under stress is a function of load duration and temperature. It tends to behave like an elastic solid at a low temperature or at short loading period, while exhibiting properties of viscous liquid at high temperature or at prolonged loading period.

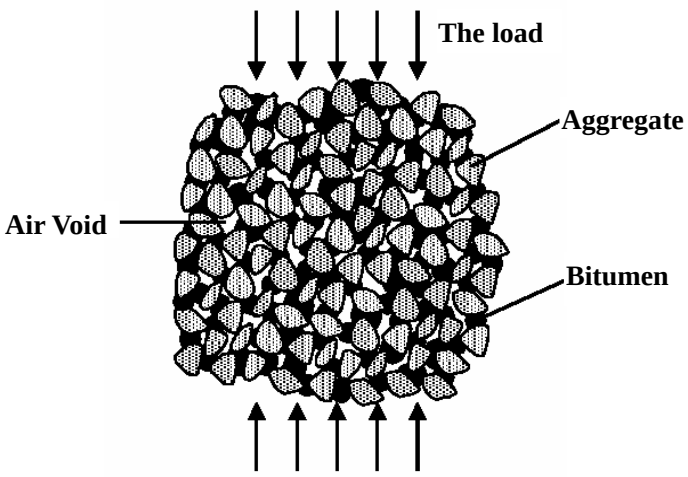

Figure 6.2 Schematic of Multi-Phase Asphalt Concrete

In order to create a geometric model for the finite element analysis, some assumptions were made. One must note that the transformation from physical model (reality) to geometric model (idealisation) requires the simplification of the geometry. Normally the geometric model simplifies details on geometry, kinematics, material laws, and boundary conditions and so on. SMA composes of aggregate,

bitumen, and air voids, which evolved the simplification around the allowable aggregate shape and the binder geometry.

6.3.1 Aggregate Generation Algorithm

Aggregate geometry mainly includes particle size, shape, angularity and texture. In general, SMA contains aggregates of diverse sizes and irregular geometries as shown in Figure 6.3(a). One approach is to allow such variable sizes, shapes, and angularity using a simple polygonal aggregate model as showed in Figure 6.3(b).

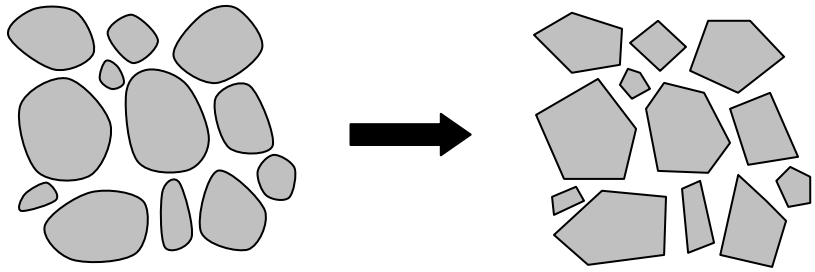

Aggregates in physical model (a) Aggregates in geometric model (b)

Figure 6.3 Aggregate Modelling

The developed algorithm for aggregate generation allows control of size, shape, angularity and elongation of aggregates. The idea of the algorithm is fully illustrated in Figure 6.4. Different particle shapes are generated by inscribing a polygon with a specified number of sides (n) into an ellipse and randomly choosing angles between adjacent vertices. With this technique, the size of particles is determined by the mean radius (r) of the ellipse, the particle elongation is controlled by the ellipse eccentricity (e) and angularity of particles depends on the number of sides per polygon. In this study, a limited number of numerical experiments with different particle shapes were performed in such a way that polygon with 4 to 6 sides are presented with equal probabilities.

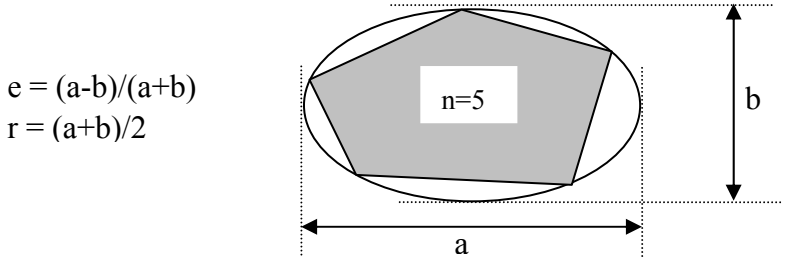

Figure 6.4 Aggregate Generation Algorithm

6.3.2 Asphalt Generation Algorithm

Asphalt is a complicated material with elastic, inelastic, and time-dependent behaviour. It is through asphalt binder that the micro-mechanical load transfer occurs between aggregates. Its behaviour cannot be easily simulated. In this study, asphalt mastic, defined as the agglomeration of binder and fine aggregates (smaller than 3.35 mm in size), was simulated instead of asphalt binder. It is simulated as a filler material that fills the voids created by the coarse aggregate and treated as a visco-elastic material.

6.3.3 Creation of Finite Element Geometric Models

According to the developed algorithm of aggregate and asphalt generations, a typical model reflecting inter-granular interactions between aggregate and asphalt mastic was mathematically derived as shown in Figure 6.5. Generally, forces acting on a particle arise from direct interaction between neighbouring grains and interaction with the mastic that fills voids created by the particles. Therefore, the

particle is subjected to a combination of distributed forces applied at a binder/particle interface and concentrated or distributed forces from neighbouring particles. In some contacts, there can be a thin film of bitumen separating particles. This is more likely when two particles form face-to-face contacts. In this study, a thin coating layer of bitumen is always assumed to be present initially and it behaves as a visco-elastic element that is connected sequentially with the elastic element that models the elasticity of particles.

Through the previous analysis described in Sections 6.3.1 and 6.3.2, the SMA mixtures investigated in connection with permanent deformation had the geometrical structure as shown in Figure 6.6. It was developed using software MATLAB. The steps involved in this type of simulation are schematically described below. The first step in the process is to create an assembly of particles by randomly generating (x, y) coordinates of particles and their sizes, shapes and elongation. Secondly, these particles are consolidated and coated with a thin film of bitumen. The compacted state depends on the thickness (t) of the thin coating layer of bitumen. Finally the voids created by the particles are filled with asphalt mastic. The microstructural parameters that controlled the properties of three parts (aggregate, asphalt mastic, and voids) of SMA are summarised as following:

(1) Aggregate: mass centre location (x, y); particle size (r-the mean radius of the ellipse); particle shape (n-the number of sides of polygon); and particle elongation (e-ellipse eccentricity).
(2) Asphalt mastic: thin film thickness of bitumen (t) and mastic area A.
(3) Voids space: 1- (aggregate + asphalt areas)/(total areas).

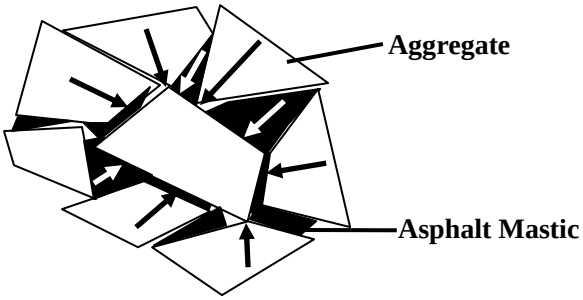

Figure 6.5 Interaction between Aggregate and Asphalt Mastic Geometry

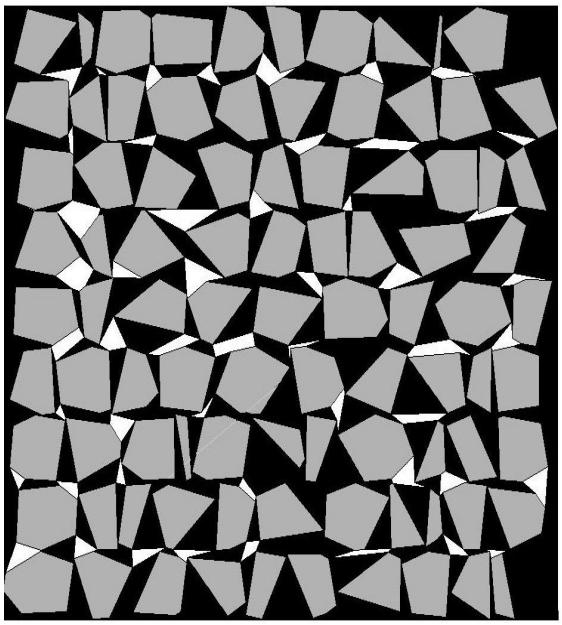

Figure 6.6 Geometric Model of SMA

In finite element analysis, the elements used for 2-D analysis include triangular and quadrilateral elements as shown in Figure 6.7. The 3-node triangular and 4-node quadrilateral elements offer linear interpolation along the element surfaces (edges), and provide solutions that are difficult to smoothen between elements. The 6-node

triangular and 8-node quadrilateral elements use quadratic interpolation and are called second order elements. The second order elements provide smoother solutions than the linear elements.

In this study, the 6-node triangular element was used for 2-D finite element analysis. Figure 6.8 presents the geometric mesh for the 2-D finite element analyses. Six-node triangular elements were used to form the finite element mesh. A brief sensitivity analysis suggested that a mesh of SMA structure would provide reasonable continuity for the stress and strain details of SMA responses under the dynamic loads.

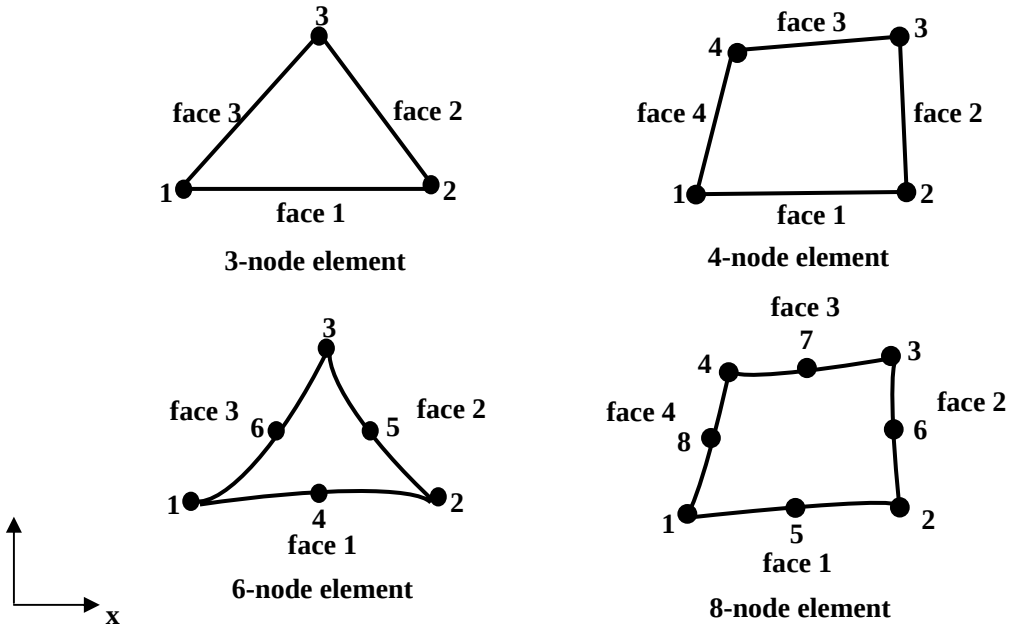

Figure 6.7 2-D Continuum Elements (ANSYS, 2004)

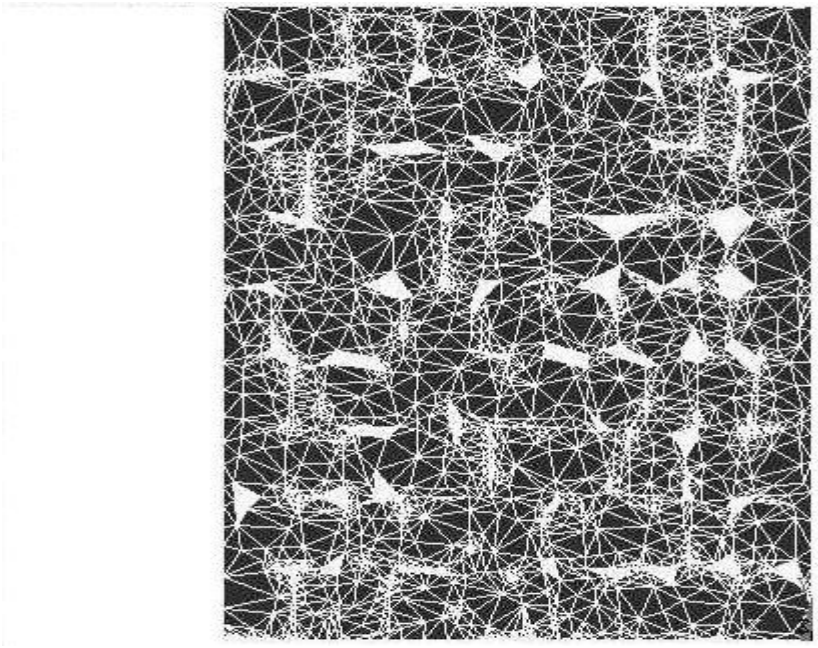

Figure 6.8 2-D Finite Element Mesh of SMA

6.4 MATERIAL MODELS FOR THE FINITE ELEMENT ANALYSIS

As described in Section 6.3, aggregates can be treated as elastic elements. On the other hand, asphalt binder exhibits elastic behaviour at low temperature or at low stress and behaves like a viscous liquid at high temperature or at prolonged loading period. It can be treated as a visco-elastic material.

6.4.1 Visco-elastic Micromechanical Model

The visco-elastic behaviour of binders can be described by mechanistic models fitted to Dynamic Shear Rheometer (DSR) measurements (Baumgaertel and Winter,

1989). These models consist of combinations of linear springs and dash-pots, e.g., the Generalised Maxwell model as shown in Figure 6.9. Papagiannakis et al. (2002) utilised the methodology described by Baumgaertel and Winter (1989) to fit a generalised Maxwell model to DSR binder measurements obtained at different strain levels. The resulting expressions for the shear relaxation modulus $G_R(t)$ is

$$G_R(t) = R_1 + \sum_{n=2}^{N} R_n \exp(-t/\frac{\eta_n}{R_n}) \qquad (6.1)$$

where R_1 and R_n =elastic spring constants; and η_n =viscosity constants of the generalised Maxwell model.

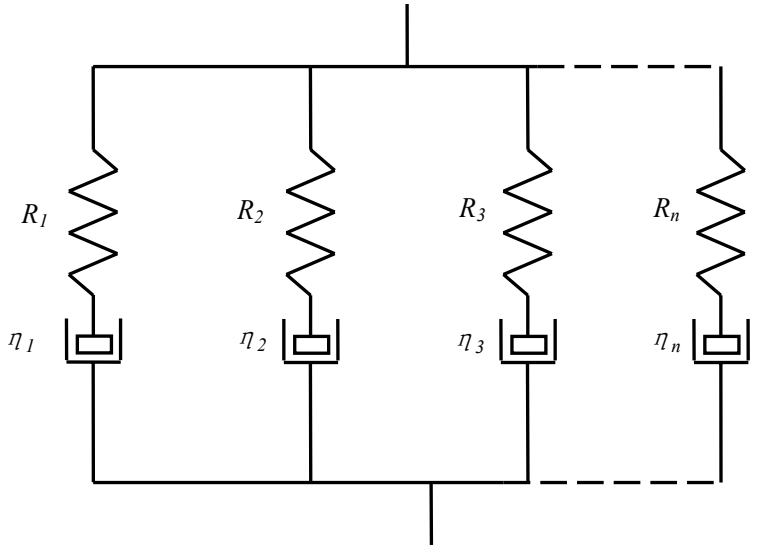

Figure 6.9 Mechanistic Asphalt Binder Model

The corresponding bulk relaxation modulus $K_R(t)$ is

$$K_R(t) = K_1 + \sum_{n=2}^{N} K_n \exp(-t/\frac{\eta_n^{K}}{K_n}) \qquad (6.2)$$

where the constants K_1, K_n, and η_n^{K} =bulk stress variants of R_1, R_n, and η_n related through the Poisson's ratio $v(t)$, satisfying

$$K_R(t) = G_R(t)\frac{2(1+v(t))}{3(1-2v(t))} \tag{6.3}$$

The long-term and the instantaneous modulus can be obtained from Equations (6.1) and (6.2) and are shown in Equations (6.4) and (6.5).

$$G_R(\infty) = R_1$$
$$G_R(0) = R_1 + \sum_{n=2}^{N} R_n \tag{6.4}$$

$$K_R(\infty) = K_1$$
$$K_R(0) = K_1 + \sum_{n=2}^{N} K_n \tag{6.5}$$

Obtaining the Poisson's ratio $v(t)$ is particularly challenging, because it requires binder testing under both normal and shear stress states. This could be possible by combining the DSR measurements with those obtained with a bending beam rheometer. However, these two tests are conducted at different temperatures and it is not practical to apply a temperature shift between them. As a result, a simplifying assumption needs to be made with respect to the Poisson's ratio of the binder. Accordingly, a value of 0.35 was assumed for the instantaneous Poisson's ratio $v(0)$, and the resulting instantaneous bulk modulus $K_R(0)$ was assumed to remain constant for loading times larger than zero (Abbas et al., 2004).

A FEM model allows definition of linear visco-elasticity in terms of Equations (6.1) and (6.2), referring to them as Prony Series. The formulation for this Prony Series approach in the case of plane strain is described in the following.

Upon application of the load, the elastic response is instantaneous while the viscous part occurs over time. Within the context of small strain theory, the constitutive equation for an isotropic visco-elastic material is defined using a hereditary integral formulation (ANSYS, 2004).

$$\begin{aligned}\sigma_{ij}(t) &= S_{ij}(t) + \frac{\sigma_{kk}(t)}{3}\delta_{ij} \\ &= \int_0^t 2G_{ijkl}(t-\tau)\frac{de_{kl}(\tau)}{d\tau}d\tau + \int_0^t 2K_{ijkl}(t-\tau)\frac{d\varepsilon_{vkl}(\tau)}{d\tau}\delta_{kl}d\tau\end{aligned} \tag{6.6}$$

where $\sigma_{ij}(t) = ij^{\text{th}}$ component of the stress tensor; $S_{ij}(t) = ij^{\text{th}}$ component of the deviatoric stress tensor; $\sigma_{kk}(t)/3 =$ first invariant of the stress tensor; $G_{ijkl}(t) = ijkl^{\text{th}}$ component of the shear relaxation tensor; $K_{ijkl}(t) = ijkl^{\text{th}}$ component of the bulk relaxation tensor; $de_{kl}(\tau)/d\tau = kl^{\text{th}}$ component of the first derivative of the deviatoric strain tensor at reduced time τ; and $d\varepsilon_{vkl}(\tau)/d\tau = kl^{\text{th}}$ component of the first derivative of the volumetric strain tensor at reduced time τ.

To evaluate the stress in Equation (6.6), the deviatoric and the volumetric parts are treated separately. The deviatoric stress is

$$\begin{aligned}S_{ij}(t) &= \int_0^t 2G_{ijkl}(t-\tau)\frac{de_{kl}(\tau)}{d\tau}d\tau \\ &= \int_0^t 2(R_1 + \sum_{n=2}^{N} R_n \exp(-(t-\tau)/\frac{\eta_n}{R_n}))\frac{de_{ij}(\tau)}{d\tau}d\tau \\ &= 2G_R(0)\int_0^t (1 - \sum_{n=2}^{N}\frac{R_n}{G_R(0)} + \sum_{n=2}^{N}\frac{R_n}{G_R(0)}\exp(-(t-\tau)/\frac{\eta_n}{R_n}))\frac{de_{ij}(\tau)}{d\tau}d\tau \\ &= 2G_R(0)\int_0^t (1 - \sum_{n=2}^{N}\frac{R_n}{G_R(0)}(1-\exp(-(t-\tau)/\frac{\eta_n}{R_n})))\frac{de_{ij}(\tau)}{d\tau}d\tau \\ &= 2G_R(0)e_{ij}(t) - 2G_R(0)\int_0^t (\sum_{n=2}^{N}\frac{R_n}{G_R(0)}(1-\exp(-(t-\tau)/\frac{\eta_n}{R_n})))\frac{de_{ij}(\tau)}{d\tau}d\tau\end{aligned} \tag{6.7}$$

Equation (6.7) includes the elastic and viscous components of the deviatoric stress. It is integrated numerically, assuming linear variation of strain with reduced time. Each of the summation components is thus integrated as

$$e_{ijn}(t) = \int_0^t (1 - \exp(-(t-\tau)/\frac{\eta_n}{R_n})) \frac{de_{ij}(\tau)}{d\tau} d\tau \tag{6.8}$$

and the modular ratios are abbreviated as

$$\alpha_n = \frac{R_n}{G_R(0)} \tag{6.9}$$

Using a time increment of Δt, the viscous strain at time $t + \Delta t$ is calculated as

$$\begin{aligned} e_{ijn}(t+\Delta t) = & \int_0^t (1 - \exp(-(t+\Delta t-\tau)/\frac{\eta_n}{R_n})) \frac{de_{ij}(\tau)}{d\tau} d\tau + \\ & \int_t^{t+\Delta t} (1 - \exp(-(t+\Delta t-\tau)/\frac{\eta_n}{R_n})) \frac{de_{ij}(\tau)}{d\tau} d\tau \end{aligned} \tag{6.10}$$

and

$$\begin{aligned} 1 - \exp(-(t+\Delta t-\tau)/\frac{\eta_n}{R_n}) = & 1 - \exp(-\Delta t/\frac{\eta_n}{R_n}) + \exp(-\Delta t/\frac{\eta_n}{R_n}) \\ & - \exp(-\Delta t/\frac{\eta_n}{R_n}) \exp(-(t-\tau)/\frac{\eta_n}{R_n}) \end{aligned} \tag{6.11}$$

Substituting Equation (6.11) into Equation (6.10), gives

$$\begin{aligned} e_{ijn}(t+\Delta t) = & (1 - \exp(-\Delta t/\frac{\eta_n}{R_n})) e_{ij}(t) + \exp(-\Delta t/\frac{\eta_n}{R_n}) e_{ijn}(t) \\ & + \frac{\Delta e_{ij}}{\Delta t} \int_t^{t+\Delta t} (1 - \exp(-(t+\Delta t-\tau)/\frac{\eta_n}{R_n})) d\tau \end{aligned} \tag{6.12}$$

Subtracting $e_{ijn}(t)$ from both sides of Equation (6.12) gives

$$\Delta e_{ijn} = (1-\exp(-\Delta t/\frac{\eta_n}{R_n}))e_{ij}(t) + (\exp(-\Delta t/\frac{\eta_n}{R_n})-1)e_{ijn}(t) + \frac{\Delta e_{ij}}{\Delta t}(\Delta t - \frac{\eta_n}{R_n}(1-\exp(-\Delta t/\frac{\eta_n}{R_n}))) \quad (6.13)$$

The change in deviatoric strain, Δe_{ij}, can be calculated from the change in the strain, $\Delta\varepsilon_{ij}$, and the change in volumetric strain, $\Delta\varepsilon_v$ (i.e., $\Delta\varepsilon_{xx}+\Delta\varepsilon_{yy}$). Also, in the first step of the analysis, the deviatoric strain, $e_{ij}(0)$, and the viscous strain, $e_{ijn}(0)$, are zero. Subtracting $S_{ij}(t)$ from $S_{ij}(t+\Delta t)$ results in

$$\Delta S_{ij} = S_{ij}(t+\Delta t) - S_{ij}(t) = 2G_R(0)(\Delta e_{ij} - \sum_{n=2}^{N}\alpha_n \Delta e_{ijn}) \quad (6.14)$$

The rate of change in deviatoric stress with respect to the change in the deviatoric strain defines the shear tangent modulus G^T. The bulk tangent modulus K^T could be derived using an analogous procedure

$$G^T = \frac{\partial \Delta S_{ij}}{\partial \Delta e_{ij}} = G_R(0)(1-\sum_{n=2}^{N}\frac{\alpha_n}{\Delta t}\frac{\eta_n}{R_n}((-\Delta t/\frac{\eta_n}{R_n})+\exp(-\Delta t/\frac{\eta_n}{R_n})-1)) \quad (6.15)$$

$$K^T = \frac{\partial \Delta \sigma_{kk}}{\partial \Delta \varepsilon_v} = K_R(0)(1-\sum_{n=2}^{N}\frac{\alpha_n{}^K}{\Delta t}\frac{\eta_n{}^K}{K_n}((-\Delta t/\frac{\eta_n{}^K}{K_n})+\exp(-\Delta t/\frac{\eta_n{}^K}{K_n})-1)) \quad (6.16)$$

The final step of this formulation involves updating the stress tensor at time increment Δt

$$\begin{aligned}\sigma_{ij}(t+\Delta t) &= S_{ij}(t+\Delta t) + \frac{\sigma_{kk}(t+\Delta t)}{3} \\ &= 2\mathrm{G}^{\mathrm{T}}\Delta e_{ij} + 2G_R(0)e_{ij}(t)(1-\sum_{n=2}^{N}\frac{R_n}{G_R(0)}(1-\exp(-\Delta t/\frac{\eta_n}{R_n}))) - \\ &\quad 2G_R(0)\sum_{n=2}^{N}\frac{R_n}{G_R(0)}\exp(-\Delta t/\frac{\eta_n}{R_n})e_{ijn}(t) + K^T\Delta\varepsilon_v + \\ &\quad \mathrm{K}_R(0)\varepsilon_v(t)(1-\sum_{n=2}^{N}\frac{K_n}{K_R(0)}(1-\exp(-\Delta t/\frac{\eta_n^{\ K}}{K_n}))) - \\ &\quad K_R(0)\sum_{n=2}^{N}\frac{K_n}{K_R(0)}\exp(-\Delta t/\frac{\eta_n^{\ K}}{K_n})\varepsilon_{vn}(t)\end{aligned} \tag{6.17}$$

and defining the Jacobian matrix

$$\text{Jacobian matrix} = \begin{bmatrix} \frac{\partial\Delta\sigma_{xx}}{\partial\Delta\varepsilon_{xx}} & \frac{\partial\Delta\sigma_{xx}}{\partial\Delta\varepsilon_{yy}} & \frac{\partial\Delta\sigma_{xx}}{\partial\Delta\varepsilon_{zz}} & \frac{\partial\Delta\sigma_{xx}}{\partial\Delta\gamma_{xy}} \\ \frac{\partial\Delta\sigma_{yy}}{\partial\Delta\varepsilon_{xx}} & \frac{\partial\Delta\sigma_{yy}}{\partial\Delta\varepsilon_{yy}} & \frac{\partial\Delta\sigma_{yy}}{\partial\Delta\varepsilon_{zz}} & \frac{\partial\Delta\sigma_{yy}}{\partial\Delta\gamma_{xy}} \\ \frac{\partial\Delta\sigma_{zz}}{\partial\Delta\varepsilon_{xx}} & \frac{\partial\Delta\sigma_{zz}}{\partial\Delta\varepsilon_{yy}} & \frac{\partial\Delta\sigma_{zz}}{\partial\Delta\varepsilon_{zz}} & \frac{\partial\Delta\sigma_{zz}}{\partial\Delta\gamma_{xy}} \\ \frac{\partial\Delta\sigma_{xy}}{\partial\Delta\varepsilon_{xx}} & \frac{\partial\Delta\sigma_{xy}}{\partial\Delta\varepsilon_{yy}} & \frac{\partial\Delta\sigma_{xy}}{\partial\Delta\varepsilon_{zz}} & \frac{\partial\Delta\sigma_{xy}}{\partial\Delta\gamma_{xy}} \end{bmatrix}_{\text{symmetric}} \tag{6.18}$$

This matrix defines the changes in stress with respect to changes in strain and allows advancing the numerical solution in time increments of Δt. Using the chain rule, where applicable, gives

$$\frac{\partial\Delta\sigma_{xx}}{\partial\Delta\varepsilon_{xx}} = \frac{\partial\Delta S_{xx}}{\partial\Delta e_{xx}}\frac{\partial\Delta e_{xx}}{\partial\Delta\varepsilon_{xx}} + \frac{\partial\Delta\sigma_{kk}}{\partial\Delta\varepsilon_v}\frac{\partial\Delta\varepsilon_v}{\partial\Delta\varepsilon_{xx}} = \frac{4}{3}G^T + K^T \tag{6.19}$$

$$\frac{\partial\Delta\sigma_{yy}}{\partial\Delta\varepsilon_{xx}} = \frac{\partial\Delta S_{yy}}{\partial\Delta e_{xx}}\frac{\partial\Delta e_{xx}}{\partial\Delta\varepsilon_{xx}} + \frac{\partial\Delta\sigma_{kk}}{\partial\Delta\varepsilon_v}\frac{\partial\Delta\varepsilon_v}{\partial\Delta\varepsilon_{xx}} = -\frac{2}{3}G^T + K^T \tag{6.20}$$

$$\frac{\partial\Delta\sigma_{zz}}{\partial\Delta\varepsilon_{xx}} = \frac{\partial\Delta S_{zz}}{\partial\Delta e_{xx}}\frac{\partial\Delta e_{xx}}{\partial\Delta\varepsilon_{xx}} + \frac{\partial\Delta\sigma_{kk}}{\partial\Delta\varepsilon_v}\frac{\partial\Delta\varepsilon_v}{\partial\Delta\varepsilon_{xx}} = -\frac{2}{3}G^T + K^T \tag{6.21}$$

$$\frac{\partial \Delta \sigma_{xy}}{\partial \Delta \varepsilon_{xx}} = \frac{\partial \Delta S_{xy}}{\partial \Delta e_{xx}} \frac{\partial \Delta e_{xx}}{\partial \Delta \varepsilon_{xx}} = 0 \tag{6.22}$$

$$\frac{\partial \Delta \sigma_{xy}}{\partial \Delta \gamma_{xy}} = \frac{\partial \Delta S_{xy}}{\partial \Delta e_{xy}} \frac{\partial \Delta e_{xy}}{\partial \Delta \gamma_{xy}} = G^T \tag{6.23}$$

Analogous expressions can be written for the remaining terms of the Jacobian matrix. The calculated result of the whole Jacobian matrix is

$$\text{Jacobian matrix} = \begin{bmatrix} \frac{4}{3}G^T + K^T & -\frac{2}{3}G^T + K^T & -\frac{2}{3}G^T + K^T & 0 \\ \vdots & \frac{4}{3}G^T + K^T & -\frac{2}{3}G^T + K^T & 0 \\ \vdots & \vdots & \frac{4}{3}G^T + K^T & 0 \\ \cdots & \cdots & \cdots & G^T \end{bmatrix}_{\text{symmetric}} \tag{6.24}$$

6.4.2 Material Parameters

In the developed FEM model, aggregate elements were modelled as linear elastic. Its material parameters mainly include Young's modulus and Poisson's ratio. Asphalt mastic elements, defined as agglomerations of binder and aggregate fines, were modelled as visco-elastic using the visco-elastic model as described above. In this study, the material parameters of the visco-elastic model are complicated by the properties of asphalt mastic which substitutes the asphalt binder. The visco-elastic parameters for the asphalt binder were obtained from the DSR test at different strain level (Bahia, 2001). They are shown in Table 6.1. The stiffness of the mastic was computed from the stiffness of the binder by considering the stiffening effect of the fines and the effect of actual mastic film thickness in the mixture. The study by Papagiannakis et al. (2002) revealed that the mastic is 3 to 30 times stiffer than the binder (In this study 30 times were used). Therefore, three different groups of material parameters of asphalt mastic (Group 1, 2, and 3 with 20, 15, and 10 times

asphalt binder stiffness.) were used in the finite element analyses to determine the optimal group of material parameters. Table 6.2 presents the material parameters used in the finite element simulation.

6.5 NUMERICAL SIMULATION OF SMA

A series of numerical simulations were carried out on the SMA microstructural model as described in Section 6.3. The binder visco-elastic model described above was implemented into the microstructural model. The objective of these simulations is to determine the optimal group of material parameters reflecting experimentally known properties of SMA. All simulated tests correspond to the repeated load uniaxial test.

Table 6.1 Constants for Model on Figure 6.9 from DSR test (Bahia, 2001)

Constant	1% Strain	21% Strain	42% Strain
R_1 (Pa)	8671	9105	6512
R_2 (Pa)	66391	59993	35173
η_2 (Pa • s)	142963	139525	155465
R_3 (Pa)	4239580	2744270	1751532
η_3 (Pa • s)	16791	13360	14742
R_4 (Pa)	467179	273276	186315
η_4 (Pa • s)	43402	29407	40634

Table 6.2 Material Parameters Used for Finite Element Analyses

Material		**Aggregate**	**Asphalt Mastic**		
			Group 1	**Group 2**	**Group 3**
Material Model		Elastic	Visco-elastic		
Elastic Modulus E (MPa)		2.5×10^4	--		
Poisson's Ratio υ		0.25	0.35		
Shear Relaxation Modulus at time=0 (MPa) $G_R(0)$		--	96	72	48
Shear Relaxation Modulus at time=infinity (MPa) $G_R(\infty)$		--	0.17	0.13	0.09
Bulk Relaxation Modulus at time=0 (MPa) $K_R(0)$		--	286	215	143
Bulk Relaxation Modulus at time=infinity (MPa) $K_R(\infty)$		--	0.51	0.39	0.27
The Modulus Ratios	α_1	--	0.001806		
	α_2		0.013831		
	α_3		0.029784		
	α_4		0.883246		

Note: -- not applicable; Aggregate values were obtained from (Abbas et al., 2004); Asphalt mastic values were computed according to the values controlled in 1% strain level in (Bahia, 2001) and based on the Equations as given in Section 6.4.1.

In the numerical simulations, a total of three typical SMA mixtures with different particle packing (90, 100, and 110% rodded unit weight of coarse aggregate,

respectively) were analysed for the finite element analysis. Since each SMA mixture has three different material parameters used in the finite element analysis, there are nine numerical simulations altogether. The results from these sets of numerical modelling are presented for comparison and discussion.

The FEM model used for the comparison involved a planar rectangular domain (50 × 63.5 mm) due to axisymmetry of the specimen (100 × 63.5 mm) and loading used in the repeated load uniaxial test. The boundary conditions of the model consisted of a lower boundary fixed in both directions and a left boundary fixed in the horizontal direction. A sinusoidal dynamic vertical stress was applied to the upper boundary. It is shown in Figure 6.10. The geometric parameters that represent fundamental physical properties were assigned to the developed FEM model. Different geometric parameters reflect the different aggregate packing of the SMA mixtures. Different material parameters reflect the different properties of the asphalt mastic. Table 6.3 presents the summary of the geometric and material parameters used in the numerical simulations. Some parameters were obtained primarily from the results of the material characterisation tests as described in Chapters 4 and 5.

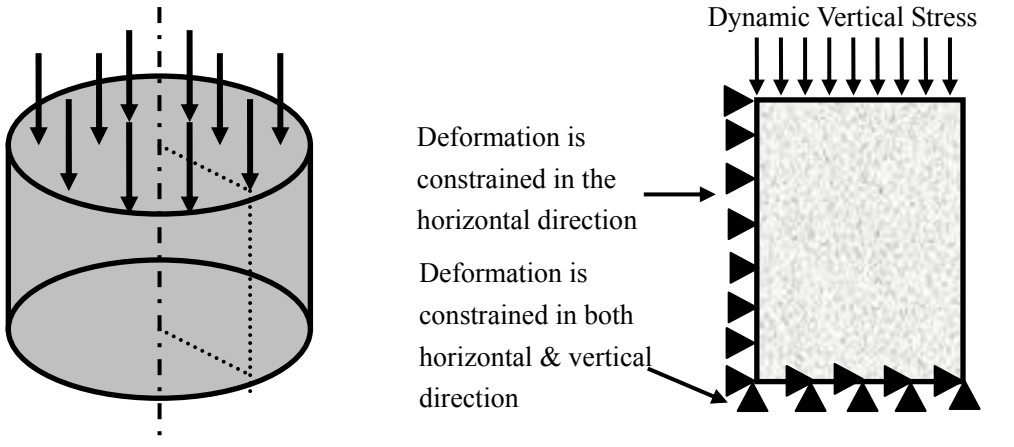

Figure 6.10 FEM Model of SMA Mixture Subjected to Dynamic Loading

Table 6.3 Geometric and Material Parameters Used in the Numerical Simulations

Material				90% RUW	RUW	110% RUW
Model Size (mm)				50 × 63.5		
Aggregate	Volume fraction (%)			54.3	59.8	64.2
	Particle size			standard sieve size from 14 mm to 3.35 mm		
	Particle shape*			the number of sides of polygon is between 4-6		
	Particle elongation*			ellipse eccentricity is equal to 0.5		
	Elastic modulus (MPa)			2.5×10^4		
	Poisson's ratio			0.25		
Asphalt Mastic	Poisson's ratio			0.35		
	Shear relaxation modulus (MPa)	$G_R(0)$	Group 1	96		
			Group 2	72		
			Group 3	48		
		$G_R(\infty)$	Group 1	0.17		
			Group 2	0.13		
			Group 3	0.09		
	Bulk relaxation modulus (MPa)	$K_R(0)$	Group 1	286		
			Group 2	215		
			Group 3	143		
		$K_R(\infty)$	Group 1	286		
			Group 2	215		
			Group 3	143		
	The Modulus Ratios	α_1		0.001806		
		α_2		0.013831		
		α_3		0.029784		
		α_4		0.883246		

Table 6.3 Geometric and Material Parameters Used in the Numerical Simulations (continued)

Material	90% RUW	RUW	110% RUW
Air Voids (%)*	4 (4.21)	4 (3.85)	4 (3.69)
Loading Path	dynamic vertical stress		

* The number of sides of polygon from 4 to 6 has equal probability in each sieve size.
* The ellipse eccentricity is computed according to the elongation ratio 3:1. The fraction of elongation is 10% and has equal probability for each sieve size.
* Air voids in the bracket is the actual value in the material model and this parameters was not used for simulation.

Figures 6.11 to 6.13 illustrate the results of permanent strain for the three simulated SMA mixtures with different aggregate packing (geometric parameters) and different material parameters of asphalt mastic from the finite element analysis. In order to determine the optimal material parameters of asphalt mastic, the experimental results for each studied SMA mixture are also plotted in these figures.

It is noticeable that the deformation behaviour of the simulated mixes with 90% RUW, 100% RUW, and 110% RUW showed an identical trend when the material parameters of asphalt mastic change with the decrease in the relaxation modulus of the asphalt mastic, the accumulated permanent strain increased accordingly. Comparing the simulated results with the experimental data, it is obvious that the permanent strain for each three simulated SMA mixtures using Group 2 material parameters showed the best simulation with the experimental data. The largest difference between the permanent strain using Group 2 material parameters and experimental data is 6%, 7%, and 7%, respectively, for SMA mixtures with 90% RUW, 100% RUW, and 110% RUW. However, it can be concluded that there was

no significant difference between these simulated values and the experimental data at 95% confidence level through a statistical t-test (Their P values are 0.03, 0.03, and 0.03, respectively, which are all smaller than 0.05.). Therefore, in the numerical simulation of SMA, Group 2 material parameters were determined as the optimal material parameters of asphalt mastic in this research study.

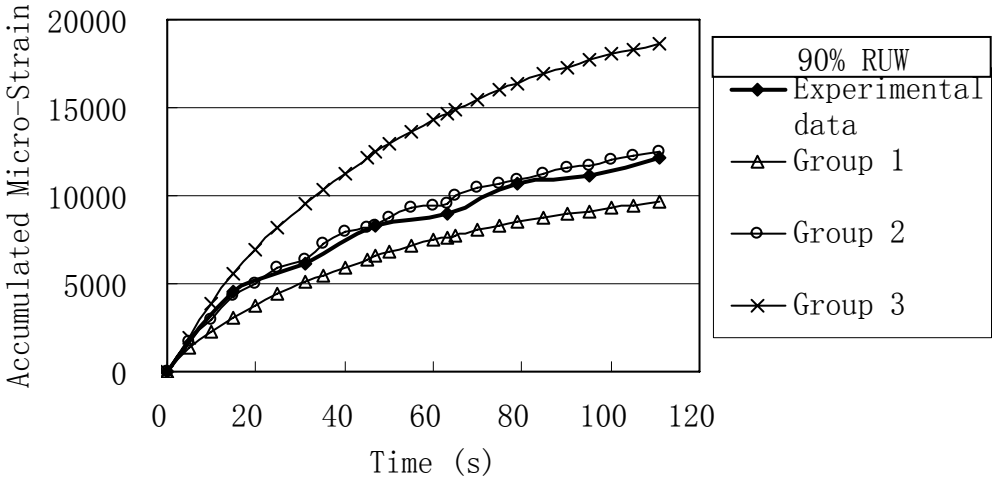

Figure 6.11 Permanent Strain for Asphalt Mixtures with 90% RUW

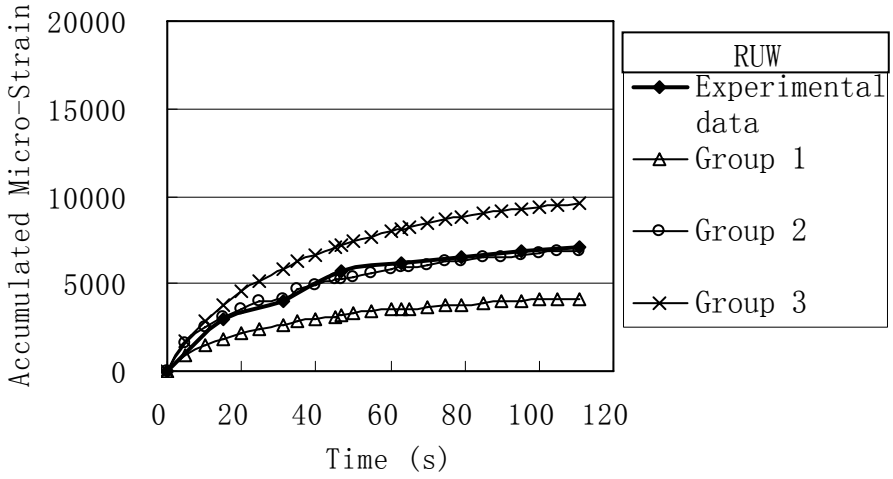

Figure 6.12 Permanent Strain for Asphalt Mixtures with RUW

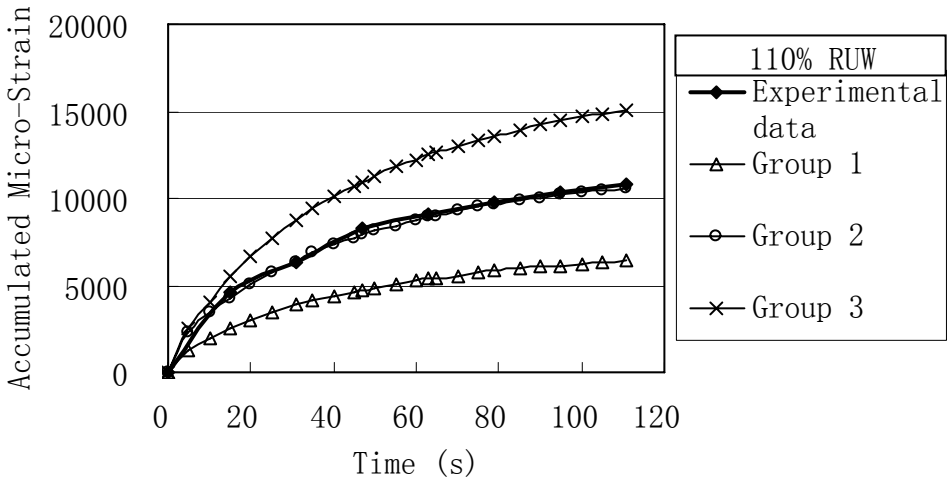

Figure 6.13 Permanent Strain for Asphalt Mixtures with 110% RUW

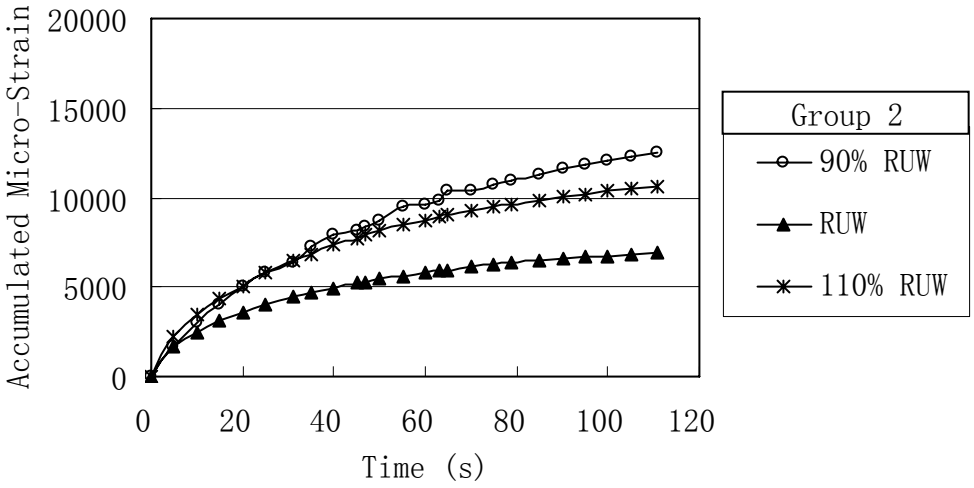

Figure 6.14 Permanent Strain for Simulated Asphalt Mixtures

Consider the simulated results using Group 2 material parameters (optimal material parameters) and plotting them in Figure 6.14, the accumulated micro-strain of the three simulated mixes was significantly different with different geometric parameters of aggregates. Mixes with 100% RUW obtained the smallest permanent deformation, while mixes with 90% RUW had the highest value. Additionally, it is

also noted that mixes with 100% RUW showed a lower permanent deformation rate as compared to the other two mixes. This trend is similar to the experimental results as described in Chapter 5, where different volume fractions of coarse aggregate resulted in different aggregate packing. For the simulated mixes with 100% RUW, the generated coarse aggregates in the finite element model were packed together and formed a firmly coarse aggregate skeleton, thus a high shear resistance to plastic deformation.

6.6 VALIDATION STUDY AND EXPANSIONS

Section 6.5 developed three simulated models for determining the optimal material parameters reflecting experimentally known properties of SMA. Based on these material parameters of asphalt mastic and the created FEM model set up, validation study for comparing the predicted performance of SMA mixtures with the experimental results obtained in Chapter 5 were conducted.

SMA mixture with 105% RUW, which had the highest rutting resistance in this study, was chosen and simulated and compared with its experimental results obtained in Chapter 5 . The simulated results and the experimental data of this SMA mixture are plotted in Figure 6.15 and discussed below.

Comparing the two curves in Figure 6.15, the modelling results matched well with the experimental data. Figure 6.16 gives the residual analysis of the simulated results and the experimental data. This analysis of residuals identifies the existence of any difference between the predicted and the measured value. It is a visual identification of trends in the ordered test residual output.

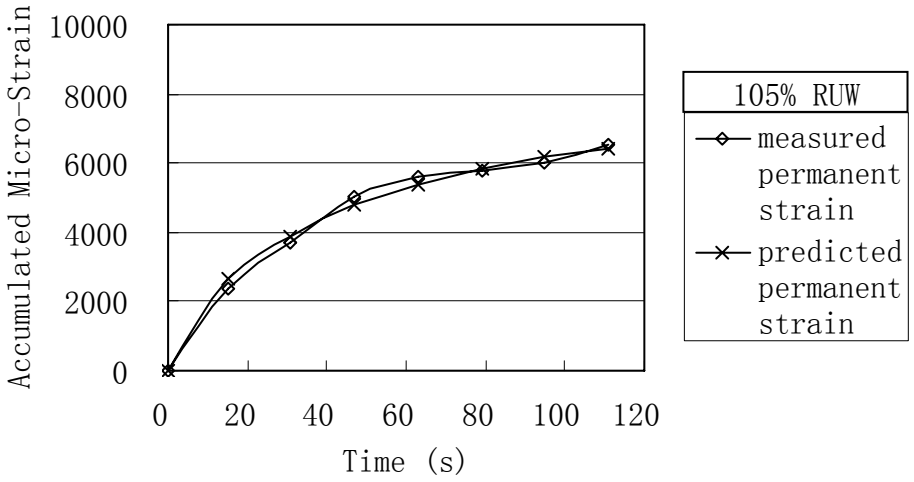

Figure 6.15 Measured and Predicted Permanent Strain for Asphalt Mixtures

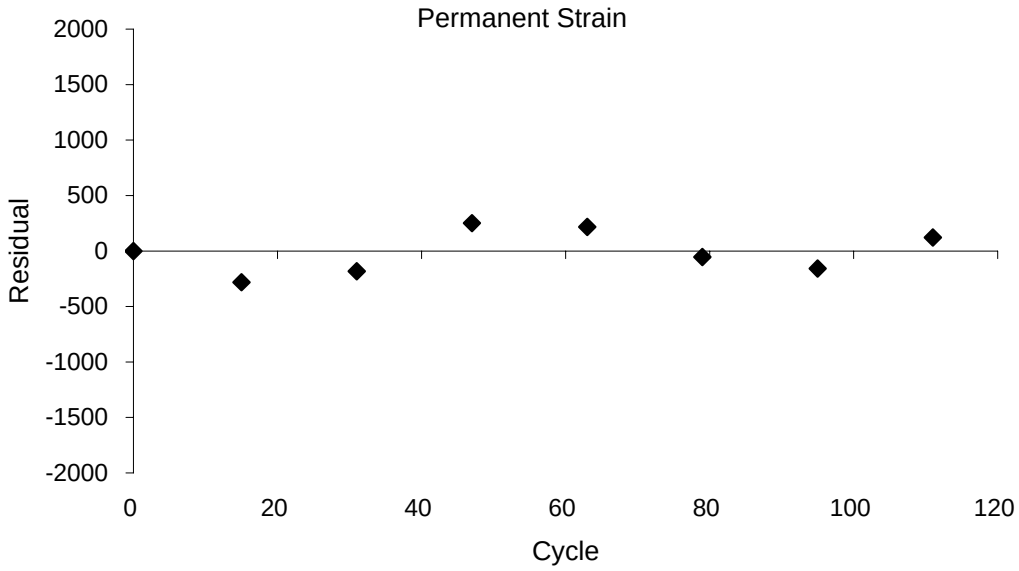

Figure 6.16 Residual Plot for the Predicted and Measured Permanent Strain

From Figure 6.16, one can note that it does not show any large difference in the simulated values with the experimental data of the SMA mixture. The residual of permanent strain is randomly scattered about the average (0 on the Y axis of the residual plot) with little to no trend in the scatter plot, which signifies the normality of the finite element analysis.

The numerical simulations of SMA described above allow control of the properties of aggregates (such as size, shape, angularity and eccentricity) with some basic assumptions on the behaviour of the aggregates. However, the same aggregate properties (maximum aggregate size, particle shape, and particle elongation) were used in these finite element analyses according to the experimental results in order to validate the numerical model. Therefore, it is necessary to develop a numerical simulation of SMA which has different aggregate properties so that the experimental results can be expanded.

Table 6.4 presents the summary of the geometric and material parameters used in the expanded numerical simulation. In order to compare the effect of different aggregate properties on the performance of SMA, the parameters of SMA mixture with 105% RUW used in the original simulation are also listed in the table. These two simulated model of SMA mixtures have different maximum aggregate size, particle shape, and particle elongation and the same material parameters.

Figure 6.17 illustrates the results of permanent strain for the expanded numerical simulation of SMA mixtures with 105% RUW. The original results of the SMA mixture with 14 mm maximum aggregate size are also plotted in the figure to be used for comparison. In the initial phase, the two simulated mixtures almost had the same permanent strain. But with the increase in the number of loading cycles, the expanded simulated model with 19 mm maximum aggregate size showed a higher

deformation resistance. This may be attributed to a larger maximum aggregate size (19 mm) and not having elongation particle (ellipse eccentricity is equal to 0), which resulted in forming a more firm coarse aggregate skeleton, thus, a high deformation resistance.

In essence, the basic approach in this study generally involves a methodology for combining the measured behaviour of the bitumen with some simple assumptions about the behaviour of the aggregate. However, the developed numerical simulation results of SMA did match very well with the experimental data.

Table 6.4 Comparisons of Parameters Used in the Numerical Simulations

Material			**105% RUW**	
			Expanded	**Original**
Model Size (mm)			50 × 63.5	
Aggregate	**Volume fraction (%)**		62.1	63.6
	Particle size		standard sieve size from 19 mm to 3.35 mm	standard sieve size from 14 mm to 3.35 mm
	Particle shape*		the number of sides of polygon is 5	the number of sides of polygon is between 4-6
	Particle elongation		ellipse eccentricity is equal to 0	ellipse eccentricity is equal to 0.5
	Elastic modulus (MPa)		2.5×10^4	
	Poisson's ratio		0.25	
Asphalt Mastic	**Poisson's ratio**		0.35	
	Shear relaxation modulus (MPa)	$G_R(0)$	72 (Group 2)	
		$G_R(\infty)$	0.13 (Group 2)	

Table 6.4 Comparisons of Parameters Used in the Numerical Simulations (continued)

Material			105% RUW	
			Expanded	Original
Asphalt Mastic	Bulk relaxation modulus (MPa)	$K_R(0)$	215 (Group 2)	
		$K_R(\infty)$	215 (Group 2)	
	The Modulus Ratios	α_1	0.001806	
		α_2	0.013831	
		α_3	0.029784	
		α_4	0.883246	
Air Voids (%)*			4 (4.12)	4 (3.78)
Loading Path			dynamic vertical stress	

* The number of sides of polygon from 4 to 6 has the equal probability in each sieve size.

* Air voids in the bracket is the actual value in the material model and

* Group 2 material parameters (optional) were used.

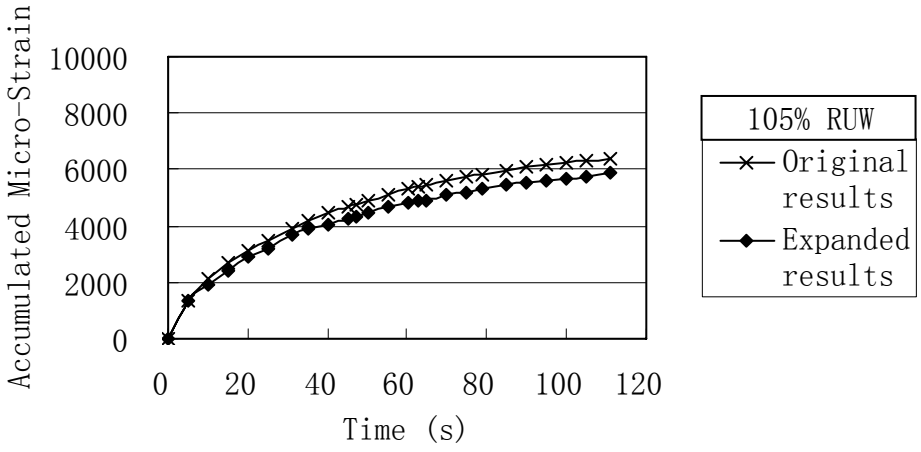

Figure 6.17 Predicted Permanent Strain for SMA with Different Aggregate Properties

6.7 SUMMARY OF NUMERICAL SIMULATION OF SMA

A two dimensional dynamic finite element procedure was developed to simulate SMA mixtures in connection with permanent deformation. Visco-elastic models were successfully used in the finite element software, ANSYS, to simulate the dynamic responses and to predict the permanent deformation (rutting) of SMA mixtures. A numerical study of finite element analyses was conducted through three typical asphalt mixtures (SMA mixtures with 90, 100, and 110% RUW) with different particle packing and different material parameters. The optimal material parameters reflecting experimentally known properties of SMA mixtures were determined. Finally, the numerical results of SMA mixture with 105% RUW were compared with the experimental data obtained in Chapter 5 and was expanded to other SMA mixture with different aggregate properties. The following observations can be made.

- Two dimensional dynamic finite element analyses can be simulated using the commercial finite element software, ANSYS, to simulate SMA mixtures;
- Two dimensional dynamic finite element analyses were able to predict the dynamic strain responses of the asphalt mixture with time;
- Visco-elastic models incorporated into the 2-D dynamic finite element procedure were able to predict the viscous characteristics of the asphalt mastic material under the traffic loading;
- Permanent deformation (rutting) could be predicted through the application of a visco-elastic model incorporated into the 2-D dynamic finite element procedure;
- The generated geometric model reflected well the inter-granular interactions between aggregate and asphalt mastic. The particle size, shape and elongation

can be controlled by the microstructural parameters, thus, the experimental results can be expanded to other SMA mixtures with different aggregate properties through the numerical simulation of SMA.

CHAPTER SEVEN

CONCLUSIONS AND RECOMMENDATIONS

Stone Mastic Asphalt mixtures can provide an extremely high rutting resistance. However, most SMA design procedures still based their mix design on empirical procedures. As in most mixture designs, there is little or no mixture performance analysis involved during the design procedure, especially the analysis of coarse aggregate stone-to-stone contact. The aggregates were combined on a weight basis in past studies of SMA. This method is rather limited as combining aggregates by weight cannot evaluate the degree of aggregate interlock because of differing specific gravities of coarse and fine aggregates, including mineral fillers. This research has provided a methodology of quantifying coarse aggregate stone-to-stone contact in SMA with different aggregate packing by volume to yield high rutting resistance; thus, developing a new mix design procedure and leading to an improved SMA mixture design and performance. The concepts that utilised aggregate interlock and aggregate packing are proposed to develop coarse aggregate stone-to-stone contact. A total of thirty-seven mixtures were tested to evaluate the effects of various aggregate combinations on the stone-to-stone contact of SMA

mixtures. Each mixture composed of different combinations of the aggregate gradation and asphalt binder. Tests were conducted to characterise the volumetric properties, resilient modulus, resistance to permanent deformation, and rut susceptibility of these mixtures. A 2-D dynamic finite element procedure was developed during this study. Advanced material model of visco-elastic behaviour was incorporated into the 2-D dynamic finite element procedure. This procedure was used to expand the experimental results to other aggregate types and maximum aggregate sizes to investigate their coarse aggregate stone-to-stone contact.

7.1 CONCLUSIONS

Within the context of the experimental study, the following general observations and conclusions could be made:

- The proposed methodology to develop a new mix design procedure for SMA can quantify coarse aggregate stone-to-stone contact;
- The method that utilised aggregate interlock and aggregate packing to combine aggregates would give a rational approach to select the appropriate volume of coarse and fine aggregates to develop aggregate stone-to-stone contact. The ratios for the analysis of gradation has provided a method to quantify the packing of the aggregates in the SMA that relates to the volumetric and mechanical properties in the material;
- Particle packing concepts are important in the understanding of the combination of the aggregates. The packing of spheres had provided a background for the study of aggregate packing. From the packing of spheres, an estimate of the size of voids in the coarse aggregate is given by the characteristic particle diameter ratio of 0.22; and
- With SMA mixtures controlled by the concepts of particle packing presented in

this study, different SMA mixtures can be designed by changing the design unit weight of the coarse aggregate in the mixture.

Volumetric properties are highly influenced by the change in the volume of coarse aggregate in the mixture; thus, affecting the coarse aggregate stone-to-stone contact.

- The volumetric property tests indicated that with an increase in the volume of coarse aggregate from 90% RUW (Rodded Unit Weight) to 105% RUW, the large aggregate particles would interlock and resist deformation, thereby giving an increase of voids in SMA mixtures; and
- VCA_{dry} and VCA_{mix} can be used as a design criterion in SMA mixtures as an identifier of coarse aggregate stone-to-stone contact when compared with the design unit weight of coarse aggregate;

Ascertaining these important volumetrics by carrying out the physical mixture tests, the following conclusions are made:

- The resilient modulus test did not give conclusive findings related to the coarse aggregate stone-to-stone contact of SMA mixtures;
- The rutting tests indicated that SMA mixtures designed with the proposed concepts exhibited excellent rutting resistance as compared to the dense-graded mixture. SMA mixtures designed with the unit weight of the coarse aggregate between 95 and 105% RUW performed much better than those SMA with other percentages of RUW. Also, the higher the degree of stone-to-stone contact, the higher would be the rutting resistance;
- The asphalt binder content had a significant effect on the performance of SMA mixtures. Asphalt content of 5.5% was found to be sufficient for the designed aggregate gradation of SMA mixture. In addition, asphalt binder content was a more significant variable as compared with aggregate gradation in explaining the performance of asphalt mixtures;

- Aggregate gradation is important in the material properties of SMA. The gradation of the coarse aggregate would change the size of the voids, which translates to a change in the development of coarse aggregate stone-to-stone contact. However, the gradation of the fine aggregate has little effect on the aggregate stone-to-stone contact of the SMA mixtures; and
- Evaluation of gradation with aggregate packing ratios would provide a new tool for examining aggregate gradations of SMA. These ratios, based on particle packing, would provide a distinct relationship with the resulting air voids and permanent strain of the SMA mixtures;

Through the results of the experimental study, a new mix design procedure for SMA to ensure stone-to-stone contact was established. This procedure is suitable for any aggregate type and maximum aggregate size (for example, see Appendix A 'Aggregate Blending Example Calculations'). It can also be used to check aggregate gradation for stone-to-stone contact (for example, see Appendix A 'Validation for LTA SMA Mix Specification').

The material used in this study is mainly based on Singapore conditions, which utilises only one type of crushed granite aggregate with a 14 mm maximum aggregate size, 10% mineral filler and 5.5% optimum binder content. This has somewhat limited the experimental findings. Therefore, a two dimensional dynamic finite element procedure was developed to expand the applicability of the mix design to other aggregate types, maximum aggregate sizes, and binder content. Within the context of the modelling and validation study undertaken in the research, the following general observations can be made:

- Permanent deformation (rutting) could be predicted through the application of a visco-elastic model that incorporated into the 2-D dynamic finite element procedure; and

- The generated geometric model reflected well the inter-granular interactions between aggregate and asphalt mastic. The particle size, shape and elongation can be controlled by the microstructural parameters, thus, the applicability of the mix design can be expanded to other SMA mixtures with different aggregate properties through the numerical simulation of SMA.

The results in this study improved the SMA mixture design by providing a method to characterise coarse aggregate stone-to-stone contact in SMA mixtures through the fundamental principles of particle packing. The design concepts outlined in this study would provide the foundation for a new procedure of SMA mixture design.

Within the context of the research study, a number of limitations had been encountered. They are briefly listed below:

- The experimental study in this research is mainly based on Singapore conditions;
- Field performance of pavements containing SMA mixtures was not conducted due to the limited time frame; and
- In the developed numerical simulation of SMA, mostly material parameters were used from published data, especially the stiffness of asphalt mastic.

7.2 RECOMMENDATIONS

Based on the aforementioned limitations, the following recommendations are offered:

- If the developed mix design procedure for SMA is to be used in other localites (different from Singapore conditions), the loose and the rodded unit weight of coarse aggregate and the rodded unit weight of fine aggregate need to be

determined again;

- In the developed numerical simulation procedure of SMA, asphalt mastic is composed of the agglomeration of polymer modified binder and fine aggregates (smaller than 3.35 mm in size). Its stiffness was estimated to be 20 times stiffer than the binder based on the conditions of 5.5% asphalt binder content, fine aggregates smaller than 3.35 mm in size, and 10% mineral filler. If these conditions were changed, its stiffness would be different as well. Therefore, asphalt mastic stiffness need to be further validated through Dynamic Shear Rheometer (DSR) test; and
- The developed SMA mixture in this study is mainly based on the laboratory performance. It is necessary to correlate pavement field performance to the fundamental engineering properties. Therefore, further study is needed to build pavement test sections to compare the field performance of pavements containing SMA mixtures designed by the proposed concepts in this study with those pavements constructed with dense-graded mixtures.

Implementation of these recommendations should result in a better way to design SMA mixtures and serve to improve the performance and to enhance the economic advantages that SMA has over other paving mixtures.

REFERENCES

AASHTO, (1991). Report on the 1990 European Asphalt Study Tour, American Association of State Highway and Transportation Officials, Washington DC.

AASHTO T-85-91, (2004). Specific Gravity and Absorption of Coarse Aggregate, American Association of State Highway and Transportation Officials, Washington DC.

Abbas, A.R., Papagiannakis, A.T., and Masad, E.A., (2004). "Linear and Nonlinear Viscoelastic Analysis of the Microstructure of Asphalt Concretes." Journal of Materials in Civil Engineering, ASCE, Vol. 16, No. 2, pp 133-139.

Ahlrich, R.C., (1996). Influence of Aggregate Gradation and Particle Shape/Texture on Permanent Deformation of Hot Mix Asphalt Pavements, Technical Report GL-96-1, US Army Corps of Engineers Waterways Experiment Station, Vicksburg, MS.

Aim, R.B. and Goff, P.L., (1967). Effet de Paroi dans les Empilements Desordonnes de Spheres et Application a la Porosite de Melanges Binaries, Powder Technology (cited in Vavrik, 2002).

ANSYS, (2004). Online Documentation: Finite Element Software Package, Version 8.0, ANSYS Inc.

Asphalt Institute (AI), (1993). Mix Design Methods for Asphalt Concrete and Other Hot Mix Types, MS-2, Sixth Edition.

ASTM Designation C29-78, (1998). Standard Test Method for Unit Weight and Voids in Aggregate, American Society for Testing Materials Annual Book of ASTM Standards, Vol. 04-02.

ASTM Designation C1252-93, (1998). Standard Test Methods for Uncompacted Void Content of Fine Aggregate, American Society for Testing Materials Annual Book of ASTM standards, Vol. 04-02.

ASTM Designation D6390-99, (2001). Standard Test Method for Determination of Draindown Characteristics in Uncompacted Asphalt Mixtures, American Society for Testing Materials Annual Book of ASTM Standards, Vol. 04-03.

Australian Standard (AS), (1995). Determination of the Permanent Compressive Strain Characteristics of Asphalt, Method of Sampling and Testing Asphalt, Australian Standard, Method 12.1, Australia.

Australian Standard (AS), (1995). Determination of the Resilient Modulus of Asphalt: Indirect Tensile Method, Australian Standard, Method of Sampling and Testing Asphalt, Australian Standard, Method 13.1, Australia.

Bahia H., (2001). Superpave Protocols for Modified Asphalt Binders, NCHRP Study 9-10, Draft Final Report.

Baumgaertel, M. and Winter, H.H., (1989). "Determination of Discrete Relaxation and Retardation Time spectra from Dynamic Mechanical Data." Rheologica Acta, Vol. 28, pp 511-519.

Bellin, P., (1992). Use of Stone Matrix Asphalt in Germany: State-of-the-Art, Paper Presented to the A2F02 Committee, Transportation Research Board, National Academy of Science, Washington, DC.

Bellin, P., (1997). Designing Stone Mastic Asphalt Mixtures, Stone Mastic Asphalt Status Report, European Asphalt Pavement Association Technical Committee, Breukelen, the Netherlands.

Bellin, P., (1998a). Stone Mastic Asphalt in Germany, The Asphalt Yearbook, The Institute of Asphalt Technology, Middlesex, United Kingdom.

Bellin, P., (1998b). Heavy Duty Surfaces: The Arguments for SMA, European Asphalt Pavement Association Technical Committee, Breukelen, the Netherlands.

Bourbie, T., Coussy, O., and Zinszner, B., (1987). Acoustics of Porous Media, Gulf Publishing Co., Houston.

British Standard Institution (BSI), (1996). Methods of Test for the Determination of Wheel Tracking Rate, BSI, London, BS 598: Part 110.

British Standard Institution (BSI), (1998). Methods of Test for the Determination of Wheel Tracking Rate and Depth, BSI, London, BS 598: Part 110.

Brown, E.R., (1993a). Evaluation of SMA Used in Michigan, NCAT Report No. 93-3, the National Centre for Asphalt Technology.

Brown, E.R., (1993b). Experience with Stone Matrix Asphalt in the United States, NCAT Report No. 93-4, the National Centre for Asphalt Technology.

Brown, E.R. and Manglorkar, H., (1993). Evaluation of Laboratory Properties of SMA Mixtures, NCAT Report No. 93-5, the National Centre for Asphalt Technology.

Brown, E.R. and Mallick, R.B., (1994). Stone Matrix Asphalt Properties Related to Mixture Design, NCAT Report No. 94-2, the National Centre for Asphalt Technology.

Brown, E.R., Haddock, J.E., Crawford, C., Hughes, C.S., and Lynn, T.A., (1995). Designing Stone Matrix Asphalt Mixtures, Volume II - Research Results, Interim Report, National Cooperative Highway Research Program Project 9-8, Transportation Research Board, National Research Council, Washing, DC.

Brown, E.R. and Mallick, R.B., (1995). "Evaluation of Stone-on-Stone Contact in Stone-Matrix Asphalt." Journal of the Transportation Research Board, Record No. 1492, pp 208-219.

Brown, E.R., Haddock, J.E., Crawford, C., and Mallick, R.B., (1996). Designing Stone Matrix Asphalt Mixtures, Volume II - Research Results, Draft Final Report, National Cooperative Highway Research Program Project 9-8, Transportation Research Board, National Research Council, Washing, DC.

Brown, E.R., Haddock, J.E., Mallick, R.B., and Lynn, T.A., (1997a). "Development of a Mixture Design Procedure for Stone Matrix Asphalt (SMA)." Journal of the Association of Asphalt Paving Technologists, Vol. 66, pp 1-30.

Brown, E.R., Rajib B.M., and Haddock, J.E., (1997b). Performance of Stone Matrix Asphalt (SMA) Mixtures in the United States, NCAT Report No. 97-3, the National Centre for Asphalt Technology.

Brown, S.F. and Scholz, T.V., (1998). "Permanent Deformation Characteristics of Porous Asphalt Determined in the Confined Repeated Load Axial Test." Highways and Transportation, Vol. 45, No. 12, pp 7-10.

Buncher, M.S., (1995). Evaluating the Effects of the Wet and Dry Processes for Including Crumb Rubber Modifier in Hot Mix Asphalt, PhD Thesis, Auburn University, Alabama.

Cheung, C.Y., (1995). Mechanical Behaviour of Bitumen and Bituminous Mixes, PhD Thesis, Cambridge University Engineering Department.

Cheung, C.Y., Cocks, A.C. F., and Cebon, D., (1999). "Isolated Contact Model for an Idealized Asphalt Mix." Journal of Mechanics Science, Vol. 41, pp 767-792.

Cocks, A.C.F., (1994). "The Structure of Constitutive Laws for the Sintering of Fine Grained Materials." Acta Metallurgica et Materialia, Vol. 42, No. 7, pp 2191-2210.

Cooley, Jr. and Brown, E.R., (2003). Potential of using Stone Matrix Asphalt (SMA) for thin overlays, NCAT Report No. 2003-01, the National Centre for Asphalt Technology.

Davidson, J.K. and Kennepohl, G.J., (1992). Introduction of Stone Mastic Asphalt in Ontario, Report for AAPT meeting in Charleston, South Carolina, February 24-26.

Davis, R., (1980). Improved Aggregate Structure Through Gap Gradation, Personal Paper Rough Draft (cited in Vavrik, 2002).

de Larrard, F. and Sedran, T., (1994). "Optimization of Ultra-High-Performance Concrete by the Use of a Packing Model." Cement and Concrete Research, Vol. 24, No. 6, pp 997-1009.

Deshpande, V.S., (1995). Deformation Behaviour of Idealized Bituminous Mixes, Master Thesis, Cambridge University Engineering Department, U.K.

Deshpande, V.S., (1997). Steady-State Deformation Behaviour of Bituminous Mixes, PhD Thesis, Cambridge University, Engineering Department, U.K.

Deshpande, V.S. and Cebon, D., (2004). "Micromechanical Modelling of Steady-State Deformation in Asphalt." Journal of Materials in Civil Engineering, ASCE, Vol. 16, No. 2, pp 100-106.

Drake, R., (1991). Asphalt-Mix Technology Puts Emphasis on Aggregate, Pit and Quarry.

Dvorkin, J., Amos, N., and Hezhu, Y., (1994). "Effective Properties of Cemented Granular Materials." Mechanics of Materials, Vol. 18, pp 351-366.

Eaton, M., (1991a). "Wisconsin Tests New Stone Mastic Asphalt Technique." Roads and Bridges, Vol. 29, No. 9, pp 45.

Eaton, M., (1991b). "Over 300 Gather for European SMA FHWA Michigan Demo Project." Roads and Bridges, Vol. 29, No. 10, pp 98.

Foo, K.Y., (1994). Predicting Rutting in Hot Mix Asphalt, PhD Thesis, Auburn University, Alabama.

Frohlich, H. and Sack, R., (1946). Theory of the Rheological Properties of Dispersions (cited in Deshpande and Cebon, 2004).

Fujita, D., (2002). Untitled and Unpublished Report (cited in Lynn, 2002).

Gabrielson, J.R., (1992). Evaluation of Hot Mix Asphalt (HMA) Static Creep and Repeated Load Tests, PhD Thesis, Auburn University, Alabama.

Germany Specification, (1984). Zusazliche Technische Vertragsedingungen und Richilinien fur den Bau von Farahndeckenaus Asphalt (cited in Lynn, 2002).

Goltermann, P., Johansen, V., and Palbol, L., (1997). "Packing of Aggregates: An Alternative Tool to Determine the Optimal Aggregate Mix." ACI Materials Journal, Vol. 94, No. 5, pp 435-443.

Goode, J.F. and Lufsey, L.A., (1962). "A New Graphical Chart for Evaluating Aggregate Gradation." Proceedings of the Association of Asphalt Paving Technologists, Vol. 31, pp 176-207.

Haddock, J.E., Liljedahl, B., Kriech, A.J., and Huber, G.A., (1993). "Stone Matrix Asphalt: Application of European Design Concepts in North America." Canadian Technical Asphalt Association Proceedings, Canada, pp 183-209.

Haddock, J.E., (1998). Characterization of Stone Matrix Asphalt mortars, PhD Thesis, Auburn University, Alabama.

Hills, J.F., (1973). "The creep of Asphalt Mixes." Journal of the Institute of Petroleum, Vol. 59-570, pp 247-262.

Hsu, T.W. and Leu, J.T., (1998). Evaluation of Permanent Deformation of Stone Matrix Asphalt Mixtures, Paper Presented to the 77th Annual Meeting of the Transportation Research Board, National Academy of Sciences, Washington, DC.

Huber, G.A. and Shuler, T.S., (1992). Providing Sufficient Void Space for Asphalt Cement: Relationship of Mineral Aggregate Voids and Aggregate Gradation, American Society for Testing and Materials, ASTM, STP 1147.

Huber, G.A. and Decker, D.S., (1994). Engineering Properties of Asphalt Mixtures and the Relationship to Performance, American Society for Testing and Materials, ASTM, STP 1265.

Hudson, S.B. and Davis, R.L., (1962). "Relationship of Aggregate Voids to Gradation." Proceedings of the Association of Asphalt Paving Technologists, Vol. 31.

Johansen, V. and Andersen, P.J., (1991). "Particle Packing and Concrete Properties." Materials Science of Concrete, South American Ceramic Society, Vol. 2, pp 244-253.

Kandhal, P.S., Foo, K.Y., and Mallick, R.B., (1998). A Critical Review of VMA Requirements in Superpave, NCAT Report No. 98-1, the National Centre for Asphalt Technology.

Kandhal, P.S. and Mallick, R.B., (1999). Evaluation of the Asphalt Pavement Analyser for HMA Mix Design, NCAT Report No. 99-4, the National Centre for Asphalt Technology.

Kast, O.E., (1985). Long-Term Experience with Splittmastixasphalt in the Federal Republik of Germany, Eurobitume Symposium.

Kight, D. and Crockford, W., (1998). Tailgates, Beer Mugs, Napkins and No. 2 Pencils – Mix Design on A Budget, Copyright Bill Crockford.

Kim, Y.R., Lee, H.J., and Little, D.N., (1997a). Mechanistic Evaluation of Fatigue Damage Growth and Healing of Asphalt Concrete: Laboratory and Field Experiments, In Proceedings of the 8th International Conference on Asphalt Pavements, Vol. II, International Society of Asphalt Pavements, pp 1089-1108.

Kim, Y.R., Lee, H.J., and Little, D.N., (1997b). "Fatigue Characterization of Asphalt Concrete Using Viscoelasticity and Continuum Damage Theory." Journal Association of Asphalt Paving Technologists, Vol. 66, pp 520-569.

Kosmatka, S.H., and Panarese, W.C., (1988). Design and Control of Concrete Mixtures, Portland Cement Association, Thirteenth Edition.

Kuennen, T., (1991). "Split Mastic Asphalt-Next Overseas Import." Roads and Bridges, Vol. 29, No. 1, pp 48.

Lau H. P., (1999). Creep Characteristics of Stone Mastic Asphalt mixtures, Final Year Project Report, School of Civil and Structural Engineering, Nanyang Technological University, Singapore.

Lee, H.J., and Kim, Y.R., (1998). "Viscoelastic Continuum Damage Model of Asphalt Concrete with Healing." Journal of Engineering Mechanics, ASCE, Vol. 124, No. 11, pp 1-9.

Liljedahl, B., (1990). Heavy Duty Asphalt Pavement, Swedish Asphalt Pavement Association, Sweden.

Lu, Y., Lu, L., and Wright, P.J., (2002). "Visco-Elastoplastic Method for Pavement Performance Evaluation." Transport, Vol. 153, No. 4, pp. 227-234.

Lum, K.M. and Hassabo N.I., (2003). "Binder Influence Type on Deformation Resistance of Stone Mastic Asphalt." Proceedings of the Institution of Civil Engineers, Transport, Vol. 156, No. 1, pp 43-49.

Lynn, T.A., (2002). Evaluation of Aggregate Size Characteristics in Stone Matrix Asphalt (SMA) and Superpave Designed Mixtures, PhD Thesis, Auburn University, Alabama.

Mallick, B.R., Ahlrich, R.C., and Brown, E.R., (1994). Potential of Dynamic Creep to Predict Rutting (cited in Huber and Decker, 1994).

Mavko, G., Mukerji, T., and Dvorkin, J., (1998). Tools for Seismic Analysis in Porous Media, The Rock Physics Handbook, Cambridge University Press.

Mogawer, W.S., and Stuart, K.D., (1994). Evaluation of Stone Matrix Asphalt Versus Dense-graded Mixtures, Paper presented to the 73rd Annual Meeting of the Transportation Research Board, National Academy of Sciences, Washington, DC.

Monismith, C.L., Hicks, R.G., Finn, F.N., Sousa, J., Harvey, J., Weissman, S., Deacon, J., Coplantz, J., and Paulsen, G., (1994). Permanent Deformation Response of Asphalt Aggregate Mixes, Report No. SHRP-A-415, Strategic Highway Research Program, National Research Council, Washington, DC.

National Asphalt Pavement Association (NAPA), (1994). Guidelines for Materials, Production, and Placement of Stone Matrix Asphalt (SMA), IS-118.

National Stone, Sand and Gravel Association (NSSGA), (1991). The Aggregate Handbook, National Stone, Sand and Gravel Association, Arlington.

Nijboer, L.W., (1948). Plasticity as a Factor in the Design of Dense Bituminous Road Carpets, Elsevier, 1948.

Nobel Industry, (1991). An Introduction to Stone Mastic Asphalt (SMA), Introductory Handout.

Nunn, M.E., Brown, A.J., and Guise, S.J., (1998). Assessment of Simple Tests to Measure Deformation Resistance of Asphalt, Transport Research Laboratory Project Report PR/CE/92/98.

Papagiannakis, A.T., Abbas, A.R., and Masad, E.A., (2002). "Micromechanical Analysis of Viscoelastic Properties of Asphalt Concretes." Journal of the Transportation Research Board, Record No. 1789, pp 113-120.

Parson, R.H., (1991). "European Paving Technology Spurs American Thought." American Association of State Highway and Transportation Officials, Vol. 70, No. 4

Phoon Y.L., (1997). Resilient Modulus Characteristics of Stone Mastic Asphalt, Final Year Report, School of Civil and Structural Engineering, Nanyang Technological University, Singapore.

Powers, T. C., (1964). "Geometric Properties of Particles and Aggregates." Journal of the PCA Research and Development Laboratories, Portland Cement Association, Vol. 6.

Pryor, C., (1991). Stone Mastic Asphalt: A Potential Rutting Solution, Stone Review.

Reed, J.S., (1988). Introduction to the Principles of Ceramic Processing, John Wiley & Sons, New York.

Richter, E., (1991). Verleichende Untersuchungen an stabilisierenden Zusatzen fur Splittmastixasphalt (cited in Lynn, 2002).

Rinckes, G., (1989). "Steenmastiekasfalt op Plaatsen met Zware Belastingen." (cited in Lynn, 2002).

Roberts, F.L., Kandhal, P.S., Brown, E.R., Lee, D.Y., and Kennedy, T.W., (1996). Hot Mix Asphalt Materials, Mixture Design, and Construction, National Asphalt Pavement Association Education Foundation, Lanham, MD.

Rothenburg, L., Bogobowicz, A., Haas, R., Jung, F.W., and Kennepohl, G, (1992). Micromechanical Modelling of Asphalt Concrete in Connection with Pavement Rutting Problems, In Proceedings of the 7th International Conference on the Structural Design of Asphalt Pavements.

Roy, D.M., Scheetz, B.E., and Silsbee, M.R., (1993). Processing of Optimized Cements and Concretes Via Particle Packing, MRS Bulletin.

Sardal, K., (1988). Slitlager au HABS, A Translation of the Swedish Road Specification, Gothenburg, Sweden.

Schapery, R.A., (1987). "Deformation and Fracture Characterization of Inelastic Composite Materials Using Potentials." Polymer engineering, Vol. 27, pp 63-76.

Scherocman, J.A., (1991). "Stone Mastic Asphalt Reduces Rutting, Better Roads." Vol. 61, No.11, pp 26.

Scherocman, J.A., (1992). Construction of SMA Test Sites in the U.S., the Association of Asphalt Paving Technologists (AAPT) Meeting.

Schwartz, C.W., Gibson, N.H., Schapery, R.A., and Witczak, M.W., (2002). Viscoplasticity Modelling of Asphalt Concrete Behaviour, Department of Civil & Environmental Engineering, University of Maryland.

Seward, D.L., Hinrichsen, J.A., and Ries, J.L., (1996). "Structural Analysis of Aggregate Blends Using Strategic Highway Research Program Gyratory Compactor." Journal of the Transportation Research Board, Record No. 1545.

Shilstone, J.M., (1990). Concrete Mixture Optimization, Concrete International, American Concrete Institute, Farmington Hills, MI. pp 33-39.

Shilstone, J.M., (1993). "High Performance Concrete Mixtures for Durability." High Performance Concrete, American Concrete Institute, Vol. 3486, pp 310.

Sigurjonsson, S. and Ruth, B. E., (1990). "Use of Gyratory Testing Machine to Evaluate Shear Resistance of Asphalt Paving Mixture." Transportation Research Record, No. 1259, pp 63-78.

Stuart, K.D., (1992). Stone Mastic Asphalt (SMA) Mixture Design, Federal Highway Administration Report, Number FHWA-RD-92-006, Federal Highway Administration, Washington DC.

Tappeneir, W.J., (1990). Splittmastixasphalt, Novophalt America, Inc.

Tashman, L., Masad, E., Zbib, H., Little, D., and Kaloush, K., (2000). Anisotropic Viscoplastic Continuum Damage Model for Asphalt Mixes, 15th Engineering Mechanics Division Conference, Columbia University, New York.

Toh C.L., (1998). Flexural Stiffness Characteristics of Stone Mastic Asphalt, Final Year Report, School of Civil and Structural Engineering, Nanyang Technological University, Singapore.

Tons, E., and Goetz, W.H., (1967). Packing Volume Concept for Aggregates, Joint Highway Research Project Technical Paper No. 24, Purdue University.

Torquato, S., Truskett, T.M., and Debenedettie, P.G., (2000). Is Random Close Packing of Spheres Well Defined?, Physical Review Letters, The American Physical Society.

Toufar, W., Born, M., and Klose, E., (1976). Beitrag zur Optimierung der Packungsdichte Polydisperser Korniger Systeme (cited in Vavrik, 2002).

Toufar, W., Klose, E. and Born, M., (1977). Berechnung der Packungsdichte von Korngemischen (cited in Vavrik, 2002).

Van der Poel, C., (1958). On the Rheology of Concentrated Dispersions (cited in Deshpande and Cebon, 2004).

Vavrik, W.R., Pine, W.J., Carpenter, S.H., and Bailey, R., (2002). Bailey Method for Gradation Selection in HMA mixture Design, Transportation Research Circular, Number E-C044, Transportation Research Board.

Walsh, I.D., (1993). Stone Mastic Asphalt Wearing Course, Clause 995 AK, Kent County Council Specification.

Walter, P.H., (2000). Influence of Aggregate Type and Gradation on Critical Voids in the Mineral Aggregate in Asphalt Paving Mixtures, PhD Thesis, School of Civil Engineering, Iowa State University, Iowa.

Warren, J.M., (1991). SMA Comes to the USA, Hot Mix Asphalt Technology, National Asphalt Pavement Association.

Zhu, H., Chang C.S. and Rish, J.W., (1996a). "Normal and Tangential Compliance for Conforming Binder Contact Ⅰ: Elastic Binder." Intl. J. Solids Structure, Vol. 33, pp. 4337-4349.

Zhu, H., Chang C.S. and Rish, J.W., (1996b). "Normal and Tangential Compliance for Conforming Binder Contact Ⅱ: Viscoelastic Binder." Intl. J. Solids Structure, Vol. 33, pp. 4351-4363.

Zhu, H., (1998). Contact Mechanism Based Asphalt Concrete Modelling, the 12th ASCE Engineering Mechanics Conference, San Diego, California.

Zhu, H. and Nodes, J.E., (2000). "Contact Based Analysis of Asphalt Pavement with the Effect of Aggregate Angularity." Mechanics of Materials, Vol. 32, No. 3, pp 193-202.

APPENDIX A:

AN EXAMPLE DESIGN OF SMA AGGREGATE GRADATION

Aggregate Blending Example Calculations

The calculations in Figure A.1 provide an example of a SMA mix design using one coarse aggregate gradation, one fine aggregate gradation, and 7.5% mineral filler. This design uses aggregate packing concept to show how aggregates are blended together by volume. All aggregates used are based on Singapore conditions.

The following steps are presented to provide a general example of blending aggregates by volume:

Step 1: According to stockpile gradations of aggregate, determine the loose and rodded unit weight of coarse aggregate and the rodded unit weight of fine aggregate using Uncompacted Void Content of Aggregate Test Apparatus. Bulk specific gravity of each aggregate is also determined. They are shown in Figure A.1.

Step 2: Select the design unit weight of coarse and fine aggregates.

$$DUW_c = RUW_c * 105\% = 1610 * 105\% = 1691 kg/m^3$$

$$DUW_f = RUW_f = 1840\,kg/m^3$$

Note: suffix "c" indicates coarse aggregate; while suffix "f" indicates fine aggregate.

Material		
Coarse Aggregate	**Fine Aggregate**	**Mineral Filler**
Crushed granite Maximum size is 14 mm	Crushed granite Maximum size is 5 mm	Crushed granite All passing 0.075 mm

Bulk Specific Gravity		
Coarse Aggregate	**Fine Aggregate**	**Mineral Filler**
9.5 – 19. mm 2.683 6.3 – 9.5 mm 2.673 3.35 – 6.3 mm 2.643	0.075 – 3.35 mm 2.536	Passing 0.075 mm 2.78

Stockpile Gradation of Aggregate					
Coarse Aggregate		**Fine Aggregate**		**Mineral Filler**	
Sieve size	Passing	Sieve size	Passing	Sieve size	Passing
19 mm	100	19 mm	100	19 mm	100
14 mm	90	14 mm	100	14 mm	100
9.5 mm	68	9.5 mm	100	9.5 mm	100
6.3 mm	32	6.3 mm	100	6.3 mm	100
3.35 mm	6	3.35 mm	97	3.35 mm	100
2.36 mm	2	2.36 mm	73	2.36 mm	100
1.18 mm	2	1.18 mm	52	1.18 mm	100
0.6 mm		0.6 mm	34	0.6 mm	100
0.3 mm		0.3 mm	20	0.3 mm	100
0.15 mm		0.15 mm	5	0.15 mm	100
0.075 mm		0.075 mm	2	0.075 mm	100

Combined bulk specific gravity (G_{sb}) and unit weight of aggregates					
Coarse Aggregate		**Fine Aggregate**		**Mineral Filler**	
G_{sb}	2.663	G_{sb}	2.544	G_{sb}	2.78
LUW	1400 kg/m^3	RUW	1840 kg/m^3	Desired Content: 7.5%	
RUW	1610 kg/m^3	DUW	100% RUW		
DUW	105% RUW				

	Coarse Aggregate	**Fine Aggregate**	**Mineral filler**
Volume of Aggregate	73.5%	36.5%	
Initial blend % by weight	71.6%	28.4%	7.5%
Adjusted blend % by weight	75.0%	18.0%	7.0%

Figure A.1 An Example Design of SMA Aggregate Gradation

Step 3: Calculate the volume of voids in the coarse aggregate at the design unit weight. It is filled by the fine aggregate with rodded unit weight.

$$VCA = (1 - \frac{DUW_c}{G_{sb} * 1000}) * 100 = (1 - \frac{1691}{2.660 * 1000}) * 100 = 36.5$$

Note: VCA – voids in coarse aggregate.

Step 4: Determine the unit weight contributed by fine aggregate according to the desired volume blend of fine aggregate. This is the unit weight that fills the voids created by coarse aggregate.

$$\text{Unit weight contribution of fine aggregate} = DUW_f * VCA$$
$$= 1840 * 36.5\%$$
$$= 671\,kg/m^3$$

Step 5: Determine the unit weight for the total aggregate blend and convert to individual aggregate blend percentages.

$$\text{Unit weight of blend} = \text{unit weight contribution of coarse and fine aggregates}$$
$$= 1691 + 671$$
$$= 2362\,kg/m^3$$

CA: Percent by weight = 1691/2362 = 71.6%

FA: Percent by weight = 671/2362 = 28.4%

Step 6: Determine the size of Break Point Sieve (BPS). Calculate the percentages of the coarse aggregate for the amount of fine aggregate they contain and the fine aggregate for the amount of coarse aggregate they contain in order to maintain the desired blend by volume of coarse and fine aggregate.

$$BPS = 0.22 * NMAS = 0.22 * 14\,mm = 3.08\,mm \approx 3.35\,mm\ \text{sieve size}$$

CA: $\text{Percent of fine aggregate in blend} = 6\% * 71.6\% = 4.3\%$

FA: Percent of coarse aggregate in blend = $(100-97)\% * 28.4\% = 0.9\%$

Step 7: Determine the adjusted blend percentages of each aggregate by weight.

CA: Adjusted percent in blend = $71.6\% + 4.3\% - \frac{71.6\% * 0.9\%}{71.6\%} = 75.0\%$

FA: Adjusted percent in blend = $28.4\% + 0.9\% - \frac{28.4\% * 4.3\%}{28.4\%} = 25.0\%$

Step 8: Determine the adjusted blend percentage of mineral filler by weight.

CA: Percent of mineral filler in blend = 0%

FA: Percent of mineral in blend = $25.0\% * 2\% = 0.5\%$

MF: Percent in blend = $7.5\% - 0.5\% = 7.0\%$

Step 9: Determine the final blend percentage of fine aggregate by adding the percentage of mineral filler to the fine aggregate.

FA: Final blend percentage = $25.0\% - \frac{25.0\% * 7.0\%}{25.0\%} = 18.0\%$

Results: The final blending percentages are taken from the above results:

CA: 75.0%

FA: 18.0 %

Mineral filler: 7.0%

The blended aggregate gradation is shown in Table A.1.

Table A.1 Blended Aggregate Gradation of SMA

Sieve size (mm)	Percent passing at various sieve sizes (%)
19	100
14	92
9.5	76
6.3	49
3.35	29
2.36	22
1.18	18
0.6	13
0.3	11
0.15	8
0.075	7

Validation for LTA SMA Mix Specification

The proposed new procedure of SMA mixture design can also be used to validate whether LTA SMA Mix specification (shown in Table 1.1) is a truly gap-graded gradation in nature. The information about stockpile gradations of aggregate, the loose and rodded unit weight of coarse aggregate, the rodded unit weight of fine aggregate, their bulk specific gravity has been shown in Figure A.1.

The following steps are presented to validate this procedure:

Step 1: Assume the design unit weight of coarse aggregate is X;

Step 2: Calculate the volume of voids in the coarse aggregate at the design unit weight. It is filled by the fine aggregate with rodded unit weight.

$$VCA = (1 - \frac{X}{G_{sb} * 1000}) * 100 = (1 - \frac{X}{2.660 * 1000}) * 100 \qquad (A.1)$$

Step 3: Determine the unit weight contributed by fine aggregate according to the desired volume blend of fine aggregate. This is the unit weight that fills the voids created by coarse aggregate.

$$\begin{aligned}&\text{Unit weight contribution of fine aggregate}\\&= DUW_f * VCA\\&= 1840 * (1 - \frac{X}{2660}) * 100\end{aligned} \qquad \text{(A.2)}$$

Step 4: Determine the unit weight for the total aggregate blend and convert to individual aggregate blend percentages.

$$CA: \text{Percent by weight} = \frac{X}{X + 1840 * (1 - X/2660)} * 100 \qquad \text{(A.3)}$$

$$FA: \text{Percent by weight} = \frac{1840 * (1 - X/2660)}{X + 1840 * (1 - X/2660)} * 100 \qquad \text{(A.4)}$$

Step 5: Calculate the percentages of the coarse aggregate for the amount of fine aggregate they contain and the fine aggregate for the amount of coarse aggregate they contain in order to maintain the desired blend by volume of coarse and fine aggregate.

Denote the initial percent by weight of coarse and fine aggregates as CA_0 (Eq. A.3) and FA_0 (Eq. A.4), respectively.

$$CA: \text{Percent of fine aggregate in blend} = 6\%CA_0 \qquad \text{(A.5)}$$

$$FA: \text{Percent of coarse aggregate in blend} = 3\%FA_0 \qquad \text{(A.6)}$$

Step 6: Determine the final blend percentages of coarse aggregate by weight.

$$\text{CA : Adjusted percent in blend} = CA_0 + 6\%CA_0 - \frac{CA_0 * 3\%FA_0}{CA_0} \qquad (A.7)$$

Step 7: Determine the design unit weight (X) of coarse aggregate.

From Table 1.1 it is known that the final percent by weight of coarse aggregate is 68%.

$$CA_0 + 6\%CA_0 - \frac{CA_0 * 3\%FA_0}{CA_0} = 68 \qquad (A.8)$$

Put equations A.3 and A.4 into A.8, there is only one unknown variable X. Therefore, it can be calculated from Equation A.8.

Design unit weigh of coarse aggregate: 1500 kg/m^3

Rodded unit weight of coarse aggregate: 1610 kg/m^3

Ratio: R=1500/1610*100%=93%

DUW=93% RUW

Results: From the conclusion of this study, coarse aggregate stone-to-stone contact is developed when the design unit weight of coarse aggregate is between 95 and 105% RUW. Thus, LTA SMA Mix specification is not a truly gap-graded gradation.

APPENDIX B:

VOLUMETRICS AND PHYSICAL TEST RESULTS AND STATISTICAL TEST RESULTS (ENCLOSED IN CD)

FOLDER: VOLUMETRICS AND PHYSICAL TEST RESULTS

File Name	Description
Aggregate Specific Gravity and Absorption Test Results	Crushed Granite Aggregate Specific Gravity and Absorption
Uncompacted Void Content of Aggregate Test Results	Air Voids in the Aggregates and Unit Weight of Aggregates
Blended Aggregate Gradations for Asphalt Mixtures	Aggregate Gradations for All Asphalt Mixtures
Aggregate Ratios for the Evaluation of Aggregate Gradations	Coarse Aggregate Ratio, Fine Aggregate Coarse Ratio, and Fine Aggregate Fine Ratio
Draindown Test Results	Draindown Value of SMA Mixtures
Volumetric Test Results	Volumetric Properties of Asphalt Mixtures
Resilient Modulus Test Results	Resilient Modulus of Asphalt Mixtures
Repeated Load Uniaxial Test Results	Permanent Deformation of Asphalt Mixtures
Wheel Tracking Test Results	Rut Depth of Asphalt Mixtures

FOLDER: STATISTICAL TEST RESULTS

File Name	Description
ANOVA Results of Air Voids for All Blocks	Significant Effect of DUW, CA, FA and AC on Air Voids
ANOVA Results of Air Voids for Block 1	Significant Effect of DUW and AC on Air Voids
ANOVA Results of Air Voids for Blocks 2 and 3	Significant Effect of DUW, CA, and FA on Air Voids
Linear Regression Results for Air Voids	Relationship between Air Voids and Aggregate Ratios
Modified Linear Regression Results for Air Voids	Relationship between Air Voids and Aggregate Ratios
ANOVA Results of Resilient Modulus	Significant Effect of DUW, CA, FA and AC on Resilient Modulus
ANOVA Results of Permanent Strain	Significant Effect of DUW, CA, FA and AC on Permanent Strain
Linear Regression Results for Permanent Strain	Relationship between Permanent Strain and Aggregate Ratios
Modified Linear Regression Results for Permanent Strain	Relationship between Permanent Strain and Aggregate Ratios
Linear Regression Results for Permanent Strain and Rut Depth	Relationship between Permanent Strain and Rut Depth

Note: DUW – Design Unit Weight of Coarse Aggregate;

CA – Coarse Aggregate;

FA – Fine Aggregate;

AC – Asphalt Content.